ENHANCED SENSITIVITY OF LATERL FLOW STRIP BIOSENSORS BASED ON ENYZMATIC REACTION AND NANOMATERIALS

A Dissertation
Submitted to the Graduate Faculty
of the
North Dakota State University
of Agriculture and Applied Science

By

Hui Xu

In Partial Fulfillment of the Requirements
for the Degree of
DOCTOR OF PHILOSOPHY

Major Department:
Chemistry and Biochemistry

May 2014

Fargo, North Dakota

North Dakota State University
Graduate School

Title

ENHANCED SENSITIVITY OF LATERL FLOW STRIP BIOSENSORS BASED ON ENYZMATIC REACTION AND NANOMATERIALS

By

Hui Xu

The Supervisory Committee certifies that this ***disquisition*** complies with North Dakota State University's regulations and meets the accepted standards for the degree of

DOCTOR OF PHILOSOPHY

SUPERVISORY COMMITTEE:

Guodong Liu
Chair

D.K. Srivastava

Sivaguru Jayaraman

Xiwen Cai

Approved:

07-31-2014
Date

Gregory Cook
Department Chair

ABSTRACT

Ultrasensitive detection for trace amount of proteins plays pivotal role in the diagnosis of specific diseases in clinical application, basic discovery research and the improvement of proteomics. Recently, lateral flow strip biosensor (LFSB) has gained considerable attention for protein analysis. Compared with the traditional immunoassays, LFSB has several advantages: user-friendly format, short assay time (generally several minutes), less interference due to chromatographic separation, a relatively low cost, and no requirements for skilled technicians. This ideal technique is suitable for on-site testing by people who are untrained. Traditional gold nanoparticles (GNPs) based LFSB have been used for qualitative and semiquantitative analysis, the application of GNP-based LFSB is limited by its low sensitivity. In this dissertation, different nanomaterials and advanced detection technologies have been used to enhance the LFSB sensitivities.

An ultrasensitive LFSB based on horseradish peroxidase (HRP)/GNP dual labels was developed for qualitative (Yes/No) and quantitative detection of protein. The LFSB signal was enhanced dramatically by introducing the second tracer (enzyme) on the GNP surface. The detection limit of LFSB was 100 times lower than that of GNP-based LFSB.

A fluorescence LFSB based on enzyme tracers was developed for sensitive detection of proteins. Alkaline Phosphatase (ALP) was selected as a label to prepare the LFSB. The signal was from the fluorescent emission of the ELF-97 alcohol precipitate which was the product of ALP catalyzed dephosphorylation of ELF-97 phosphate.

ALP-conjugated antibody (ALP-Ab) functionalized gold nanoparticles (GNPs) were used as labels for the development of a chemiluminescence-based quantitative LFSB. The use of

chemiluminescence detection and GNPs as enzyme carriers allowed accurate and sensitive analyte detection.

GNP-decorated silica nanorods (GNP-SiNRs) were synthesized and employed as the labels for ultrasensitive detection of proteins on the LFSB. Owing to its biocompatibility and convenient surface modification, SiNRs were used as carriers to load numerous GNPs. The signal of the GNP-SiNR based LFSB was enhanced significantly compared to the GNP-based LFSB since more GNPs were captured through the sandwich-type immunoreactions.

ACKNOWLEDGMENTS

I would like to express my greatly thankful my advisor, Dr. Guodong Liu, who always provided his support, encouraged me to face difficulties, and guided me to the right direction throughout my whole research work. His passion for research inspires me and sets a spectacular example for me to develop myself as an independent researcher.

I wish to give my sincere thanks my committee members, Dr. D.K. Srivastava, Dr. Sivaguru Jayaraman and Dr. Xiwen Cai, for their support, guidance, comments and suggestions during my graduate study. I would like to thank Wendy Leach, Linda Stoetzer, Christina Exner, David Tacke and Karla Wohlers, who always helped me with great patience whenever I approached them for any support. I want to thank all other staffs and faculty members in the department for their help. I also want to thank Dr. Xiaojun Zhao in University of North Dakota, who provided silica nanorods in my research.

I want to give my thanks to my lab members: Meenu Baloda, Anant Gurung, Sunitha Takalkar, Kwaku Baryeh and Xiaoguang Zhang; visiting scholars and students: Dr. Yunhui Yang, Dr. Guangyu Shen, Dr. Yafeng Zheng, Wei Wen, Xuefei Gao, Lu Wang, Wanwei Qiu and Zebin Guo. They are kind-hearted and supportive either in the research or in my personal life. I also want to thank my friends, Shuang Zhou, Jiao Chen, Yue Li, Jing Zhang, Qixin Zhou, Qun Sun, Xuelian Bai, Qunshu Zhang and all the graduate students in the department for their support and guidance.

I would like to give my heartfelt thanks to my family and my boyfriend. I would not have gone so far without their support, concern and encouragement.

I want to thank the Department of Chemistry and Biochemistry and North Dakota State University.

TABLE OF CONTENTS

LIST OF FIGURES

LIST OF ABBREVIATIONS

Ab……...Antibody

AEC……3-Amino-9-ethylcarbazole

AFB_2……...Aflatoxin B_2

ALP…….Alkaline phosphatase

AMI…….Acute myocardial infarction

BSA…….Bovine serum albumin

CCD…….Charge-coupled device

CEA…….Carcinoembryonic antigen

CL……Chemiluminescence

CPPU……...Phytoregulator forchlorfenuron

DIBA……...Dot immunobinding assay

DNA…….Deoxyribonucleic acid

EDS……..Energy-dispersive X-ray spectroscopic

ELISA……..Enzyme-linked immunosorbent assay

GNP……..Gold nanoparticle

$HAuCl_4 \cdot 3H_2O$……...Gold (III) chloride trihydrate

HBsAg……...Hepatitis B surface antigen

hCG……Human chorionic gonadotropin

HCV……...Hepatitis C virus

HIV…….Human immunodeficiency virus

HRP……....Horseradish peroxidase

Hs-cTNI……..High-sensitivity cardiac troponin I

IgG……..Immunoglobulin G

IGSS……....Immunogold–silver staining

IL6……...Interleukin 6

K_2CO_3……..Potassium carbonate

LC-MS/MS……..Liquid chromatography–mass spectrometry

LFA……..Lateral flow assay

LFI……Lateral flow immunoassay

LFSB……....Lateral flow strip biosensor

microRNA……....miRNA

MnGMs……Magnetic nanogold microspheres

MS……Mass spectrometry

Na_3Ct……Sodium citrate

$Na_3PO_4•12H_2O$…….Sodium phosphate tribasic dodecahydrate

$NaBH_4$……...Sodium borohydride

NALFA……..Nucleic acid lateral flow assay

NH_4OH……..Ammonium hydroxide

NMR……..Nuclear magnetic resonance

PBS……Phosphate buffer saline

PBST……..PBS with 0.05% Tween 20

PCa…….Prostate cancer

PCR……Polymerase chain reaction

PDGF-BB……...Platelet derived growth factor-BB

PfHRP2……...*Plasmodium falciparum* histidine-rich protein 2

POCT……..Point-of-care testing

PSA…….Prostate-specific antigen

PVP…….Polyvinylpyrrolidone

Qdot……Quantum dot

QISB……...Quantitative immunochromatographic strip biosensor

RIA……..Radioimmunoassay

RNA……Ribonucleic acid

SEM……Scanning-electron microscope

sIgE…….Specific IgE

SiNRs……..Silica nanorods

SiNWs…….Silica nanowires

SNPs……Single nucleotide polymorphisms

SPR……..Surface plasmon resonance

TB……Tuberculosis

TEOS……...Tetraethylorthosilicate

TNFα……...Tumor necrosis factor alpha

TNT……..2, 4, 6-trinitrotoluene

UPT……...Upconverting phosphor technology

α-AFP……Alfa-fetoprotein

1. INTRODUCTION

Identification and quantification of disease-specific biomarkers have obtained an increasing attention in the past a few decades. A biomarker, defined as an indicator of specific biological processes, is found in biological fluids in patients functioning for the diagnostic, prognostic and predictive of cancer-related disease.[1] It is demonstrated that the DNA methylation, changes in RNA or protein abundances, cell death or proliferation could be used as biomarkers of disease-related biological process.[2] Early detection of cancer has a significant impact on improving the survival rate of patients with many cancers, such as breast, colon, kidney, skin, pancreas and lung cancer. The clinical treatment is more effective and more successful if the disease is detected at a curable stage.[3] Proteins which are the important biomolecules in living organisms, demonstrate vital functions in storage and metabolism of energy and cellular regulations.[4] The abnormal expression of protein biomarkers in serum and tissue often correlates with cancer-related disease. The detection of these proteins which expressed at the lowest level at their earliest incidence could largely reduce patient's suffering and lower mortality rates.

Numerous techniques have been exploited for the sensitive detection of protein biomarkers with exceptional sensitivity and high selectivity. Mass spectrometry (MS),[5-7] western blotting,[8] gel electrophoresis,[9-10] enzyme-linked immunosorbent assay (ELISA),[11] protein microarray,[12-14] and nuclear magnetic resonance (NMR)[15-16] are often such assays which play pivotal role in the biomarker detection. However, these techniques with multiple washing steps, complex procedures, and expensive instruments are limited to well-financed central testing laboratories. Therefore researches have aimed at developing fast, simple, low-cost, disposable,

and easy-to-use platforms for multiplex proteins detection, especially in developing countries, resource-limited and remote regions.

1.1. Point-of-care testing

Point-of-care testing (POCT), or bed-side testing is defined as medical testing at or near the site of patient care. The driving notion behind POCT is to bring the test conveniently and immediately to the patient. This increases the likelihood that the patient, physician, and care team will receive the results quicker, which allows for immediate clinical management decisions to be made. POCT includes: blood glucose testing, blood gas and electrolytes analysis, rapid coagulation testing (PT/INR, Alere, Microvisk Ltd), rapid cardiac markers diagnostics (TRIAGE, Alere), drugs of abuse screening, urine strips testing, pregnancy testing, fecal occult blood analysis, food pathogens screening, hemoglobin diagnostics, infectious disease testing and cholesterol screening. By performing the procedures with shorter assay time, less sample amount, easier data collecting and management, as well as lower medical cost, POCT devices have been widely used in screening diseases, monitoring drug abuse and testing the safety of water or food. The lateral flow assay (LFA) or lateral flow chromatographic assay, introduced in 1988 by Unipath, is the commonest POCT diagnostics format available in the laboratory or in commercial market.[17] Paper chromatographic strips combined with conventional immunoassay have been developed as a popular platform for qualitative or semi-quantitative detection of many types of targets.

1.2. Principle of lateral flow chromatographic assay

Typical lateral flow chromatographic assay is performed on a lateral flow strip biosensor (LFSB, Figure 1.1), which is composed of porous membranes, recognition elements, and a

signal-generating system (commonly colored particles as the labels). The LFSB consists of four components: sample pad, conjugate pad, nitrocellulose membrane and absorption pad. The movement of liquid along the strip is essential in the LFSB, thus each part overlaps onto one another to ensure the migration. One end of the strip is located a sample pad which is usually made of cellulose for loading sample solution. The conjugate pad, made from glass fiber, is attached with the sample pad; colored particles labeled with recognition elements are dispensed/pipetted, and dried on the conjugate pad. The nitrocellulose membrane acts as detection zone with sprayed at least two lines: a test line and a control line; the test line is use to recognize the sample analyte and capture the colored particles to generate the detectable signal, while the control line is to validate the proper performance of the strip. The attached absorption pad at the other end of the strip is to maintain the flow of the liquid since the capillary force of the strip material is the driving force for the movement of the liquid.

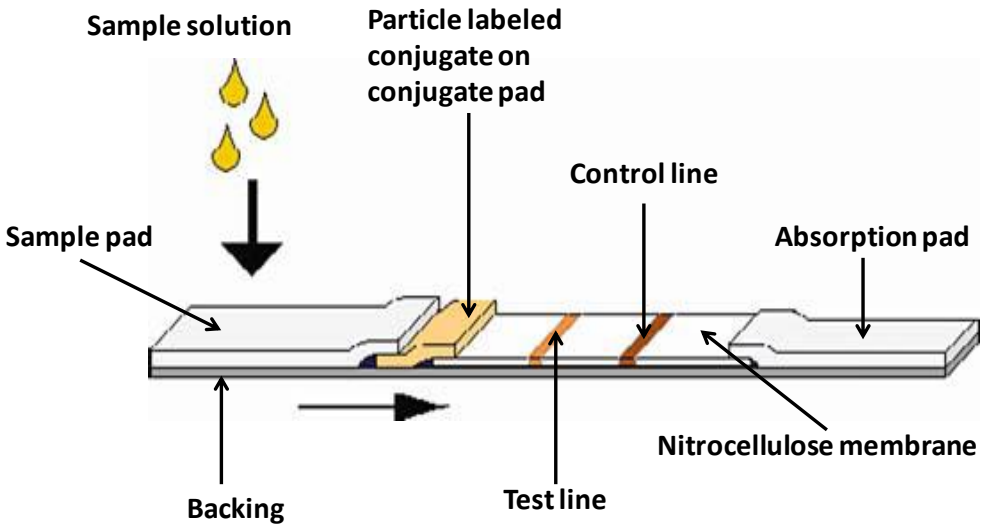

Figure 1.1. Typical configuration of lateral flow strip biosensor.[18]

1.3. Classification of lateral flow assay

According to the different recognition elements applied in the tests, the LFA could be classified as ‘lateral flow immunoassay (LFI)’ and ‘nucleic acid lateral flow assay (NALFA)’. LFI is based on antibody-antigen immunoreaction, and the antibodies are widely used in the LFI configuration for recognizing analyte. There are two major detection formats reported for LFI: competitive and sandwich-type formats. Competitive format is most often designed for detection of small molecule with single antigenic determinants, which could not bind with two antibodies simultaneously. In a typical competitive format, antibody is immobilized on the test line, labeled analyte is dispensed on the conjugate pad and the analyte in the sample solution competes with the labeled-analyte for binding the antibodies on the test line (Figure 1.2); instead of antibody, analyte-protein complex also could be sprayed at the test line, and the labeled-antibody is immobilized at the conjugate pad.[19] Generally, the secondary antibody is dispensed on the control line to capture the excess labeled-antibody. Under the competitive condition, the response is negatively related to the analyte concentration.

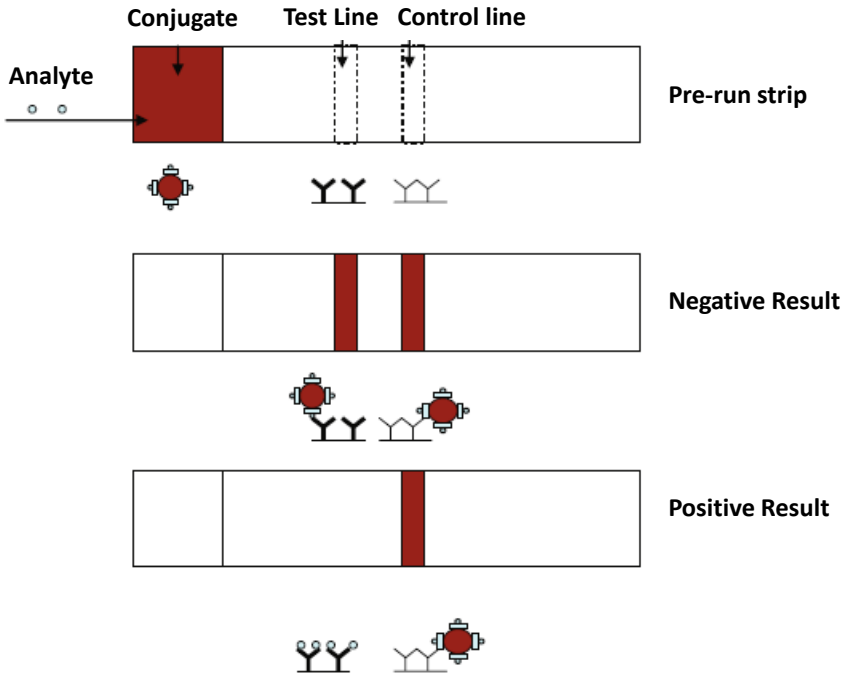

Figure 1.2. Competitive detection format of lateral flow immunoassay. (Adapted from original source)[18]

On the other hand, sandwich-type format is applied for the analytes with more than one epitope such as proteins. A pair of antibodies specifically recognizing different binding sites on the analyte are introduced: the colored particles labeled with the reporter antibody is applied on the conjugate pad, the other antibody called capture antibody is immobilized on the test line. Analyte in the sample solution interacts with the report antibody-labeled particles initially to form antibody-analyte complex on the colored particle surface, then continues migrating along the strip toward test line. Detectable signal is achieved when the complex is captured by the capture antibody on the test line through the second immunoreaction. The excess amount of colored particles is captured by the secondary antibody on the control line. The more analyte presents, the higher response from test line is obtained. The signal intensity is directly proportional to the concentration of analyte in the sample solution. (Figure 1.3)

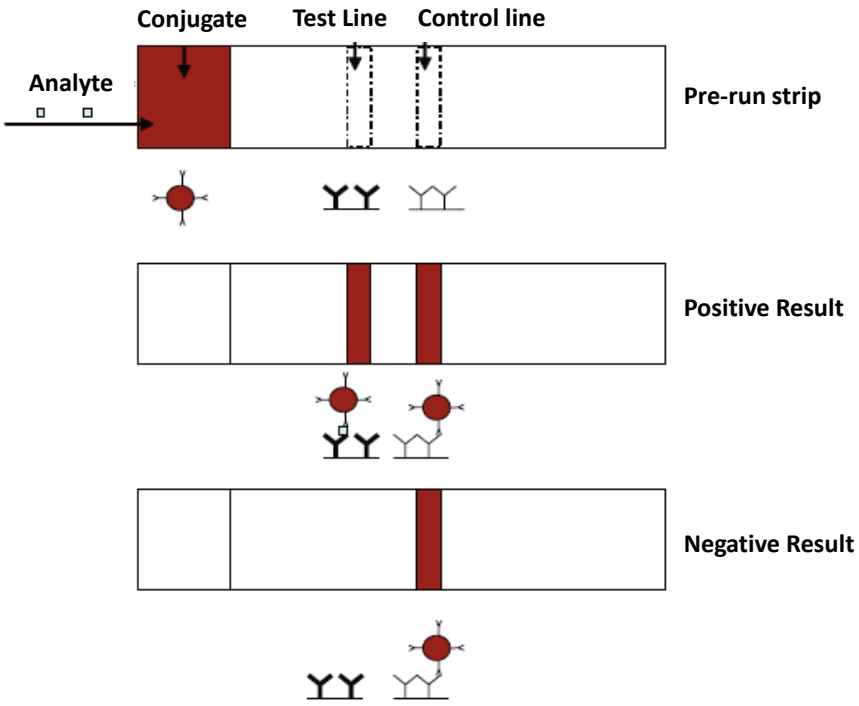

Figure 1.3. Sandwich detection format of lateral flow immunoassay. (Adapted from original source)[18]

NALFA platform has been used to detect the sequences of nucleic acids. Typically the analyte is a specific sequence of nucleic acid (DNA or RNA) of the organism. The colored particles labeled with an oligonucleotide probe (reporter probe), which is partially complementary to the analyte, is applied on the conjugate pad; another partially complementary DNA probe is immobilized on the test line as capture probe. The immobilization of capture probe on the nitrocellulose membrane could be achieved either using bovine serum albumin (BSA) conjugated capture probe, or through the interaction between biotinylated capture probe and streptavidin/avidin sprayed at test line (Figure 1.4). Capillary force drives the sample solution from the sample pad toward another end of the strip. The reporter probe on the colored particle surface hybridizes to the part of the target sequence and move together to the test line. The

response is formed at test line when the capture probe hybridizes to the other part of the target. Similar to the sandwich-type format of LFI, the response of the test line is proportional to the amount of analytes in the sample solution. More recently, with a significant development of aptamers (the artificial nucleic acid ligands), NALFA has been employed toward a wider range of targets, such as small molecules (e.g. cocaine),[20] proteins[21] and whole cells.[22]

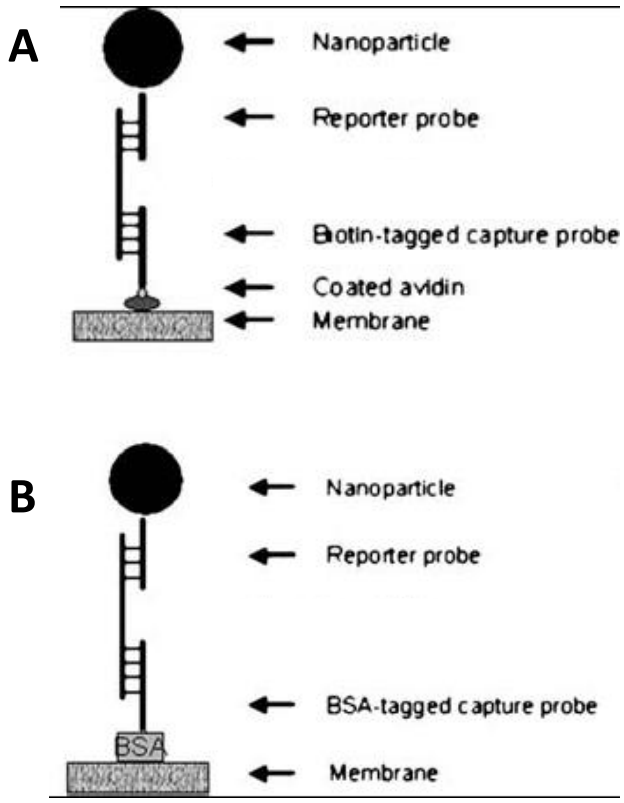

Figure 1.4. Schematic representation of immobilization methods in nucleic acid lateral flow assay. (A) Particles labeled reporter probe and biotinylated capture probe, immobilized through the interaction between biotin and avidin/streptavidin; (B) Particles labeled reporter probe and BSA labeled capture probe.[19]

1.4. Applications of lateral flow assay

Being a powerful POCT device, LFA has shown its promising applications in a wide range of research and clinical fields.

Proteins are common targets for LFA. The pregnancy test kit is the best-known commercial POCT device based on the measurement of the pregnancy hormone human chorionic gonadotropin (hCG).[17] Detection of protein cancer biomarkers is shown of greatly essential applications in cancer prevention and treatment. The visual detection of free and total prostate specific antigen in female serum, which is the most reliable tumor marker to detect prostate cancer (PCa), was realized on the lateral flow device.[23] Carcinoembryonic antigen (CEA) has been widely used as a biomarker in clinical diagnosis of breast cancers, colon cancers and lung cancers. The quantitative immunochromatographic strip biosensor (QISB) was reported for the analysis of CEA in human serum sample.[24] The LFA has been used to detect other disease-specific protein markers. For example, LFA was used for detection of hepatitis C virus (HCV) core antigen, and offered an easy and fast screening method for early diagnosis of HCV infection.[25] An aptamer-based LFA was reported for the detection of thrombin in human serum.[21] To achieve the rapid and accurate evaluation of patients with acute myocardial infarction (AMI), a novel lateral flow immunoassay test was developed and was capable of simultaneous detection of high-sensitivity cardiac troponin I (hs-cTnI) and myoglobin in patients.[26] Worsley et al.[27] reported a rapid duplex immunoassay for assessments of wound healing and treatment. Two common inflammatory wound biomarkers, interleukin 6 (IL6) and tumor necrosis factor alpha (TNFα) were successfully tested in plasma. The LFA was also used to detect specific IgE (sIgE) to bee venom and wasp wenom in insect venom allergic patients. The results demonstrated that the allergy LFA would be a reliable and versatile tool for the diagnosis of insect venom allergy.[28] Recently, Fang et al.[29] reported a lateral flow biosensor for the detection of DNA-binding proteins and the measurement of the activity of transcription factors in cell samples.

The NALFA has been used to detect specific nucleic acid sequences to determine the genomic detail of patient and to determine the special sequences for invading pathogens. Lateral flow nucleic acid biosensor with isothermal strand-displacement polymerase reaction was developed for detecting extracted human genomic DNA, and a good specificity was obtained when HCV RNA, tuberculosis (TB) DNA and swine DNA were used as negative controls. [30] Prostate-specific antigen (PSA) cDNA and HCV RNA from Human Plasma were detected by combining PCR and the dry-reagent strip biosensor.[31] Single nucleotide polymorphisms (SNPs), which are mainly correlated with genetic diseases, drug resistance of infectious agents and disease susceptibility, were detected by using lateral flow biosensor with high sensitivity.[32] The specific RNA after isothermal amplification was assayed for the detection of *Bacillus anthracis*.[33] The hybridization-based *Streptococcus pneumoniae* DNA assay in a complex matrix was reported for the identification of *Streptococcus pneumoniae* infection.[34] The NALFA was also used for the detection of microRNA (miRNA)-215 from A549 cell lysate.[35]

In addition, the detection of small molecules or metal ions on the lateral flow devices expanded the applications of LFA for testing and monitoring the safety of water, food and animal feed. Various tests have been developed for the detection of toxin compounds including Aflatoxin B_1 in pig feed extracts,[36] Carbarly and endosulfan from extracts of cereals and vegetables,[37] Fumonisin B_1 in extracts of cereals and peanuts,[38] (Dihydro) streptomycin in raw milk.[39] The release of heavy metals has shown the significant impact on the environment. The amount of heavy metal ions should be carefully monitored. The detection of Mercury (Hg^{2+}),[40] Chromium ions (Cr),[41] Cadmium (Cd^{2+}),[42] Lead (Pb^{2+})[43] and Copper (Cu^{2+})[44] on the lateral devices has shown great promise for the applications of LFA in environmental protection and monitoring toxic compounds.

More Recently, it has been recognized that LFA could be directly used for whole-cell assay, such as visual detection of Ramos cells[22], multiplexed detection of *Escherichia coli* (non-pathogenic or pathogenic),[45] multiplex immuno-disc sensor for the specific detection of *Pseudomonas aeruginosa* and *Staphylococcus aureus*.[46]

1.5. Labels used in lateral flow assay

Labels used in LFA play very important roles for the development of LFA with high sensitivities. The intensity of test line depends on the amount of captured labels in the test zone. The ideal label for LFA would obtain several characteristics: wide detection dynamic range, high sensitivity, good stability, easy conjugation and low cost.[18] Various labels including nanoparticles (gold nanoparticles, quantum dots and magnetic nanoparticles), nanowires, nanotubes, dye-doped microbeads and hybrid nanocomposites have been utilized in LFA.

1.5.1. Gold nanoparticle (GNP)

There is no doubt that gold nanoparticle (GNP) is the most popular label in LFA because of easy preparation and conjugation, vivid color for visualization, good stability and cost-effective. A large number of tests have been done based on GNP labels for detecting infectious agents,[47-48] metabolic disorders,[49] toxic compounds.[50-52] The qualitative or semiquantitative detection of analytes would be realized by the visualization with the analysis of color intensity. However, the detection limit and sensitivity of GNP-based LFA remains to be improved, particularly for the detection of trace amount of analytes. For instance, the most of detection limits of the GNP-based LFA of proteins ranged from μg mL^{-1} (nanomolar) to ng mL^{-1} (picomolar) levels.[23-24, 53-55] However, protein detection, such as cancer biomarker detection and

early diagnosis of disease often require lower detection limits, in the range of pg mL^{-1} (fetomolar) concentration.[56-57]

An improved sensitivity for the detection of cardiac troponin I was obtained by introducing Immunogold–silver staining (IGSS) method. The color intensity of the test line was largely enhanced due to the silver deposition and the detection sensitivity was increased by 51-fold compared to the GNP-based LFA.[58] Similarly Rohrman et al. employed gold nanoparticle and gold enhancement solution to detect human immunodeficiency virus (HIV) RNA. The signal-to-noise ratio was increased by 25% due to the gold deposition on the surface of gold nanoparticles.[59]

Another effective method to amplify the intensity of the test line is the utilization of two types of GNP conjugates. The 2nd GNP conjugate was to bind with the 1st GNP conjugate which was previously captured at detection zone. The detection sensitivity for troponin I increased about a 100-fold compared to the conventional LFA.[60]

Another approach for signal amplification is the use of hybrid gold nano-composite. Magnetic nanogold microspheres (MnGMs) with Fe_2O_3 nanoparticles as core and gold nanoparticles as shell were synthesized and bio-functionalized with monoclonal anti-aflatoxin B_2 (AFB_2) antibodies. The visual detection limit was about 3-fold lower than a conventional test using GNP label.[61] Instead of making hybrid nano-composite, multiple nanoparticles were used to achieve higher analytical sensitivity of LFA. Besides of GNP, magnetic nanoparticle was applied with a magnetic field to purify and concentrate analyte in bulk serum firstly, then this enriched mixture was directly applied to the GNP-based lateral flow strip. Visual analysis of *Plasmodium falciparum* histidine-rich protein 2 (PfHRP2) was enhanced by 50-fold using magnetic enrichment assay.[62]

More recently, new detector was applied for GNP-based LFA. Instead of visual detection, thermal contrast of GNP at detection zone was used for quantitative analysis. The amount of heat generated by GNP was analyzed upon optical stimulation. The analytical sensitivity of thermal contrast was enhanced 32-fold.[63]

1.5.2. Enzyme labels

In conventional ELISA, enzyme is used extensively as a tracer for signal generation. The potential advantage of using enzyme labels is the signal amplification that may be achieved by enzyme catalytic reactions. The products resulting from the enzymatic reactions, which are related to the concentration of analytes, would be detected with different types of detectors (chemiluminescent, fluorescent, UV-vis). Enzyme labels have been used to develop sensitive LFAs.

Cho et al.[64] reported an enzyme-based LFA with horseradish peroxidase (HRP) conjugated antibody. Upon the formation of sandwich-type immunocomplex, HPR was specifically accumulated on the detection zone. Enzyme substrate was then introduced to flow through the detection zone. The color signal generated from the catalytic reaction product was used for quantitative analysis. The sensitivity of the assay was enhanced 30-fold compared to that of GNP-based LFA. In this case, only one enzyme molecular could be captured in each single immunoreaction/nucleic acid hybridization. Later on GNP was used as a carrier to load more enzyme trackers for further signal amplification. Reported DNA probe and HRP were immobilized on the GNP surface. This dual labels based nucleic acid biosensor offered a dramatic improvement in the detection of target DNA, and was capable of detecting of 0.01 pM DNA without instrumentation.[65]

In addition of visual detection, enzyme-based chemiluminescence (CL) detection has been integrated with LFA. The wide dynamic range of the CL measurement minimizes the need of sample dilution. CL detection is also less affected by interferences from sample components because of the absence of an excitation source. For example, Mirasoli et al.[66] reported a competitive LFA for fumonisins detection based on HRP-catalyzed CL and a portable charge-coupled device (CCD) camera. An accurate analyte quantification was obtained with good recovery when compared with liquid chromatography–mass spectrometry (LC-MS/MS) analysis. A CL based LFA was used for the detection of 2,4,6-trinitrotoluene (TNT) in real samples with a detection limit of 0.2 μg mL^{-1} , which is 5 times lower than that of GNP based LFA.[67]

1.5.3. Other nano-/macro- material labels

Quantum dot (Qdot) has gained an increasing attention in many areas because of the high brightness, size-tunable fluorescence emission and good stability against photobleaching. A portable dry-reagent strip biosensor was reported for the analysis of nitrated ceruloplasmin, a biomarker for cardiovascular disease, lung cancer and stress response to smoking. In this case, Qdot was introduced as fluorescent label to prepare Qdot-antibody conjugates for LFA.[68] A silica/CdTe Qdot hybrid composite was also used as labels for fluorescent LFA. Large number of CdTe Qdot bound onto silica nanoparticles to enhance the fluorescence intensity of the labels. Alfa-fetoprotein (α-AFP) was used as a model analyte to demonstrate the concept. The results indicated that the sensitivity of silica/CdTe Qdot based test strips were enhanced at least 10-fold compared to the conventional GNP-based test strips.[69]

Xia et al.[70] reported a LFA using europium chelate-loaded silica nanoparticles as the labels for fluorescent testing of hepatitis B surface antigen (HBsAg) over the range of 0.05-3.13

ng mL^{-1}. The clinical sera samples had been successfully evaluated by the method and the results were as sensitive as ELISA.

Recently carbon nanomaterials have been used as labels in LFA. Carbon nanoparticles based immunochromatographic assay was applied for the detection of the phytoregulator forchlorfenuron (CPPU). The detection limit of the CPPU-specific LFA in kiwi fruits and grapes was 33.4 mg/kg.[71] A newly introduced type of carbon nanomaterials, named carbon nanostrings, are elongated particles containing spherical particles with branched structures. Kalogianni et al.[72] developed the carbon nanostrings based lateral flow device for the detection of polymerase chain reaction (PCR) product and visual genotyping of SNP in human genomic DNA. Abera et al.[73] reported using carbon nanotubes as label for quantitative lateral flow immunosensing in competitive format. Instead of optical measurement, quantitative signal was obtained by simple resistance measurement of the detection zone.

Upconverting phosphor technology (UPT) has been introduced in LFA. UPT particles are composed of rare earth lanthanide elements doped in a crystal. Increased sensitivity in the detection of infectious diseases in saliva was observed using UPT particles as labels.[74]

1.6. Objective

Visual detection is by far the commonest LFA measurement based on gold or dye doped polymer (nano) particles. Because of its easy preparation and reasonable cost, GNPs based LFA are largely explored for POCT application. The best-known commercial device is the pregnancy test kit. Though GNPs has been demonstrated to be potentially useful in protein assay, the detection limit of GNPs-based LFA remains to be improved for trace analysis. My research project aims to improve the analytical performance of LFSB with various configurations by

integrating promising detection technologies (visualization, fluorescence and chemiluminescence) and novel nanomaterial labels.

An effective way for signal amplification of the GNPs-based LFA is to exploit enzymes as alternative types of labels, which generate an enhanced signal resulting from its catalytic reactions. In this dissertation:

1. The GNP was used as a carrier to load multiple HRP tracers for signal amplification. The more HRPs to be captured via each immune-sandwich binding event, the more enzymatic products accumulated at detection zone.
2. Integration with enzyme-based amplification, fluorescence and chemiluminescence detectors were introduced to detect the enzymatic reaction products on the enzyme/GNP based LFSB. Alkaline phosphatase (ALP), ELF-97 phosphate substrate and Lumigen APS-5 substrate were used to demonstrate the proof-of-concept.
3. The GNPs decorated silica nanorods (SiNRs) were used as labels for the development of ultrasensitive LFSB for protein assay.

2. SENSITIVE PROTEIN ASSAY USING DUAL-LABEL BASED LATERAL FLOW STRIP BIOSENSOR

2.1. Introduction

Sensitive, selective and rapid quantifications of extremely low concentration of proteins have been an area of great interest for its potential application in many fields. Such highly sensitive detection of proteins is essential for disease diagnosis, drug discovery and defense against biological threats. Conventional immunoassays, based on the antibody-antigen recognition events, have been developed to detect proteins in various formats, such as radioimmunoassay (RIA)[75], enzyme-linked immunosorbent assay (ELISA)[76], dot immunobinding assay (DIBA)[77-78] and antibody arrays (protein chips).[79-81] Although those approaches offer good sensitivities and specificities, they are often limited in point-of-care testing (POCT) and in-field detection due to safety issues, extended analysis time, complex assay procedure, expensive instruments as well as well-trained personnel. Therefore, continuing efforts have been made to seek an ideal tool for fast, sensitive, low-cost and easy-to-use detection method for proteins.

Recently, lateral flow strip biosensor (LFSB) has been widely used as a powerful tool for protein analysis, clinical diagnosis and biological warfare agents[82-84] by virtue of its user-friendly format, short assay time, low cost, and no requirement for skilled technicians. Gold nanoparticle (GNP) is the most commonly used label [85-88] in LFSB due to its advantages of facile preparation, highly stability and cost-effective. However, only high concentration of proteins can be qualitatively or semi-quantitatively detected using GNP as a colorimetric signal reporter. Therefore, quantitative LFSBs have been developed by introducing an enzyme[89-91] or

fluorophore[68, 92-93] as labels to meet the requirement of sensitive protein detection. Fluorescence based LFSBs were usually performed on expensive optical detectors and complex software for imaging and analysis, which limits its in-field and POCT applications. Recently, a horseradish peroxidase (HRP)-based LFSB in connection with a portable strip reader was used to detect Carcinoembryonic Antigen (CEA) in human plasma[89]. To date, many efforts have been made to improve detection sensitivity by signal amplification strategies.[94-96] Nanoparticles as carriers to load a large amount of enzymes have been explored to amplify the detection signals of biomolecules. Enhanced sensitivity can be obtained from the increasing amount of enzymes loading in each immunoreaction event. For example, Wu et al.[97] employed an enzyme-functionalized silica nanoparticle labels for biomarkers detection. On the basis of this strategy, the designed immunosensor displayed an improved electrochemical and chemiluminescence measurement of α-fetoprotein compared with traditional sandwich immunoassay. An et al.[98] investigated a novel electrochemical immunosensor by using an enhanced GNP labels which were fabricated by modifying the surface of GNP with HRP-Ab.

In this work, we reported a dual-label based LFSB in connection with the portable strip reader for POCT and in-field detection of ultra-low concentration of protein. Signal amplification was obtained by using HRP-labeled antibody functionalized GNP as the label. 3-Amino-9-ethylcarbazole (AEC) was chosen as an enzymatic substrate. Its insoluble end product, which is red in color, can be observed visually. Compared with the GNP based LFSB,[89] the sensitivity of GNP-HRP dual-label based LFSB increased by 25 fold. The LFSB was capable of detecting 20 pg mL^{-1} of rabbit IgG (R-IgG) in 20 min. This device has shown promise to be a fast, accurate and cost-effective tool for the detection of trace amounts of protein biomarker and may find wide applications in clinical diagnostics and other biomedical analytical fields.

2.2. Experimental section

2.2.1. Apparatus

Airjet AJQ 3000 dispenser, Biojet BJQ 3000 dispenser, Clamshell Laminator and the Guillotine cutting module CM 4000 were from Biodot LTD (Irvine, CA). A portable strip reader DT1030 was purchased from Shanghai Goldbio Tech. Co., LTD (Shanghai, China).

2.2.2. Reagents and materials

$Na_3PO_4 \cdot 12H_2O$, sucrose, Tween 20, Triton X-100, phosphate buffer saline (PBS, pH 7.4, 0.01 M), bovine serum albumin (BSA), 3-amino-9-ethyl-carbazole (AEC) were purchased from Sigma-Aldrich (St. Louis, MO). Rabbit IgG, Horseradish peroxidase conjugated goat anti-rabbit IgG (HRP-Ab), Goat anti-rabbit IgG (Primary Ab), Mouse anti-goat IgG (Secondary Ab) were obtained from Thermo Scientific (Rockford, IL). Hydrogen peroxide (30%) was purchased from VWR international (Radnor, PA). Colloidal gold (40 nm) was provided from the Diagnostic consulting network (Carlsbad, CA). Glass fibers (GFCP000800), cellulose fiber sample pads (CFSP001700), laminated cards (HF000MC100) and nitrocellulose membranes (HFB24004) were provided from Millipore (Bedford, MA).

All other chemicals were of analytical reagent grade. All buffer solutions were prepared using ultrapure (>18 MΩ cm) water from a Millipore Milli-Q water purification system (Billerica, MA).

2.2.3. Preparation of GNP-HRP-Ab conjugates

HRP-Ab was conjugated with GNP for the preparation of GNP-HRP-Ab conjugates. Briefly, at room temperature, 7.5 μg of HRP-Ab was added into 1.0 mL of 5-fold concentrated

GNP (pH 9.0). The mixture is gently incubated for 2h, and blocked by 100 μL of 1% BSA solution for 30 min. Then the solution was centrifuged at 12,000 rpm for 18 min, and the nanoparticles were washed with PBS (1% BSA) three times. The resulting ruby sediments were dispensed in 1 mL of buffer containing 20 mM Na_3PO_4•$12H_2O$, 0.25% Tween 20, 10% sucrose and 5% BSA.

2.2.4. Fabrication of dual-label based lateral flow strip biosensor

The biosensor consists of the following components: sample application pad, conjugate pad, nitrocellulose membrane and absorption pad. A schematic diagram of the biosensor was shown in Figure 2.1A. The sample application pad (17 mm×30 cm) was soaked in a buffer (pH 8.0) containing 0.25% Triton X-100, 0.05 M Tris-HCl and 0.15mM NaCl. Then it was dried and stored in desiccators at room temperature. Primary Ab with concentration of 1.2 mg mL^{-1} and secondary Ab were dispensed at the different locations of nitrocellulose membrane (25 mm × 30 mm) as test zone and control zone by using Biojet BJQ 3000 dispenser. The nitrocellulose membrane was then dried at 37 ^{0}C for 1 h. In order to reduce nonspecific binding, nitrocellulose membrane should be treated with blocking reagent (a solution of 1% BSA in PBS buffer) for 30 minutes, and this was washed with PBS as well as distilled water. Finally, all the parts were assembled on a plastic adhesive backing layer (typically an inert plastic, e.g., polyester) using the Clamshell Laminator. Each part overlapped 2 mm to ensure the solution migrating through the biosensor during the assay. The biosensor with a 3 mm width was cut by using the Guillotin cutting module CM 4000. The GNP-HRP-Ab conjugates were dropped on the conjugate pad using a pipet before each test.

2.2.5. Sample assay procedure

One-hundred and twenty microliters of sample solution containing a desired concentration of rabbit IgG was applied onto the sample application pad. After waiting for 5 minutes, additional 25 μL of PBS buffer containing 0.05% Tween 20 and 1% BSA was added. After 10 minutes, when two red bands were developed at the test zone and the control zone respectively, 60 μL of substrate solution containing 0.05% AEC and 0.015% H_2O_2 which was freshly prepared in acetate solution was applied to the sample pad. The enzymatic reaction proceeded for 5 minutes to deposit an insoluble enzymatic product on the test zone and the control zone of the biosensor. For quantitative measurements, the optical intensities of both test and control lines on the biosensor were recorded simultaneously by using a strip reader combined with the 'GoldBio strip reader' software. The numeric values of recorded data was obtained from pixel images of test and control lines.

2.3. Results and discussions

2.3.1. Principle of dual-label based lateral flow strip biosensor

The proof-of-concept of dual-label based LFSB was demonstrated by using the rabbit IgG model system. Figure 2.1A presents the configuration of the LFSB. In general, sample solution containing a desired concentration of rabbit IgG was applied onto the sample application pad. The solution migrated along the nitrocellulose membrane by capillary force and rehydrated the GNP-HRP-Ab conjugates on the conjugate pad. Then the immunoreactions between rabbit IgG and anti-IgG on the GNP surface occurred and the formed complexes continued to migrate along the membrane. When the complexes reached the test zone, they were then captured by the primary Ab immobilized on the test zone via the immunoreactions resulting in the sandwich-type

complexes and the first red band (Figure 2.1B). The excess GNP-HRP-Ab conjugates continued to migrate due to the capillary action and were captured on the control zone via the binding between the secondary antibody and the GNPs-HRP-Ab. The second red band was developed at this moment (Figure 2.1B). After several minutes the substrate solution was applied. The enzymatic reaction proceeded to deposit red enzymatic product on the test zone and control zone of the biosensor, showing two enhanced red lines on the membrane (Figure 2.1C). In the absence of rabbit IgG, only one red band on the control zone was observed (Figure 2.1b and c). In this case, the red band on the control zone (control line) shows that the biosensor has worked properly. Qualitative analysis can be simply performed by observing the color change of the test zone, and quantitative analysis can be implemented by reading the optical intensities of the red bands on the test zone with a portable strip reader (Figure 2.1D).

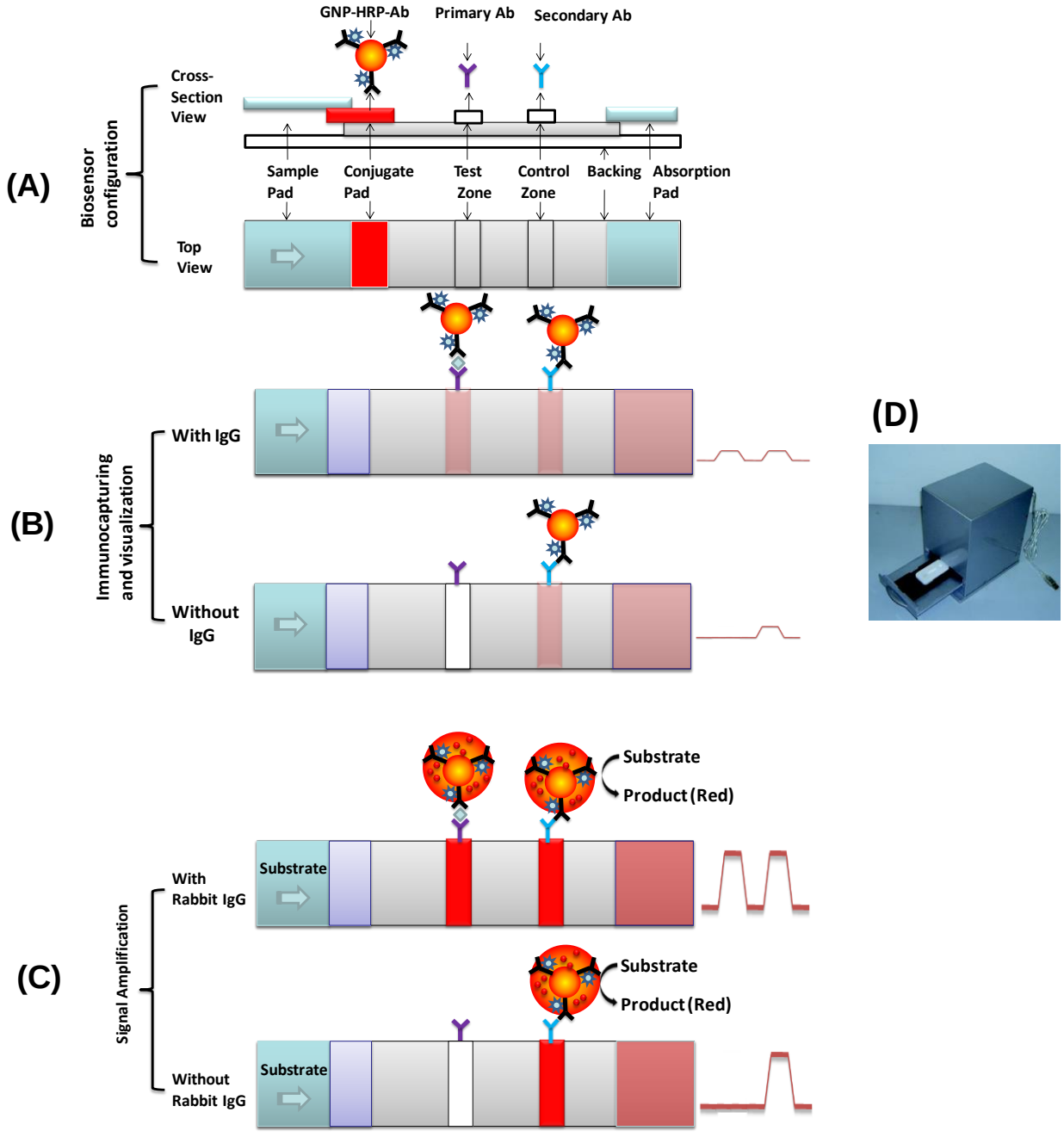

Figure 2.1. Schematic illustration of the configuration of the lateral flow strip biosensor and the principle of the test.

Figure 2.2 presents the typical photo images and corresponding optical responses of the LFSB in the presence of 0 and 10 ng mL^{-1} rabbit IgG before and after the addition of AEC substrate. Only one band could be seen in the absence of rabbit IgG (Figure 2.2A and C). Two visible red bands were observed in the presence of rabbit IgG (Figure 2.2B) and the intensities of the test line and the control line increased significantly after the addition of AEC (Figure 2.2D). The intensities of the red bands were recorded with a portable strip reader and shown on the right side of each photo image in Figure 2.2. Well-defined peaks were observed, and the peak area is proportional to the amount of captured GNPs on the test line, thus the concentration of rabbit IgG in the sample solution.

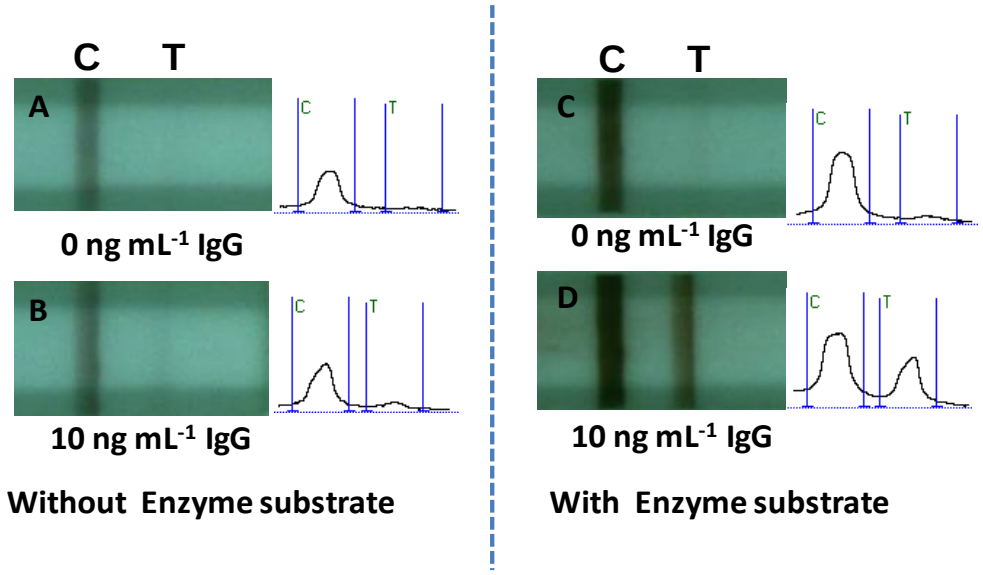

Figure 2.2. Typical images and corresponding responses on the dual-label based LFSB. (Without (left) and with (right) the addition of AEC substrate.)

2.3.2. Optimization of experimental parameters

In the current study, HRP-Ab was used to prepare GNP-HRP-Ab conjugates. The response of the biosensor depends on the amount of captured GNP-HRP-Ab conjugate on the test

zone. The excess HRP-Ab in the conjugate solution may compete with GNP-HRP-Ab and bind to the rabbit IgG target, resulting in the decrease of sensitivity. To obtain a maximum response, the optimal amount of HRP-Ab was established by measuring the signal (10 ng mL^{-1} of rabbit IgG) to noise (0 ng mL^{-1} of rabbit IgG) ratio (S/N) with an increasing amount of HRP-Ab in preparation of GNP-HRP-Ab conjugate. Figure 2.3A presents the histogram of S/N ratio of the biosensor. The maximum S/N ratio was obtained by using 7.5 μg mL^{-1} of HRP-Ab. So this concentration of HRP-Ab was used to prepare the conjugate in the following experiment.

Background signal caused by the nonspecific adsorption of protein and conjugate on the membrane is one of the essential issues in the development of dual-labels based LFSB. In the current study, there was a response coming from the control (in the absence of rabbit IgG). To minimize such nonspecific adsorption, the nitrocellulose membrane (after primary antibody and secondary antibody immobilization) was blocked with a buffer containing 1% BSA. As shown in Figure 2.3B, the S/N ratio of the LFSB pretreated with 1% BSA was much higher than that of the LFSB untreated with BSA. Such delimitation of nonspecific adsorption may be attributed to the shield effect of BSA.

The intensity of the test band depends on the amount of the GNP-HRP-Ab conjugate captured on the test zone, which relates to the amount of conjugate on the conjugate pad. Figure 2.3C presents the histogram of S/N ratios of LFSB with an increasing amount of conjugate solution. It can be seen that the S/N ratio increased up to 5 μL of GNP-HRP-Ab on the conjugate pad. The higher loading amount of GNP-HRP-Ab conjugates caused an increasingly nonspecific adsorption, resulting in a high background, and thus low S/N ratio (results not shown). So 5 μL of GNP-HRP-Ab conjugate was employed to prepare the LFSB.

Another factor affecting the sensitivity and reproducibility of the LFSB is the compositions of the running buffer. Several buffers including PBS, PBS (1%BSA), PBS with 0.05% Tween 20 (PBST) and PBST (1% BSA) were tested, and the S/N ratios of the LFSB are shown in Figure 2.3D. One can see that the best performance was obtained with the PBST (1% BSA) buffer. Therefore, a PBST (1% BSA) buffer was selected for the experiments.

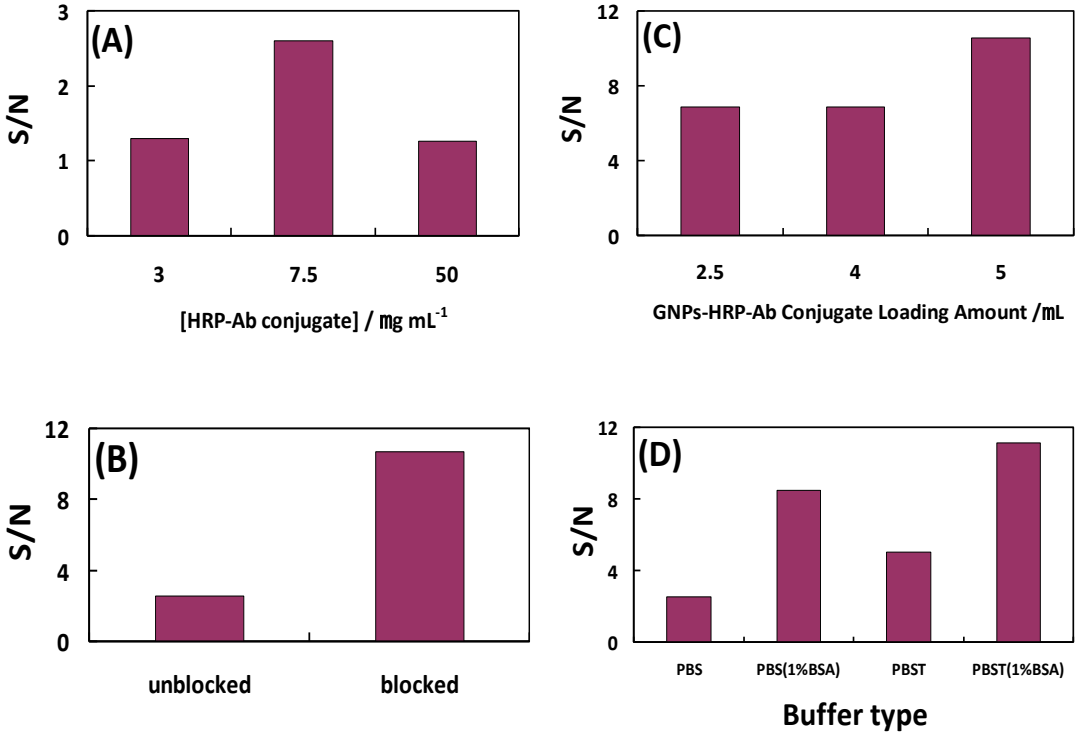

Figure 2.3. Optimization of experimental parameters. (A) Effect of HRP-Ab concentration in the conjugate solution, (B**)** Effect of BSA blocking at test zone, and (C) Effect of the loading volume of GNP-HRP-Ab conjugate on the LFSB's S/N ratio. Assay time: 20 minutes; Sample solution was prepared with PBST (1% BSA); Concentration of primary Ab for the preparation of test zone: 1.2 mg mL^{-1}; Nitrocellulose membrane was unblocked (A) and blocked (C) with 1% BSA; rabbit IgG concentration: 10 ng mL^{-1}. (D) Effect of running buffer components on the LFSB's S/N ratio. Assay time: 20 minutes; Concentration of primary Ab for the preparation of test zone: 1.2 mg mL^{-1}; Concentration of HRP-Ab for the preparation of conjugate: 7.5 μg mL^{-1}; Nitrocellulose membrane was blocked with 1% BSA; Loading volume of GNPs-HRP-Ab conjugate: 5 μL; rabbit IgG concentration: 10 ng mL^{-1}.

2.3.3. Signal amplification using GNP-HRP dual labels in lateral flow strip biosensor

In order to verify the signal amplification function of dual labels in LFSB, the performances of three biosensors based on varied labels were compared. Figure 2.4 shows the illustrations, images and corresponding responses of 10 ng mL^{-1} of rabbit IgG on GNP, HRP and GNP-HRP labels based biosensors, respectively. An increase of signal intensity on both the control zone and the test zone was observed from HRP label based biosensor, compared with the GNP label based biosensor. Such signal enhancement attributed to the deposition of red product which was formed during enzymatic reaction catalyzed by HRP. For conventional amplification strategy, using enzyme as a label, only one label can be captured in one immunoreaction event. Whereas in the dual-label strategy, a large amount of enzymes loading per immunoreaction could be achieved and result in higher signal intensity. It was observed that the signal intensity of GNP-HRP dual-label based biosensor displayed an increasing signal in comparison of HRP based biosensor at the same rabbit IgG concentration. This confirmed that signal amplification using GNP-HRP dual label came from the increasing amount of HRP captured on both control zone and test zone.

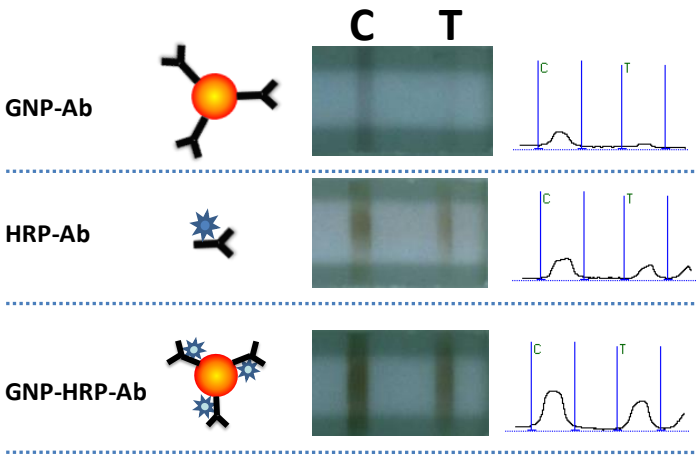

Figure 2.4. Schematic illustration, images and corresponding responses of rabbit IgG from three biosensors based on GNP, HRP and GNP-HRP labels, respectively. (Assay time: 20 minutes; Sample solution was prepared with PBST (1% BSA); Concentration of HRP-Ab for the preparation of test zone: 1.2 mg mL^{-1}; Nitrocellulose membrane was blocked with 1% BSA; rabbit IgG concentration: 10 ng mL^{-1}.)

2.3.4. Analytical performances of dual-label based lateral flow strip biosensor

Under optimal experimental conditions, we examined the performance of the dual-label based biosensor with different concentrations of rabbit IgG. The quantitative behavior was measured by monitoring the recorded signals of a biosensor with strip reader. Figure 2.5A displays typical photo images and corresponding optical responses of biosensor with increasing concentrations of rabbit IgG. A series of well-defined peaks on both control zone and test zone were observed. The resulting calibration curve of the peak area versus logarithm of [Rabbit IgG] showed two linear ranges over 0.02 ng mL^{-1} to 50 ng mL^{-1} (Figure 2.5B). Under the lower concentration range, the amount of GNP-HRP-Ab captured on test zone was small, resulting in fewer amounts of GNPs at the test zone. Therefore, optical responses predominantly came from enzymatic products produced on the test zone. While in higher concentration range, a large amount of GNPs were captured, functioning together with enzymatic products to produce the

signal of the test line. Two linear ranges attributed to the different contributions from GNPs and enzymatic products under different concentrations. The detection limit is estimated as 0.02 ng mL^{-1} (S/N=3). This detection limit is far better than that of the GNP label based LFSB (0.5 ng mL^{-1}) and comparable to that of the HRP label based LFSB (0.05 ng mL^{-1}).[89] The results also showed that the sensitive and specific response of this biosensor was coupled with high reproducibility. In series of six repetitive measurements of 10 ng mL^{-1} and 1 ng mL^{-1} rabbit IgG, the relative standard deviation of 9.5% and 7.5% were found respectively.

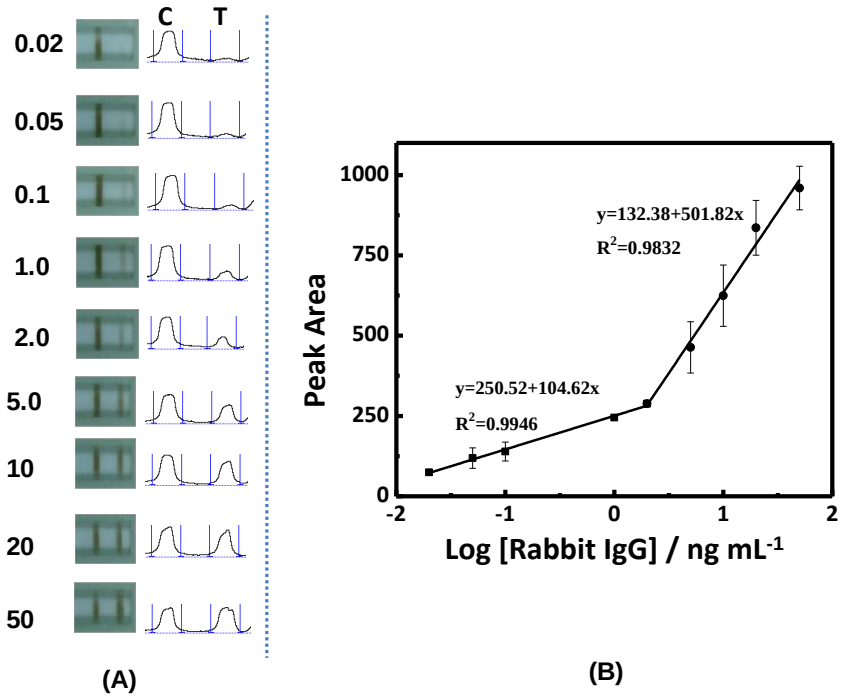

Figure 2.5. (A) Typical photo images and optical responses, as well as (B) calibration curve corresponding to the different concentrations of rabbit IgG. (Assay time: 20 minutes; Sample volume: 120 μL. (n=3))

2.4. Conclusion

We have successfully developed a dual-label based lateral flow strip biosensor for rapid, sensitive and quantitative detection of protein. The concept was demonstrated by using a rabbit

IgG model system. Under optimal conditions, the LFSB was capable of detecting a minimum 20 pg mL^{-1} of rabbit IgG in 20 min. The detection limit was 25 times lower than that of the GNP-based LFSB. The excellent analytical performances of the dual-label based LFSB make it particularly attractive for detecting extremely low concentration of protein biomarkers in decentralized analytical applications.

3. DEVELOPMENT OF FLUORESCENT LATERAL FLOW STRIP BIOSENSOR

3.1. Introduction

Lateral flow strip biosensor (LFSB), combing chromatography separation with traditional immunoassay, is designed for single use at point-of-care testing (POCT), especially outside of the laboratory. It has been widely applied for clinical diagnosis,[99-100] detection of infection disease and contamination,[101-102] monitoring toxic compounds in food, feed and water.[103-106] In comparison with conventional laboratory instrument analysis, LFSB owns many benefits, such as user-friendly, short assay time, low cost and simplified procedure. Typically the application of LFSB is performed by using a colored particle conjugated antibody to detect the presence of target analyte. Gold nanoparticle (GNP) is the commonly used particle as a label due to its vivid color, cost-effective, good stability and easy preparation. Usually the detection of analyte is limited to qualitative or semiquantitative measurement.

Many efforts have been made to improve the sensitivity of LFSB. One of the approaches is to use sensitive detectors, which can be used to quantify the captured labels on the test zone of LFSB. Fluorescent, electrochemical, and chemiluminescent detectors have been integrated with LFSB. Among these detectors, the fluorescence detectors have gained considerable attentions because it provides a sensitive, accurate and fast detection platform using fluorescent particles/fluorophores labels. Li et al.[68] reported a portable fluorescence LFSB for the detection of protein biomarker. Quantum dots (Qdots) were used as labels and conjugated with the specific antibodies to prepare the LFSB. Upon capturing Qdots labeled antibodies on the test zone in the presence of target, the quantitative detection was realized by recording the fluorescence intensity of captured Qdots. The LFSB was successfully utilized for detecting the

protein biomarker in the spiked human plasma sample. Later on more effective and more sensitive approach was reported that involves binding a large number of individual Qdots onto larger silica nanoparticles to obtain composite Qdot probes of higher fluorescence intensity.[69] Lanthanide chelates, possessed high sensitivity in time resolved fluoroimmunoassay, was coated onto porous silica nanoparticles to form the stable fluorescent nanosilica label. The proposed fluorescent nanosilica-based lateral flow immunosensor (LFI) has an excellent ability for quantitative analysis of trace amounts of clenbuterol.[107]

A drawback for fluorescent particle/fluorophore based LFSB is that some of them are very photolabile, resulting in a problem for testing and storage. Therefore enzyme-catalyzed fluorescence using fluorogenic substrate was introduced to provide greater sensitivity.[108] Recently, a new alkaline phosphatase (ALP) substrate was used to yield bright fluorescent product upon enzymatic hydrolysis. This technique provided a well-localized precipitate product and a photostable signal with a large Stokes shift.[109]

In the present work, ALP was selected as a label to conjugate with antibody. ELF-97 phosphate, a specific fluorescence substrate of ALP, was employed to initiate the fluorescent responses. Rabbit IgG was used as a model analyte to demonstrate the proof-of-concept. The maximum excitation and emission of ELF-97 alcohol, the product of ALP catalyzed reaction, were at 345 nm and 530 nm respectively. Quantitative detection was determined by recording the fluorescent intensities of the test line with the assistance of the portable lateral flow fluorescent reader. The feasibility of the biosensor was evaluated. The total assay time for a sample is less than 30 min. The detailed optimization and attractive performance are reported in the following sections.

3.2. Experimental section

3.2.1. Apparatus

Airjet AJQ 3000 dispenser, Biojet BJQ 3000 dispenser, Clamshell Laminator and the Guillotine cutting module CM 4000 were from Biodot LTD (Irvine, CA) and used for the preparation of LFSB. The intensity of fluorescence was scanned in a portable ESE-Quant Lateral Flow Reader (ESE GmbH, Germany).

3.2.2. Reagents and materials

Sodium citrate (Na_3Ct), gold (III) chloride trihydrate ($HAuCl_4 \cdot 3H_2O$, 99.9+%), $Na_3PO_4 \cdot 12H_2O$, sucrose, Tween 20, Triton X-100, phosphate buffer saline (PBS, pH 7.4, 0.01 M), bovine serum albumin (BSA), Tris-HCl (1M) were purchased from Sigma-Aldrich (St. Louis, MO). ELF-97 endogenous phosphatase detection kits (E-6601) were provided by Molecular Probes, Inc. (Eugene, OR). Rabbit IgG, alkaline phosphatase conjugated goat anti-rabbit IgG (ALP-Ab_1), goat anti-rabbit IgG (Ab_1), mouse anti-goat IgG (Ab_2) were obtained from Thermo Scientific (Rockford, IL). Glass fibers (GFCP000800), cellulose fiber sample pads (CFSP001700), laminated cards (HF000MC100) and nitrocellulose membranes (HFB18004) were provided by Millipore (Bedford, MA). All other chemicals were of analytical reagent grade. All buffer solutions were prepared using ultrapure (>18MΩcm) water from a Millipore Milli-Q water purification system (Billerica, MA).

3.2.3. Preparation of lateral flow strip biosensor

The LFSB consists of four components: sample application pad, conjugate pad, nitrocellulose membrane, and absorption pad. A schematic diagram of the LFSB is shown in Figure 3.1A. The sample application pad (17 mm×30 cm) was made from cellulose fiber (CFSP001700, Millipore) and was soaked with a buffer (pH 8.0) containing 0.25% Triton X-100, 0.05M Tris-HCl, and 0.15 M NaCl. Then it was dried and stored in desiccators at room temperature. Test zone at the nitrocellulose membrane (25mm×30 cm) was prepared by dispensing Ab_1 (1.2mg mL^{-1}) with Biojet BJQ 3000. The membrane was dried at room temperature for 1 h and stored at 4 ^{0}C. Finally, all of the parts were assembled onto a plastic adhesive backing layer using the Clamshell Laminator. Each part overlapped 2 mm to ensure the solution migrating through the LFSB during the assay. Each LFSB was cut with a 3 mm width by using the Guillotin cutting module CM 4000. The ALP-Ab_1 conjugate solution was dropped on the conjugate pad using a pipette and air-dried before each test.

3.2.4. Sample assay procedure

One hundred microliters of sample containing a desired concentration of rabbit IgG in PBS+0.5% BSA buffer was applied to the sample pad. After 5 min, another 50 µL of PBS+0.5% BSA buffer was applied to wash the LFSB. Upon the completion of immunoreaction at detection zone, 5 µL of ELF-97 phosphatase substrate (20-fold diluted in dilution buffer) was applied to the test zone. The enzymatic reaction was allowed to proceed for 3 min. The resulted enzymatic product was determined with a portable ESE-Quant lateral flow reader, and the fluorescent intensities of the test line could be analyzed by using a “Lateral flow studio” software.

3.3. Results and discussions

3.3.1. Principle of fluorescent lateral flow strip biosensor

The configuration of the biosensor based on ALP catalyzed fluorescent detection is illustrated in Figure 3.1A. Rabbit IgG was used as a model target to demonstrate the proof of concept. In a typical assay, a sample solution containing a desired concentration of rabbit IgG was applied to the sample application pad. The solution migrated along the LFSB by capillary force and rehydrated the ALP-Ab_1 on the conjugate pad. Then the immunoreaction between rabbit IgG and ALP-Ab_1 conjugate occurred and the formed ALP-Ab_1-rabbit IgG complex continued to flow toward the detection zone. Once reaching the test zone, the complex was then captured by the Ab_1 immobilized on the test zone via the second immunoreaction. The excess of ALP-Ab_1 kept moving until been captured by the Ab_2 at control line (Figure 3.1B) which was used to validate the testing. The fluorescent response from LFSB was generated after adding enzyme substrate-ELF-97 phosphates. Upon enzymatic cleavage, this weakly blue-fluorescent substrate yielded a bright yellow-green-fluorescent precipitate with good photostability (Figure 3.1C). The quantitative analysis was realized by recording the fluorescent intensities of the test zone with a portable ESE-Quant reader (Figure 3.1D). In the presence of rabbit IgG, two peaks from test line and control line could be observed by fluorescent reader (Figure 3.2A). Only one peak from the control line was detectable in the absence of rabbit IgG, indicating the LFSB was working properly (Figure 3.2B).

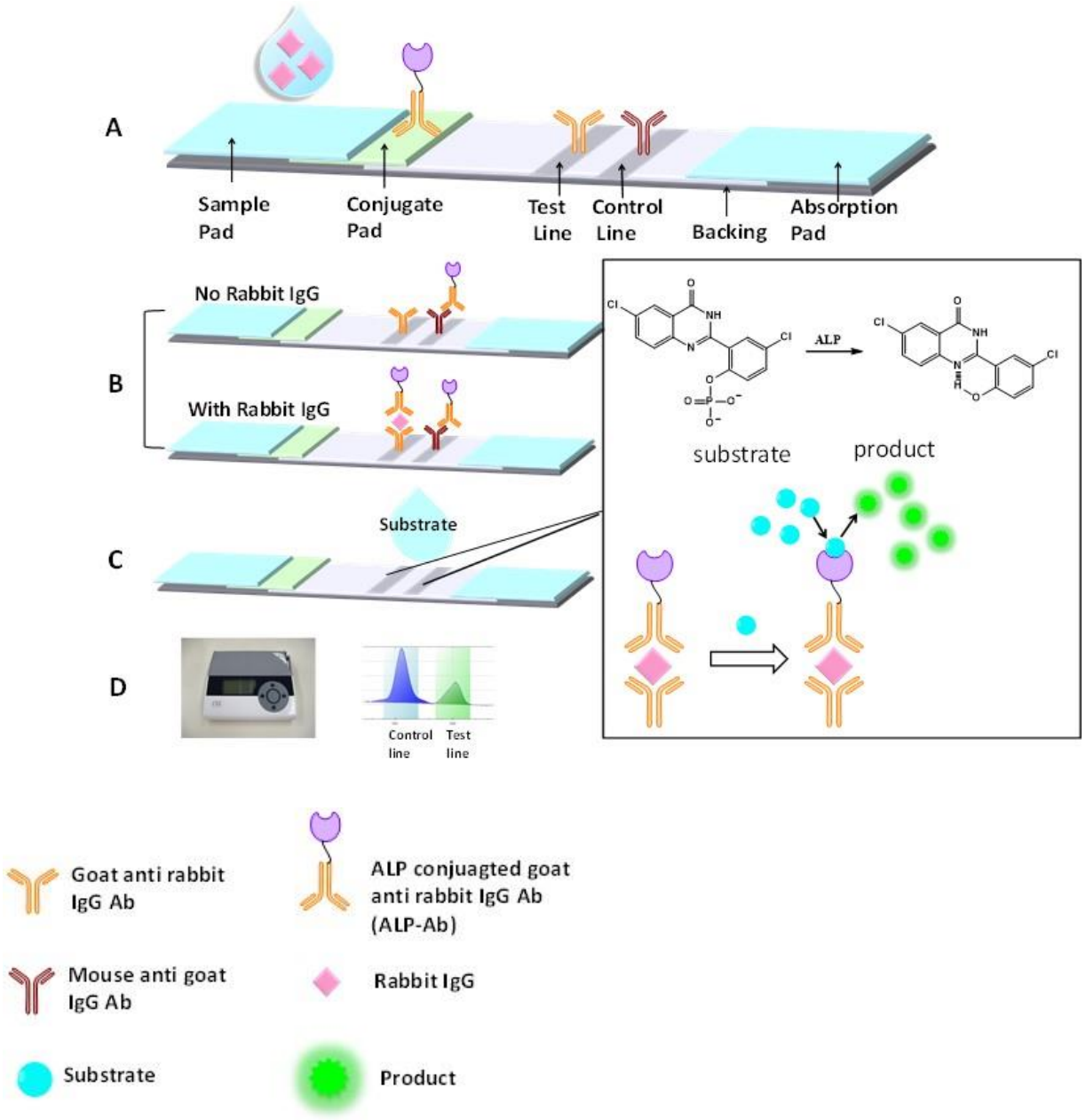

Figure 3.1. Schematic illustration of the configuration and measurement principle of the fluorescent LFSB. (A) configuration of LFSB; (B) Principle of LFSB in the presence and absence of rabbit IgG, (C) Formation of fluorescent product by adding ELF-97 phosphate substrate, (D) Portable ESE-Quant Lateral Flow Reader (left) and the typical fluorescence responses (right) recorded at test line and control line.

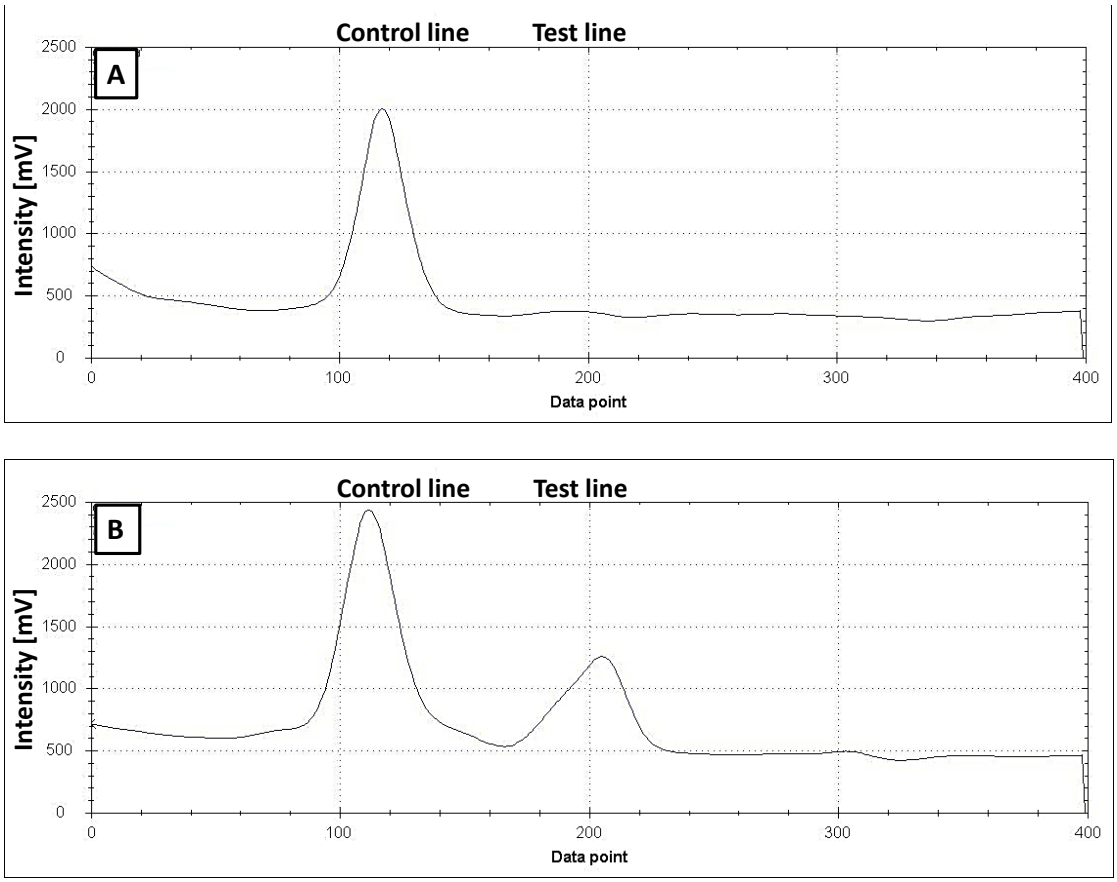

Figure 3.2. Typical fluorescence responses recorded by the portable fluorescent reader. (A) Blank solution; (B) 1 ng mL $^{-1}$ rabbit IgG. Excitation: 363 nm, and emission: 530 nm.

3.3.2. Optimization of experimental parameters

In the current study, the fluorescence intensity of test line depends on the amount of the captured ALP-Ab_1 conjugates. The concentration of ALP-Ab_1 conjugates on the conjugate pad influences the amount of the captured ALP-Ab_1 conjugates on the test line, and thus the performance of LFSB. Figure 3.3A presents the S/N ratio (ratio between 1 ng mL^{-1} rabbit IgG and 0 ng mL^{-1} rabbit IgG (control)) changes with the different concentrations of ALP-Ab_1 conjugates loaded. One can see that the highest S/N ratio was obtained with 0.06 mg mL^{-1} of ALP-Ab_1. The decrease of S/N at higher concentration was ascribed to an increasing of

fluorescence background from overloaded ALP. Therefore, 0.06 mg mL^{-1} of ALP-Ab_1 was selected as the optimal condition.

The fluorescence response of LFSB was also affected by the amount of capture Ab_1 dispensed on test zone. Figure 3.3B presents the effect of Ab_1 amount on the signal intensity of the LFSB. The amount of Ab_1 on the test zone was controlled by the dispensing cycles of the Ab_1. It was found that the highest fluorescence intensity was obtained with two dispensing cycles of Ab_1 on the test zone. Therefore, two-dispensing-cycle was used as the optimal condition in the following experiments.

Enzymatic reaction time would affect the amount of product and the fluorescence intensity of the test line of LFSB. The histogram of the S/N ratios under different enzymatic reaction time is shown in Figure 3.3C. The S/N ratio was found to be the highest for 3 min. The decrease in the S/N at longer reaction time is ascribed to the increased background signal since no stop solution was used here. Therefore, 3 min was selected as the optimal enzymatic reaction time.

The composition of the running buffer has a significant effect on the performance of the LFSB. PBS buffers containing different percentage of BSA were tested, and the results are shown in Figure 3.3D. One can see that the PBS with 0.5% BSA exhibited the best performance. Thereby, PBS (0.5% BSA) buffer was selected for the experiments.

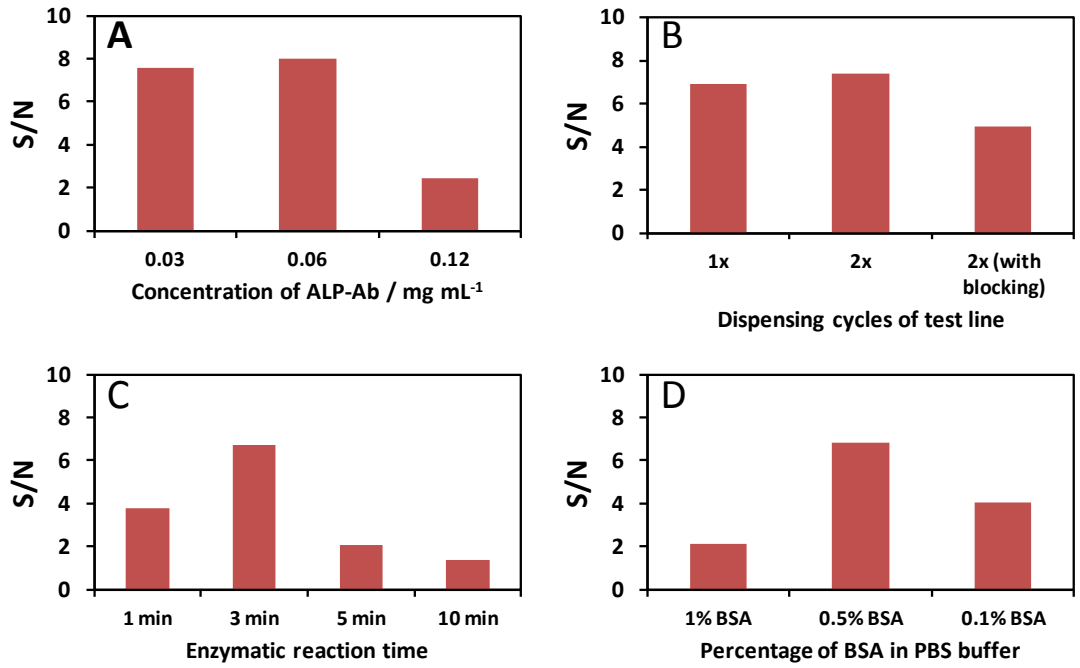

Figure 3.3. Optimization of experimental parameters. (A) Effect of ALP-Ab concentration dispensed on the conjugate pad (with 2-cycle dispensing test line, PBS+0.5% BSA as running buffer and 3 min enzymatic reaction time), (B) Effect of dispensing cycles of Ab_1 on the test zone (with 0.06 mg mL^{-1} ALP-Ab conjugate, PBS+0.5% BSA as running buffer and 3 min enzymatic reaction time), (C) Effect of enzymatic reaction time (with 2-cycle dispensing test line, PBS+0.5% BSA as running buffer and 0.06 mg mL^{-1} ALP-Ab conjugate), and (D) Effect of running buffer components (with 2-cycle dispensing test line, 0.06 mg mL^{-1} ALP-Ab conjugate and 3 min enzymatic reaction time) on the fluorescent LFSB's S/N ratio. Rabbit IgG concentration: 1 ng mL^{-1}, running buffer amount: 100 μL, substrate amount added: 5 μL.

3.3.3. Analytical performance

Under optimal experimental conditions, we examined the performance of the LFSB in the presence of different concentrations of target rabbit IgG. For quantitative analysis, the responses of the LFSB were recorded with the portable lateral flow fluorescence reader. A serial of well-defined peaks were observed, and the peak areas increased with the increasing of rabbit IgG concentration (Figure 3.4).

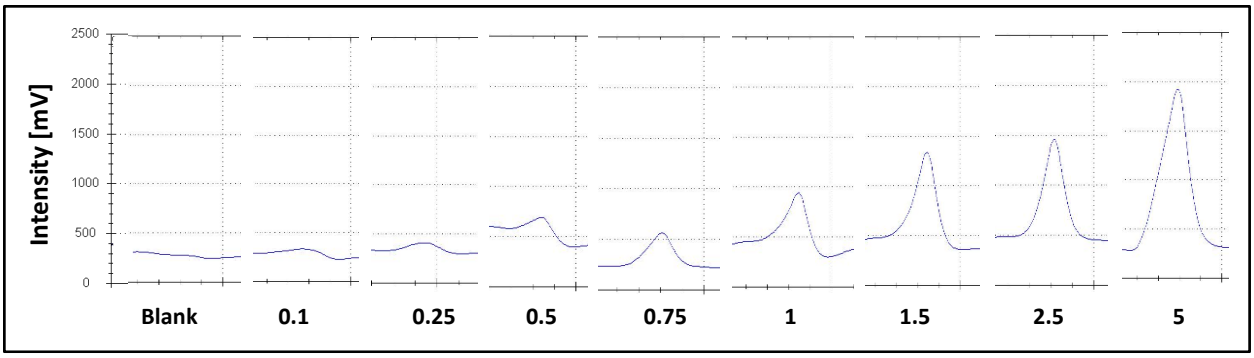

Figure 3.4. Typical fluorescence responses of LFSB corresponding to the different concentrations of rabbit IgG (ng mL^{-1}).

The resulted calibration curve (Figure 3.5) of the peak height versus rabbit IgG concentration is linear over 0.1 to 5 ng mL^{-1} range and is suitable for quantitative analysis. The detection limit of 0.1 ng mL^{-1} (based on S/N =3) was estimated in connection with a 30 min assay time.

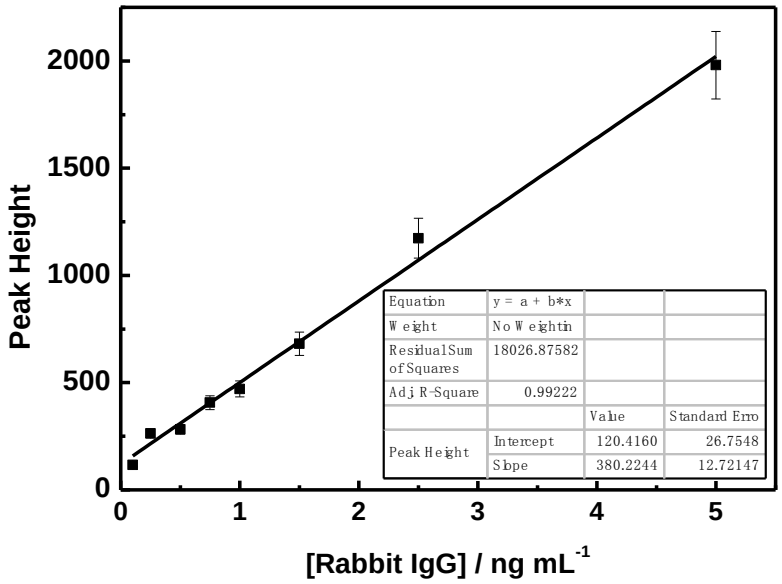

Figure 3.5. Calibration curve of fluorescent LFSB with different concentrations of rabbit IgG. (Error bars represent standard deviation: N=3.)

3.4. Conclusion

We have successfully developed an enzyme-based fluorescent LFSB for sensitive detection of protein. Rabbit IgG was used as model target to demonstrate the proof of concept. Under optimal conditions, the detection limit is 0.1 ng mL^{-1} (S/N = 3) with the linear range of 0.1-5 ng mL^{-1}. The new fluorescent LFSB provided a rapid, sensitive, low cost and quantitative tool for the detection of protein samples. It shows great promise for use of fluorescent LFSB for point-of-care or in-field detection. Further work will aim at to improve the sensitivity of the LFSB by employing nanoparticles for signal amplification, and to detect multiple proteins simultaneously.

4. DEVELOPMENT OF CHEMILUMINESCENT LATERAL FLOW STRIP BIOSENSOR

4.1. Introduction

Lateral flow assays (LFA) have gained an increasing attention for performing fast and low-cost analysis of samples at the place where the samples are collected. Compared to traditional laboratory analysis platforms, such a lateral flow assay or biosensor has some advantages for point-of-care or in-field testing: short assay time, small volume of sample, user-friendly and low cost.[21] The LFA have been used for clinical diagnosis or screening of diseases, testing drugs of abuse, monitoring the safety of water and food.[17] While conventional LFA is based on colloidal gold and latex or polystyrene beads for visual detection through the color formation. Thus this approach only allows qualitative or semi-quantitative analysis. The application of LFA is challenged for detection of trace amount analytes.[110] Therefore, it is highly desirable to develop an ultrasensitive LFA for detection of proteins.

Many efforts have been made to improve the performance of LFA. For example, enzyme [111] and fluorescent dye doped nanoparticles[27, 68, 93] have been used as labels to enhance the LFA sensitivities. Electrochemical detectors have been integrated with LFA for sensitive detection of protein biomarkers.[112-114] Chemiluminescence is a sensitive measurement tool and has been applied in life sciences, clinical diagnosis, environmental and food analysis.[115] The enzyme-based chemiluminescence reaction is initiated by using an enzyme label (usually horseradish peroxidase (HRP) or alkaline phosphatase (ALP)), upon addition of suitable substrate. Even with low quantum efficiency of chemiluminescence reactions, the approach still provides a superior analytical performance. Such high sensitivity is due to the signal amplification from enzymatic

reaction in the presence of excess enzyme substrate. In addition the wide dynamic range of the chemiluminescence detection ensures the analysis of samples with a broad range of concentrations. In addition, chemiluminescence detection due to the absence of an excitation source enhances the detectability compared to fluorescence measurement.[116]

Recently enzyme-based chemiluminescence detection has been used for LFA with improved detection sensitivity with respect to colloid gold or latex beads based LFA. Kim et al.[117] reported a chemiluminescence LFA by using HRP labeled antibodies for detecting myoglobin. Upon addition of luminol substrate, the detection limit of myoglobin was determined as 10 ng mL^{-1}, as much as 100-fold enhanced compared to colloid gold based test. The strategy also demonstrated the broadened application for detection of trace compounds in forensic and environmental fields with the aid of CCD-based light measurement instrumentation.[66-67]

In this work we describe a chemiluminescent (CL) lateral flow strip biosensor (LFSB) based on gold nanoparticles (GNPs) and ALP. Rabbit IgG was chosen as an analyte model to demonstrate the concept. Anti-rabbit IgG antibodies and ALPs were immobilized on the surface of GNPs. Using GNPs as enzyme carrier, more ALPs were captured in each antibody-antigen binding incident, resulting in more enzyme substrate to be converted to CL product. Thus the detection sensitivity was enhanced compared to the results obtained without using GNPs. The developed chemiluminescent LFSB was able to provide quantitative detection of Rabbit IgG with dynamic range from 0.05 to 2 ng mL^{-1}. The observed detection limit was 0.02 ng mL^{-1}, showing a significant improved sensitivity compared to HRP based chemiluminescent LFSB with the detection limit of 10 ng mL^{-1}.[117]

4.2. Experimental section

4.2.1. Apparatus

Airjet AJQ 3000 dispenser, Biojet BJQ 3000 dispenser, Clamshell Laminator and the Guillotine cutting module CM 4000 were from Biodot LTD (Irvine, CA). A portable strip reader DT1030 was purchased from Shanghai Goldbio Tech. Co., LTD (Shanghai, China). QuantiReader™ Benchtop Luminometer was bought from DiaCarta (Hayward, CA) for chemiluminescence detection.

4.2.2. Reagents and materials

Sodium citrate (Na_3Ct), gold (III) chloride trihydrate ($HAuCl_4 \cdot 3H_2O$, 99.9+%), $Na_3PO_4 \cdot 12H_2O$, sucrose, Tween 20, Triton X-100, phosphate buffer saline (PBS, pH 7.4, 0.01 M), bovine serum albumin (BSA), Tris-HCl (1M) were purchased from Sigma-Aldrich (St. Louis, MO). Rabbit IgG, alkaline phosphatase conjugated goat anti-rabbit IgG (ALP-Ab_1), goat anti-rabbit IgG (Ab_1), and mouse anti-goat IgG (Ab_2) were obtained from Thermo Scientific (Rockford, IL). Lumigen APS-5 was purchase from Lumigen (Southfield, Michigan). Glass fibers (GFCP000800), cellulose fiber sample pads (CFSP001700), laminated cards (HF000MC100) and nitrocellulose membranes (HFB24004) were provided from Millipore (Bedford, MA).

All other chemicals were of analytical reagent grade. All buffer solutions were prepared using ultrapure (>18 MΩ cm) water from a Millipore Milli-Q water purification system (Billerica, MA).

4.2.3. Synthesis of GNPs with different diameters

GNPs with three different diameters were prepared according to the reported methods with minor modifications.[118-119] All glassware used in the procedure was thoroughly cleaned with aqua regia (HCl: HNO_3 = 3:1), following with washing and oven-dried. The synthesis began with 50 mL of 0.01% $HAuCl_4$ heated to boil in a round bottom flask with vigorous stirring. To obtain different sizes of GNPs, sodium citrate (1%) was added with amount of 400 μL, 614 μL and 1mL to synthesize 50, 30 and 16 nm diameter of GNPs, respectively. Reflux system was used here to minimize any loss of solution from heating. Finally the obtained solutions were cooled to room temperature and stored in dark bottles at 4 Celsius.

4.2.4. Preparation of GNP-ALP-Ab_1 conjugates

ALP-Ab_1 was conjugated with GNP for the preparation of GNP-ALP-Ab_1 conjugates. Briefly, at room temperature, 7 μg of ALP-Ab_1 was added into 1.0 mL of 5-fold concentrated GNPs. The mixture is gently incubated for 2h, and blocked by 100 μL of 1% BSA solution for 1h. Then the solution was centrifuged at 12,000 rpm for 15 min, and the nanoparticles were washed with Tris-HCl (0.1 M, 1% BSA) three times. The resulting ruby sediments were dispensed in 1 mL of buffer containing 20 mM Na_3PO_4•$12H_2O$, 0.25% Tween 20, 10% sucrose and 5% BSA.

4.2.5. Fabrication of chemiluminescent lateral flow strip biosensor

The biosensor consists of the following components: sample application pad, conjugate pad, nitrocellulose membrane and absorption pad. A schematic diagram of the biosensor was shown in Figure 4.1A. The sample application pad (17 mm × 30 cm) was soaked in a buffer (pH

8.0) containing 0.25% Triton X-100, 0.05 M Tris-HCl and 0.15mM NaCl. Then it was dried and stored in desiccators at room temperature. Ab_1 with concentration of 1.2 mg mL^{-1} and Ab_2 were dispensed at the different locations of nitrocellulose membrane (25 mm × 30 mm) as test zone and control zone by using Biojet BJQ 3000 dispenser. The nitrocellulose membrane was then dried at 37 ^{0}C for 1 h. Finally, all the parts were assembled on a plastic adhesive backing layer using the Clamshell Laminator. Each part overlapped 2 mm to ensure the solution migrating through the biosensor during the assay. The biosensor with a 3 mm width was cut by using the Guillotin cutting module CM 4000. GNP-ALP-Ab_1 conjugates were dropped on the conjugate pad of the biosensor with a pipette and air-dried before the test.

4.2.6. Sample assay procedure

The chemiluminescent LFSB was dipped into a centrifuge tube containing 100 μL of sample solution with a desired concentration of rabbit IgG. After waiting for 5 minutes, additional 50 μL of Tris-HCl (0.1 M) buffer containing 1% BSA was added. Two red bands were developed at the test zone and control zone of LFSB in 20 min. Two microlitter of Lumigen APS-5 substrate was applied to the test zone and control zone. The enzymatic reaction proceeded for 1 minute to yield enzymatic products on the test zone and control zone of LFSB. The chemiluminescence intensities of test line and control line were recorded with Diacarta Benchtop Luminometer.

4.3. Results and discussions

4.3.1. Principle of chemiluminescent lateral flow strip biosensor

The proof-of-concept of chemiluminescent LFSB was demonstrated by using rabbit IgG model system, and GNP-ALP labels. Figure 4.1A present the configuration of the chemiluminescent LFSB. In general, sample solution containing a desired concentration of rabbit IgG was applied to the sample pad. The solution migrated along the nitrocellulose membrane by capillary force and rehydrated the GNP-ALP-Ab_1 conjugates on the conjugate pad. Then the immunoreactions between rabbit IgG and GNP-ALP-Ab_1 occurred and the formed complexes (GNP-ALP-Ab_1-IgG) continued to migrate along the membrane. When the complexes reached the test zone, they were then captured by the Ab_1 immobilized on the test zone via the second immunoreactions, resulting in the sandwich-type complexes (GNP-ALP-Ab_1-IgG-Ab_1) and the first red band (Figure 4.1B). The excess GNP-ALP-Ab_1 conjugates continued to migrate due to the capillary action and were captured on the control zone via the binding between Ab_2 and GNP-ALP-Ab_1. The second red band was developed at this moment (Figure 4.1B). After waiting for 5 min, two microliter of Lumigen APS-5 substrate was applied. The enzymatic reaction proceeded 1 min to produce chemiluminescent product on the detection zone (Figure 4.1C). In the absence of rabbit IgG, only one red band on the control zone was observed (Figure 4.1B). In this case, the red band on the control zone (control line) shows that the biosensor has worked properly. Quantitative analysis can be realized by recording the chemiluminescence intensities of the test line.

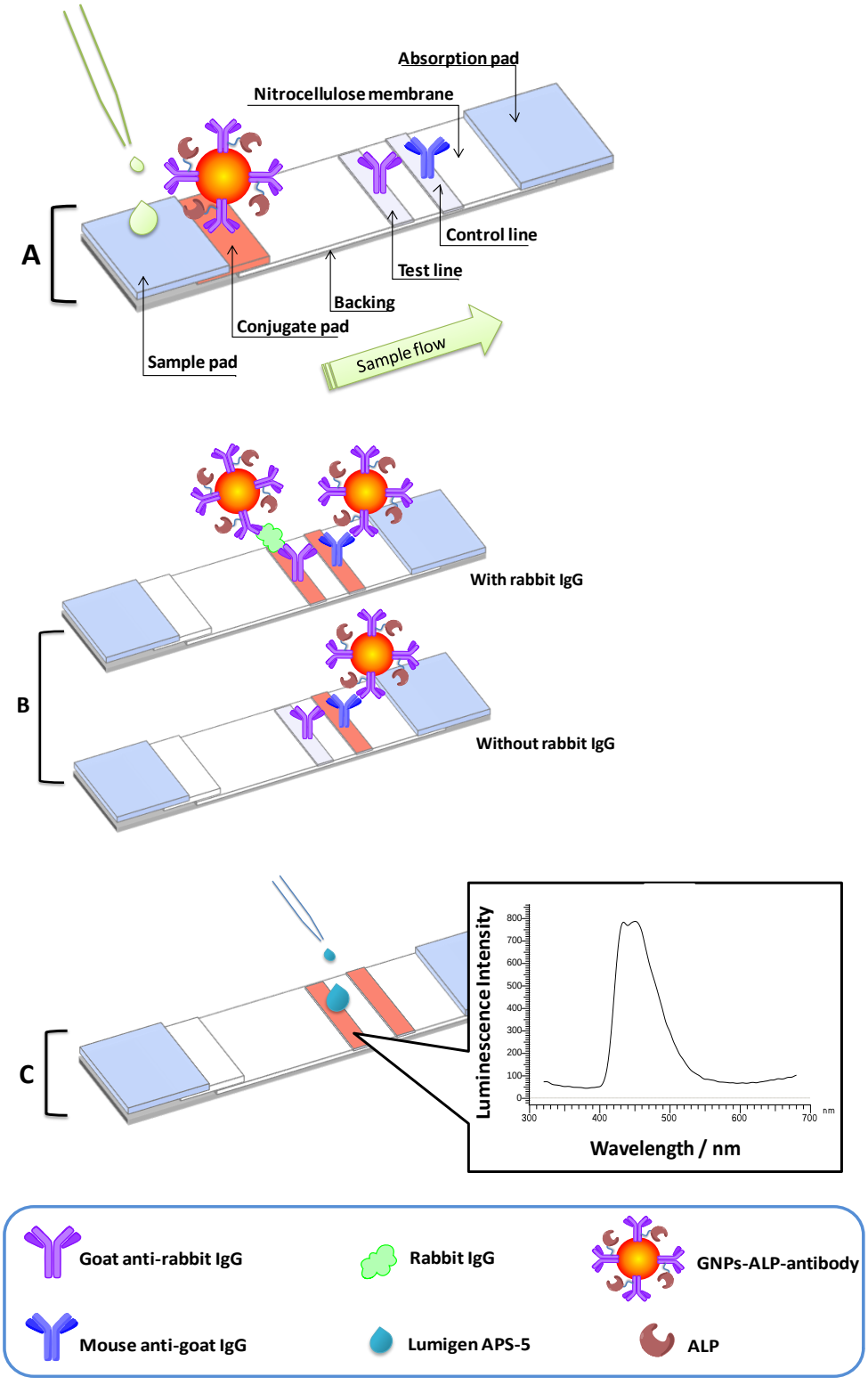

Figure 4.1. (A) Schematic illustration of chemiluminescent LFSB, (B) principle of LFSB measurement and (C) chemiluminescent measurement after adding Lumigen APS-5 substrate.

4.3.2. Optimization of experimental parameters

First, we studied the effect of GNP diameters on the response of LFSB. GNPs with three diameters of 16 nm, 30 nm and 50 nm were prepared and used to fabricate the LFSBs. It was found that the S/N ratio decreased with the increase of GNP diameter, and the best S/N ratio (the chemiluminescence response ratio of 1 ng mL^{-1} rabbit IgG to blank) was obtained with 16 nm GNP (Figure 4.2). The decreased S/N ratio with large size of GNPs may be caused by the reduced stability of large size GNPs. In addition, GNPs with large diameters required more antibodies to cover the surface. Same amount of ALP-Ab_1 was used to conjugate with different sizes of GNPs, thus the GNPs with large diameter probably would not be fully covered by ALP-Ab_1. The stability of GNP-ALP-Ab_1 conjugates prepared with large size of GNP was more interfered by the buffer components which could cause the aggregation or precipitation of the conjugate, and resulted in the reduced binding efficiency of GNP-ALP-Ab_1 toward the analyte.

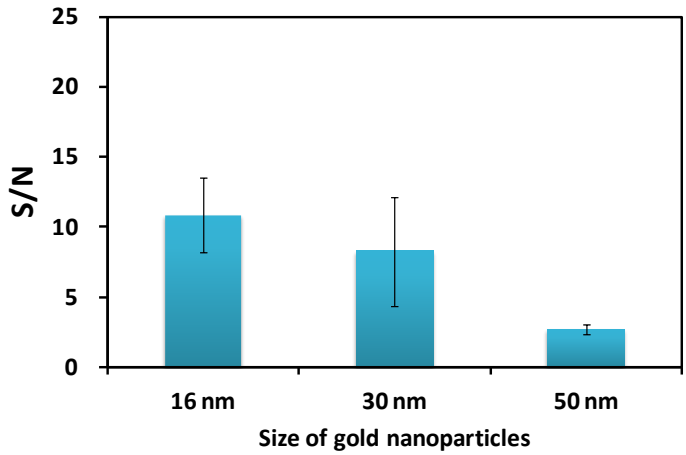

Figure 4.2. The effect of GNP diameters on the S/N of LFSB. (GNP-ALP-Ab_1 conjugate: 6 µL; test line: 2x dispensing cycles; running buffer: Tris-HCl (1%BSA); rabbit IgG concentration: 1 ng mL^{-1}.)

The enzymatic reaction time is another factor to influence the chemiluminescent response of LFSB. After adding Lumigen APS-5 substrate the chemiluminescence of enzymatic product could be recorded in just a few seconds, but dramatically declined after 5 mins. Figure 4.3A presents the chemiluminescent responses of 1 ng mL^{-1} rabbit IgG with different enzymatic reaction time. There was not significant change of chemiluninescent from 1 min to 3 min reaction time. Therefore, 1 min was chosen as the optimal enzymatic reaction time for the following procedure.

Another factor affecting the sensitivity and reproducibility of the LFSB is running buffer. The composition of running buffer has a significant effect on the performance of LFSB. Several buffers including PBS (1%BSA), PBST (1%BSA) and Tris-HCl (0.1M, 1%BSA) were tested, and the results are shown in Figure 4.3B. Comparing the S/N ratios, the best performance was obtained with the Tris-HCl (0.1M, 1%BSA) buffer. Therefore, a Tris-HCl (0.1M, 1%BSA) buffer was selected for the experiments.

The amount of capture Ab_1 on the test zone affects the response of LFSB. Figure 4.3C presents the effect of the Ab_1 amount on the signal intensity of LFSB. The amount of Ab_1 on the test zone was determined by the dispensing cycles of the Ab_1. The signal intensity was the highest for two dispensing cycles of Ab_1 on the test zone. The decreased S/N ratio with more dispensing cycles resulted from the higher background signal. Therefore, two-dispensing-cycle was used as the optimal condition in the following experiments.

The chemiluminescent intensity of the test line depends on the amount of the GNP-ALP-Ab_1 conjugate captured on the test zone, which relates to the amount of conjugate dispensed on the conjugate pad. The amount of GNP-ALP-Ab_1 conjugate was adjusted by dropping different volume of conjugate solution on conjugate pad. Figure 4.3D presents the histogram of the S/N

ratio of LFSB with an increasing amount of conjugate solution. It can be seen that the best S/N ratio was obtained with 6 µL of GNP-ALP-Ab_1 on the conjugate pad. The higher loading amount of GNP-ALP-Ab_1 conjugates caused an increasing signal from blank sample. From the above result, 6 µL of GNP-ALP-Ab_1 conjugate was employed.

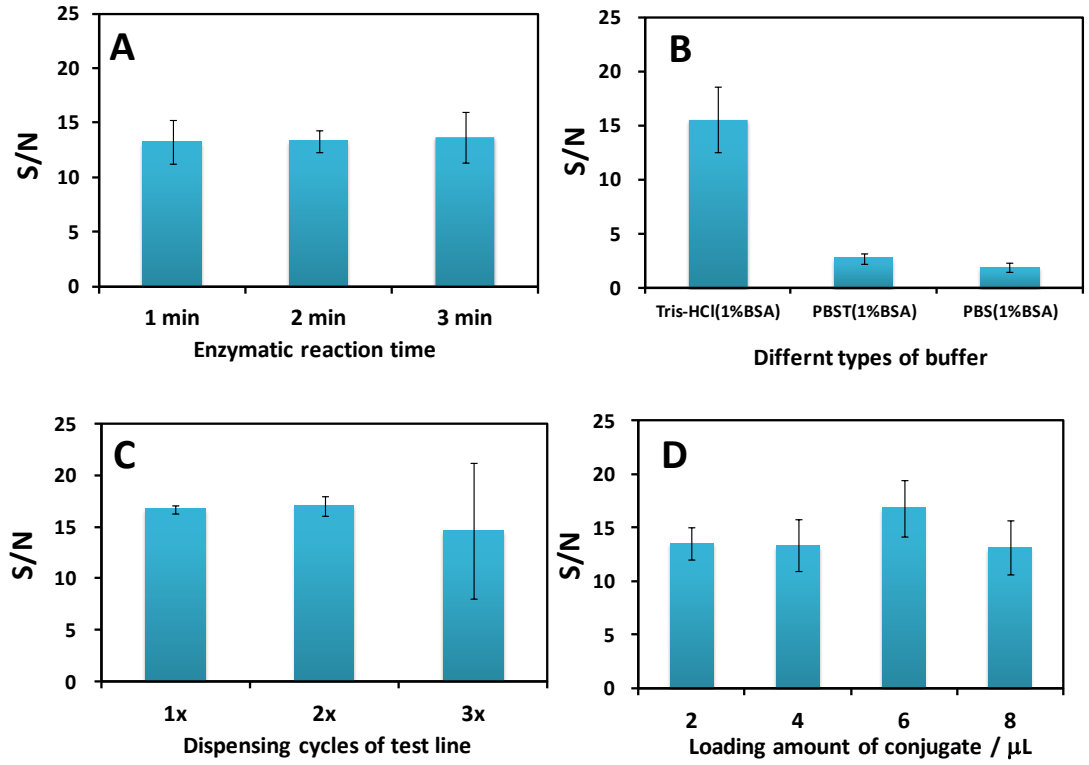

Figure 4.3. Optimization of experimental parameters. (A) Effect of enzymatic reaction time (with 2x dispensing cycle of test line, 6 µL of conjugate and Tris-HCl (1%BSA) as running buffer); (B) Effect of different types of running buffer (with 2x dispensing cycle of test line, 6 µL of conjugate and 1 min enzymatic reaction time); (C) Effect of dispensing cycles of capture antibody at test line (with 2x dispensing cycle of test line, Tris-HCl (1%BSA) as running buffer and 1 min enzymatic reaction time); and (D) Effect of loading amount of conjugates (with 2x dispensing cycle of test line, Tris-HCl (1%BSA) as running buffer and 1 min enzymatic reaction time) on chemiluminescence responses for 1 ng mL^{-1} of rabbit IgG.

4.3.3. Analytical performance of chemiluminescent lateral flow strip biosensor

Under optimal experimental conditions, we examined the performance of the chemiluminescent LFSB with different concentrations of rabbit IgG. The quantitative measurement was performed by recording chemiluminescent signals of test line. Figure 4.4 displays typical chemiluminescence responses in RLU with increasing concentrations of rabbit IgG. The resulting calibration curve of the signal intensity versus concentrations of rabbit IgG showed a good linear range over 0.05 ng mL^{-1} to 2 ng mL^{-1}. The detection limit is estimated as 0.02 ng mL^{-1} (S/N=3). This detection limit is 25-fold lower than that of the GNP label based LFSB (0.5 ng mL^{-1}),[89] and 500-fold lower than that of HRP based CL-LFI (10 ng mL^{-1}).[117]

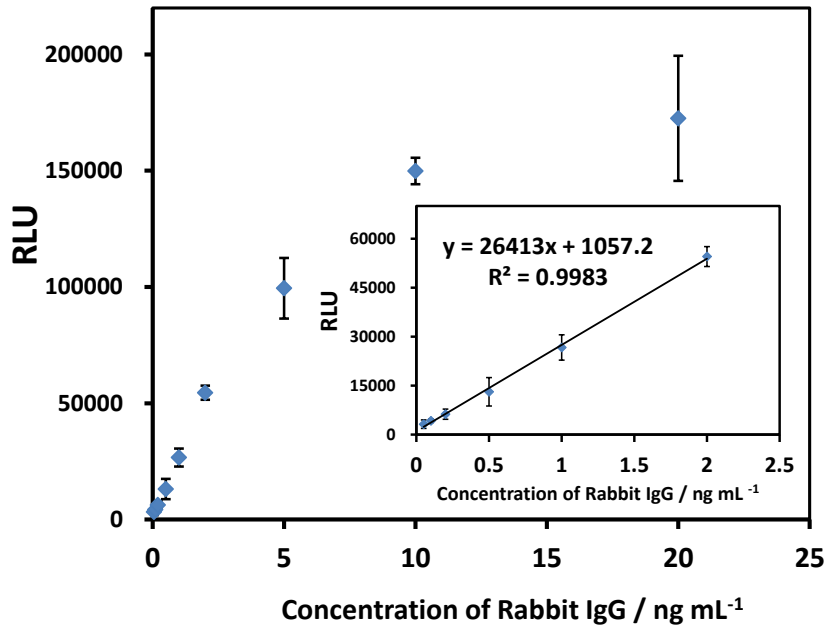

Figure 4.4. Calibration curve of chemiluminescent LFSB. (The inset shows the linear response for rabbit IgG. Each data point represents the average value obtained from three measurements.)

4.3.4. Selectivity and reproducibility.

Selectivity and reproducibility are two important parameters to evaluate the performance of a biosensor. The selectivity of the GNP-ALP-based LFSB was assessed by testing the responses of other proteins (thrombin, CEA, human IgG, and platelet derived growth factor-BB (PDGF-BB)) at 100 ng mL^{-1} level, as well as the mixtures of rabbit IgG (10 ng mL^{-1}) and those non-target protein (100 ng mL^{-1}). The histogram of the responses is shown in Figure 4.5. Excellent selectivity for rabbit IgG, over other proteins, was achieved. The sensitive and specific response was coupled with high reproducibility. The reproducibility of the GNP-ALP-based LFSB was studied by testing the sample solutions at different concentration levels (0, 1 and 10 ng mL^{-1} of rabbit IgG). Samples from the same batch preparation and at the same concentration level were tested 6 times with 6 different LFSBs and yielded RSD of 7.53%, 9.24% and 6.98%, respectively.

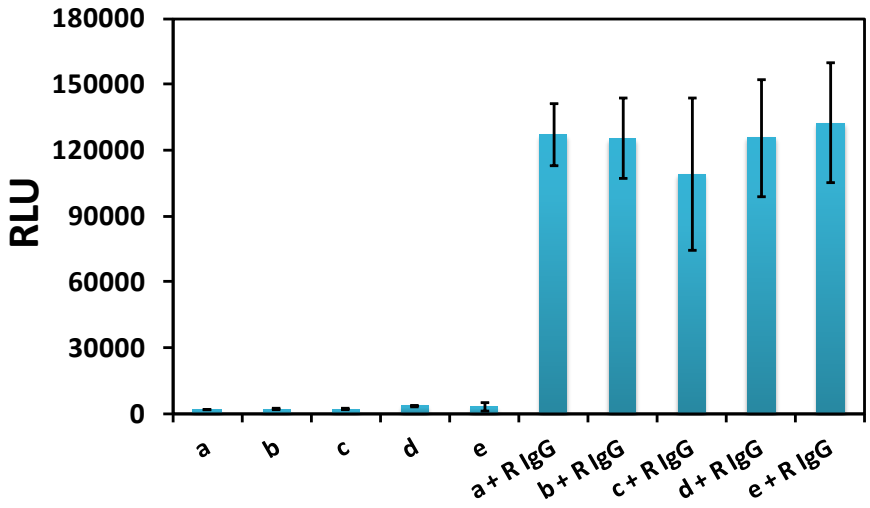

Figure 4.5. Selectivity of chemiluminescent LFSB. Histogram of LFSB responses of (a) Tris-HCl (1% BSA), (b) 100 ng mL^{-1} of CEA, (c) 100 ng mL^{-1} of Thrombin, (d) 100 ng mL^{-1} human IgG, and (e) 100 ng mL^{-1} PDGF-BBin the absence and presence of 10 ng mL^{-1} of rabbit IgG.

4.4. Conclusion

We have successfully developed a novel chemiluminescent LFSB based on GNPs and ALP dual labels for rapid, ultrasensitive and quantitative detection of proteins. The device took advantages of the loading capacity of GNPs and the high sensitivity of ALP-catalyzed CL analysis to achieve the signal amplification. Under optimal conditions, the LFSB was capable of detecting a minimum 0.02 ng mL^{-1} of rabbit IgG in 30 min. The proposed biosensor possessed high selectivity and good reproducibility. It shows great promise for use of the LFSB for point-of-care and in-field detection of proteins.

5. GOLD-NANOPARTICLE-DECORATED SILICA NANORODS BASED LATERAL FLOW STRIP BIOSENSOR FOR VISUAL DETECTION OF PROTEIN

5.1. Introduction

Sensitive detection of proteins is of tremendous interest for a broad range of applications, such as clinical diagnosis, food safety, and environmental analysis.[120-124] A variety of strategies and techniques has been developed to detect proteins, including enzyme-linked immunosorbent assay (ELISA), Western blot, agarose and polyacrylamide gel electrophoresis, and immunosensors in connection with various transducers.[125-133] The assay sensitivities were further enhanced by using nanomaterials (nanoparticles, nanowires, and nanotubes)[134-137] and novel signal-amplification approaches.[138-141] However, most nanomaterial-based signal-amplification methods generally involved a time-consuming detection process or advanced laboratory equipment. Lateral-flow immunoassay (LFI), also called immunochromatographic assay, has been studied extensively for different applications, such as pregnancy tests as well as detecting cancer biomarkers, infectious agents, and biowarfare agents.[142-143] In a typical LFI, the antibody-modified marco-nano-particles move along the strip with the analytes driven by capillary force and are eventually captured by the preimmobilized antibodies in the test zone. The captured marco-nano-particles, which are proportional to the target concentrations, can be determined by observing the color changes for the test band or by recording the fluorescence, electrical, or magnetic signals with appropriate transducers.[144-145] Gold nanoparticles (GNPs),[146-148] carbon nanoparticles,[149] quantum dots,[150-152] Fe_3O_4 nanoparticles,[153] etc. have been used as labels to develop LFIs. Although the fluorescent, magnetic, and electrical LFIs offered high sensitivity, the requirements for instrumentation and skilled personnel limit their point-of-care or in-field

applications. Among the aforementioned colored particles used for LFI, GNPs are the most applicable materials due to their unique optical properties (plasma absorption), remarkable chemical stability, and easy surface modification. The GNP-based LFIs have been applied for the qualitative and semiquantitative/quantitative detection of proteins,[154] metal ions,[155] and natural toxins.[156] Most reported LFIs for protein analysis were established with detection limit ranging from μg mL^{-1} (nanomolar) to ng mL^{-1} (picomolar).[23-24, 53-55] However, protein detection, such as cancer biomarker detection and early diagnosis of disease often require pg mL^{-1} (fetomolar) detection limit.[56-57, 157] Therefore, it is highly desirable to develop an ultrasensitive LFI for visually detecting proteins.

Recently, great efforts have been made to improve the sensitivity of the GNP-based LFIs by using a dual-labeling method. Choi et al. reported a dual-GNP conjugate-based lateral-flow assay method to analyze Troponin I.[158] The first GNP conjugate was prepared with an antibody against Troponin I. The second GNP conjugate was designed to bind with the first GNP conjugate and thus resulted in a larger size to improve the detection limit. The detection sensitivity increased about 100-fold compared to the conventional LFI. Mei et al. reported a sensitivity-enhanced LFI based on the same concept using different-sized GNPs for the visual detection of bisphenol A.[159] The LFI detection limit was 10 times lower compared to the traditional GNP-based assay. He et al. reported an ultrasensitive lateral flow strip biosensor (LFSB) based on horseradish peroxidase (HRP)-GNP dual labels.[160] Deposition of an insoluble, enzymatic catalytic product (red-colored chromogen) on the captured GNPs at the LFSB test zone offered a dramatic visual enhancement. Combining enzyme catalytic amplification with the unique optical properties of GNPs, the LFSB was capable of detecting 0.01 pM of target DNA without instrumentation. Tang et al. found that using magnetic GNP labels lowered the detection

limit 3-fold for aflatoxin B_2 compared to a conventional immunodipstick test using GNPs as colored reagents.[161]

Inspired by the signal amplification methods, the composite nanomaterial, formed by numerous GNPs evenly coated on a single substrate, would be an ideal colored reagent to enhance the LFSB sensitivity. Several materials, including carbon nanotubes and polymers,[162-165] were used as substrates to prepare the composite nanomaterials. However, most of the composite nanomaterials involved complicated or strict synthetic procedures. Silica-based nanomaterials (nanoparticles, nanowires, and nanorods) have attracted considerable interest in biomedical research because of their unique properties, such as inertness, high payload capacity, biocompatibility, and great surface-modification.[166] The silica-based nanomaterials have been utilized to develop highly sensitive biosensors and bioassays.[167-170] In this paper, we report an ultrasensitive protein assay using a gold-nanoparticle-decorated silica nanorod (GNP-SiNR) label and a LFSB. Silica nanorod was chosen as a matrix to make the GNP-SiNR hybrid. A large number of GNPs on a single SiNR provided a purple color that was much darker than the pure GNP solution. The nanohybrid, instead of GNP, was used as a colored reagent in LFSB. Rabbit IgG was used as a model target to demonstrate the proof-of-concept. A pair of antibodies capable of specifically recognizing rabbit IgG was used to prepare the LFSB (Figure 5.1). Capture antibody was immobilized on the test zone of the LFSB, and report antibody was conjugated with GNP-SiNR hybrid (Ab-GNP-SiNR). Rabbit IgG interacted with Ab-GNP-SiNR to form rabbit IgG-Ab-GNP-SiNR complex and continued to move along the strip. Accumulation of GNP-SiNR on the test zone produced a visible dark-purple band, which could be used for either qualitative or quantitative detection of rabbit IgG by a portable strip reader. Under the optimal

conditions, a detection limit of 0.01 ng mL^{-1} (10 pg mL^{-1}) was obtained. The promising properties of the GNP-SiNR-based LFSB are reported in the following sections.

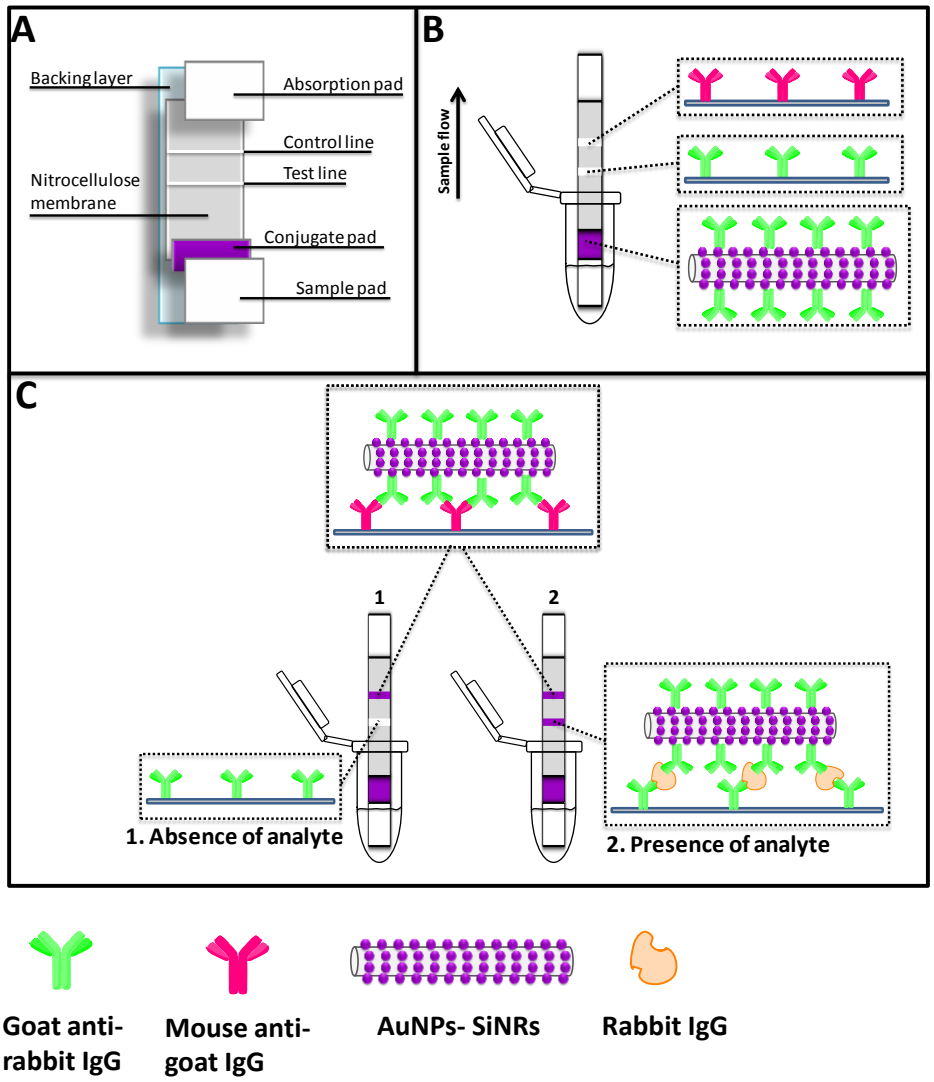

Figure 5.1. (A) Schematic representation for the configuration of the lateral flow strip biosensor, (B) reagents on the lateral flow strip biosensor, and (C) measurement principle of the lateral flow strip biosensor in the absence and presence of rabbit IgG.

5.2. Experimental section

5.2.1. Apparatus

A Hitachi SU8010 field scanning-electron microscope (SEM; Tokyo, Japan) was used to take images of the developed nanocomposites. The elemental analysis was obtained by performing energy-dispersive X-ray spectroscopic (EDS) measurements (Oxford X-Max; Concord, MA, USA), and the spectrometer was attached to a Hitachi SU8010 field-emission SEM. A Shimadzu UV-vis spectrometer (Columbia, MD, USA) was used to obtain the absorption spectra of the nanomaterials. An Airjet AJQ 3000 dispenser, Biojet BJQ 3000 dispenser, Clamshell Laminator, and the Guillotine cutting-module CM 4000 purchased from Biodot LTD (Irvine, CA, USA) were used to prepare lateral-flow strips. A portable strip reader DT1030 (Shanghai Goldbio Tech. Co.; Shanghai, China) was used for signal recording.

5.2.2. Reagents and materials

Tetraethylorthosilicate (TEOS, 98%) was purchased from Acros Organics (NJ, USA). Sodium citrate (Na_3Ct), gold (III) chloride trihydrate ($HAuCl_4 \cdot 3H_2O$, 99.9+%), hydroxylamine hydrochloride (98%, ACS grade), sodium borohydride ($NaBH_4$, >98%), $Na_3PO_4 \bullet 12H_2O$, sucrose, Tween 20, Triton X-100, phosphate buffer saline (PBS, pH 7.4, 0.01 M), phosphate buffer saline with 0.05% Tween 20 (PBST), and bovine serum albumin (BSA) were purchased from Sigma-Aldrich, Inc. (St. Louis, MO, USA). Ammonium hydroxide (NH_4OH, 28.0%-30.0%), potassium carbonate ($K_2CO_3 \cdot 1.5\ H_2O$, ACS grade), and ethanol (95%) were obtained from Fisher Scientific Co. (Pittsburgh, PA, USA). Polyvinylpyrrolidone molecule (PVP; average molecular weight M_n = 40,000) and 1-pentanol (99+%, ACS grade) were purchased from Alfa Aesar (Ward Hill, MA, USA). Rabbit IgG, goat anti-rabbit IgG (Ab_1), and mouse anti-goat IgG (Ab_2) were obtained

from Thermo Scientific (Rockford, IL, USA). Glass fibers (GFCP000800), cellulose-fiber sample pads (CFSP001700), laminated cards (HF000MC100), and nitrocellulose membranes (HFB18004) were provided by Millipore (Billerica, MA, USA). All chemicals were analytical reagent grade unless specified. All buffer solutions were prepared using ultrapure water (>18 MΩ cm) from a Millipore Milli-Q water purification system.

5.2.3. Preparation of Silica Nanorods (SiNRs)

A one-step synthetic method was used to prepare SiNRs. In a typical synthetic procedure, a total of 3.00 g of PVP was added to 30.00 mL of 1-pentanol. The mixture was sonicated for 30 min to obtain a well-mixed PVP/pentanol solution. Then, 3.00 mL of 95% ethanol, 0.84 mL of H_2O, and 0.20 mL of 0.17 M Na_3Ct were added to the PVP/pentanol mixture, followed by hand-shaking for a few seconds. After the addition of 0.30 mL of TEOS and 0.50 mL of NH_4OH, the reaction was allowed to proceed overnight at room temperature. The SiNRs were collected by centrifuging at 11,000 rpm for 30 min and removing the supernatant. The collected SiNRs were washed 3 times with ethanol and dried in the oven at 100 °C.

5.2.4. Preparation of gold seeds

Typically, 4.00 mL of 1% $HAuCl_4$ solution was added to 100.00 mL of H_2O in an ice bath, followed by the addition of 0.50 mL of 0.20 M K_2CO_3 to reduce Au(III) to Au(I). The solution is then stirred for 10 min until its color changes from yellow to light yellow or colorless. Then, 1.00 mL of freshly prepared $NaBH_4$ (0.50 mg mL^{-1}) was slowly added. The formation of a reddish solution indicated the successful synthesis of gold seeds.

5.2.5. Preparation of Gold-Nanoparticle-decorated Silica Nanorods (GNP-SiNRs)

The GNP-SiNRs were prepared according to the reported methods with slight modifications.[171] An aliquot with 1.00 mL of 10.00 mg mL^{-1} SiNR solution was added to a 40.00 mL gold-seed solution, and the mixture was stirred vigorously for 20 min. Surplus gold seeds were removed by centrifugation at a speed of 6,500 rpm for 15 min. The obtained reddish precipitate was gold-seed-decorated SiNRs and was redispersed in 10.00 mL of water for the gold-shell growth process. In the gold-shell growth process, 4.00 mL of 1% $HAuCl_4$ solution and 0.025 g of K_2CO_3 were added to 90.00 mL of water. The mixture was stirred until it turned to light yellow or colorless. Then, 10.00 mL of a gold-seed-decorated SiNR solution, 1.00 mL of 0.5 M hydroxylamine hydrochloride, and 1.00 g of PVP were sequentially added to the growth solution. After overnight reaction, the solution was centrifuged at a speed of 6,500 rpm for 15 min and was washed 3 times with water. Finally the obtained GNP-SiNRs were suspended into 10 mL of water and stored at 4 Celsius for use in the future. The size of the GNPs that decorated the SiNR's surface can be adjusted by adding different amounts of 1% $HAuCl_4$ (0, 2, 4, or 6 mL).

5.2.6. Preparation of GNP-SiNR-Ab_1 and GNP-Ab_1 conjugates

GNP-SiNR-Ab_1 and GNP-Ab_1 conjugates were prepared according to the reported methods with slight modifications.[172] Initially, 0.01 mg of Ab_1 was mixed with 1.00 mL of GNP-SiNRs (pH 9.0), followed by gentle shaking for 1 h at room temperature. Then, 0.10 mL of 10.0 wt% BSA was added, and the mixture was incubated for 30 min. The mixture was further washed with PBS (1% BSA) and centrifuged at 6,000 rpm for 5 min to remove the washing liquid. Finally, the as-prepared GNP-SiNR-Ab_1 conjugates were collected and suspended in 1.00

mL of eluent buffer containing 20.00 mM Na_3PO_4•$12H_2O$, 0.25% Tween 20, 10% sucrose, and 5% BSA.

To prepare GNP-Ab_1 conjugate, 0.01 mg of Ab_1 was added to 1.0 mL of fivefold-concentrated GNPs (pH 9.0). The mixture was gently incubated for 1 h and blocked by 0.1 mL of 10 wt% BSA for 30 min. The obtained solution was centrifuged at 12,000 rpm for 18 min, and the nanoparticles were washed with PBS (1% BSA) 3 times. The resulting ruby sediments were dispensed in 1.0 mL of buffer containing 20 mM Na_3PO_4•$12H_2O$, 0.25% Tween 20, 10% sucrose, and 5% BSA.

5.2.7. Analytical procedure

Lateral flow strip biosensors (LFSBs) were prepared according to the reported procedure with minor modifications.[49] The LFSB consisted of the following components: a sample-application pad, a conjugate pad, a nitrocellulose membrane, and an absorption pad. Both the sample-application pad and the absorption pad were made from cellulose fiber. The sample-application pad (17 mm × 30 cm) was soaked in a buffer (pH 8.0) containing 0.25% Triton X-100, 0.05 M Tris-HCl, and 0.15 mM NaCl. Then, the sample pad was dried at 37 ^oC in the oven and stored in desiccators at room temperature. Ab_1, with a concentration of 1.20 mg mL^{-1}, and Ab_2 (0.85 mg mL^{-1}) were dispensed at different locations of the nitrocellulose membrane (25 mm × 30 mm) to form the test line and the control line by using a Biojet BJQ 3000 dispenser. The nitrocellulose membrane was then dried in the oven at 37 ^oC for 1 h. Finally, all the parts were assembled on a plastic, adhesive backing layer (typically an inert plastic, e.g., polyester) using the Clamshell Laminator. Each part overlapped 2 mm to ensure that the solution migrated through the biosensor during the assay. The LFSB with a 3-mm width was cut with the Guillotin

cutting-module CM 4000. The GNP-SiNR-Ab_1 or GNP-Ab_1 conjugates were dropped on the conjugate pad using a pipet before each test.

The assay was performed by dipping the LFSB in a 1.50 mL microcentrifuge tube containing the desired concentration of rabbit IgG in 0.10 mL of running buffer (PBST with 1% BSA). The test and control zones could be evaluated visually within 20 min. The intensities of the test line and the control line were measured using a strip reader, and the results were further analyzed using the GoldBio strip-reader software.

5.3. Results and discussions

5.3.1. GNP-decorated SiNRs as colored reagents in the lateral flow strip biosensor

Silica-based nanomaterials (nanoparticles, nanorods, and nanowires) have shown great promise in various fields due to the nanomaterials' unique physical and chemical stability as well as their well-established surface modification.[173-174] In the current study, silica nanowires (SiNWs) and nanorods were used as substrates to coat GNPs due to the larger surface area per rod or wire compared to that per nanoparticle. The synthesized GNP-SiNWs and GNP-SiNRs were used as labels for the lateral-flow assays. The mobility of GNP-SiNWs was much slower than that of GNP-SiNRs on the nitrocellulose membrane due to the large size of the SiNWs. (The length of SiNWs is up to tens of micrometers; results not shown) Therefore, we chose GNP-SiNRs, which have a dark purple color and better mobility, as the colored reagents.

5.3.2. Preparation and characteristics of GNP-decorated SiNRs (GNP-SiNRs)

A two-step deposition process involving gold-seed deposition and seed growth was used to prepare the GNP-SiNRs. SiNRs with a length varying from 3.4 to 7.0 μm (Figure 5.2A) were

used as the substrate to load numerous GNPs. Gold seeds were deposited on the SiNR surface by simply mixing GNP and SiNR solutions for 20 min. Figure 5.2B presents the typical SEM image of the gold-seed-loaded SiNRs. One can see that the gold seeds with a diameter of 9.7 ± 1.6 nm are monodispersed on the SiNR surface. The gold-seed-decorated SiNRs were then added to a gold growth solution to form a uniform GNP layer. Figure 5.2C shows the SEM image of GNP-decorated SiNRs after the GNP growth process. A layer of GNPs was coated on the SiNR surface, and the density of GNPs was much higher than the gold-seed-decorated SiNRs. To further identify the formation of the GNP layer on the SiNR surface, element analysis was performed by the EDS technique. A strong peak for the gold signal was observed in the EDS spectra of GNP-SiNRs, indicating that GNPs were successfully loaded on the SiNRs (Figure 5.2D). Figure 5.2E presents the UV-vis absorption spectra of the GNP-SiNR suspension, gold-seed solution, and SiNR suspension. No UV-vis absorption (Figure 5.2E, a) was observed for the SiNR solution while a typical surface plasmon resonance (SPR) absorption peak around 514 nm of gold-seed solution was observed (Figure 5.2E, b). However, GNP-SiNRs showed a red-shifted SPR band in the near-infrared region compared to that of the gold seeds (Figure 5.2E, c).

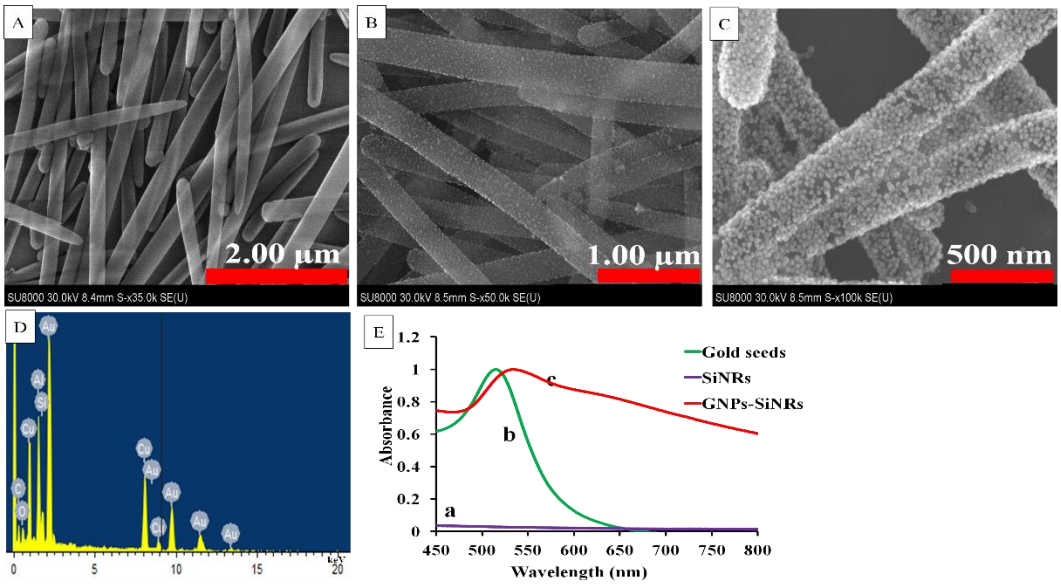

Figure 5.2. SEM images of (A) SiNRs, (B) gold-seed-decorated SiNRs, and (C) the formation of the GNP layer on the SiNR surface, (D) a representative EDS spectra of GNP-SiNRs, and (E) UV-vis spectra of SiNRs (a), gold seeds (b), and GNP-SiNRs (c).

We studied the effect of the $HAuCl_4$ concentration in the seed growth solution on the GNP size and coverage on the SiNR surface (Figure 5.3). Without the addition of a gold precursor ($HAuCl_4$) in the growth solution, the GNP size (9.7 ± 1.6 nm) did not change, and GNPs were evenly positioned on the SiNR surface (Figure 5.3A). By adding 2 mL of 1% $HAuCl_4$, gold seeds grew to bigger GNPs with a size of 16.7 ± 2.4 nm (Figure 3B). In the case of 4 and 6 mL of 1% $HAuCl_4$ addition to the growth solution, the SiNR surface was covered with a layer of GNPs (Figure 5.3C-D). However, a large number of free GNPs was synthesized when 6 mL of 1% $HAuCl_4$ solution was added. Therefore, in the following lateral-flow immunoassay application, GNP-SiNR synthesized from the addition of 4 mL of 1% $HAuCl_4$ in the growth solution was used as the colored reagent. On the basis of surface area of a SiNR (diameter: 200 nm; length: 3.4 mm) and cross section area of a GNP (diameter: 16.7 nm), it was estimated that there were 10000 GNPs coated on a single silica nanorod.

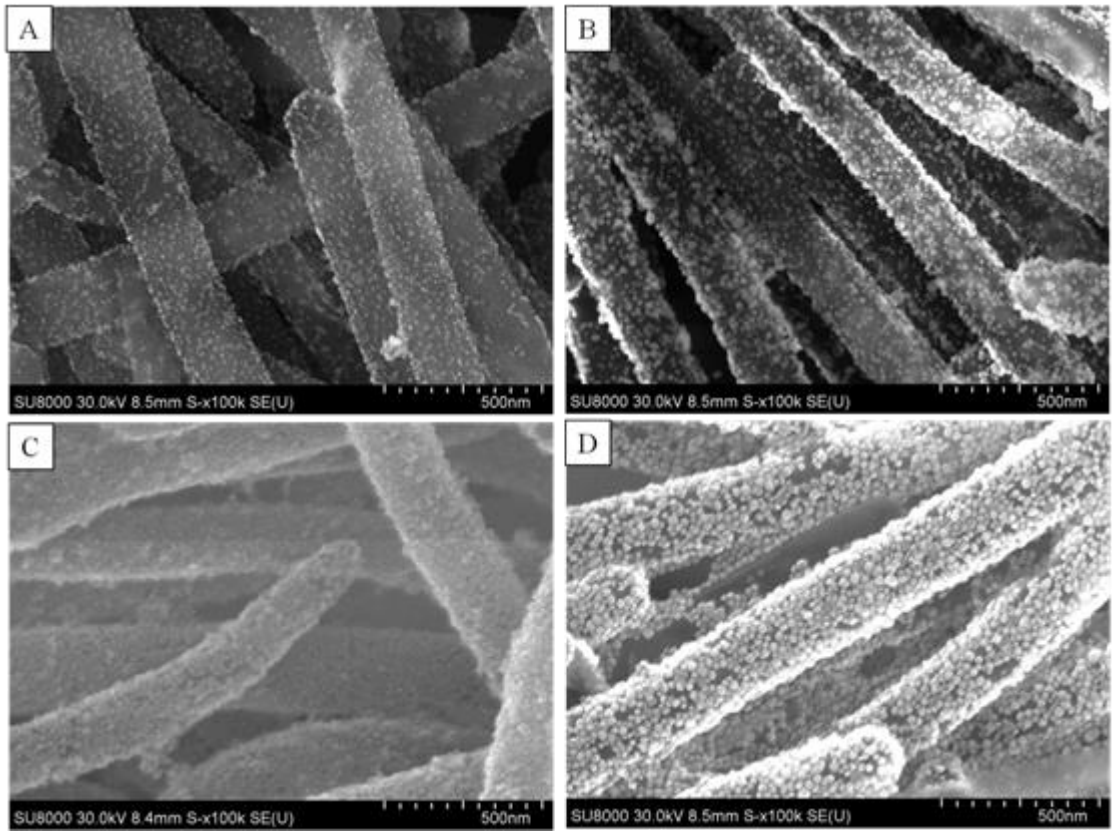

Figure 5.3. SEM images of GNP-SiNRs by adding (A) 0, (B) 2, (C) 4, and (D) 6 mL of 1% $HAuCl_4$ in the gold growth solution.

5.3.3. GNP-SiNR label based lateral flow strip biosensor

The GNP-SiNRs were, thus, used as labels to fabricate the LFSB. Rabbit IgG was used as model target to demonstrate the proof-of-concept. Figure 5.1 schematically illustrates the LFSB's configuration and measuring principle. The LFSB consisted of a sample pad, a conjugate pad, an absorption pad, and a nitrocellulose membrane (test line and control line; Figure 5.1A). All the components were assembled on a common-adhesive backing layer. Goat anti-rabbit IgG Ab_1 was conjugated with GNP-SiNRs, and the Ab_1-GNP-SiNR conjugates were dispensed on the conjugate pad. Goat anti-rabbit IgG Ab_1 was also used as the capture antibody and was dispensed on the test zone of the nitrocellulose membrane. Mouse anti-goat IgG Ab_2 was used as the

secondary antibody and was immobilized on the control zone of the nitrocellulose membrane, which was 2 mm behind the test zone (Figure 5.1B). During the assay, the LFSB was dipped into a test tube, and the sample solution moved up by capillary force. The Ab_1-GNP-SiNRs conjugates were rehydrated and released from the conjugate pad. The binding between Ab_1 in Ab_1-GNP-SiNR conjugates and rabbit IgG (target) occurred, and the formed complexes (IgG-Ab_1-GNPs-SiNRs) continued to migrate along the membrane. When reaching the test zone, the complexes were captured by the antibody on the test zone via the second immunoreaction, resulting in the accumulation of GNP-SiNRs on the test zone. A dark-purple band was observed, and the color intensity of the test band was directly proportional to the amount of analyte (IgG) in the sample solution. The solution continued to flow until it passed through the control zone where the excess Ab_1-GNP-SiNRs conjugates were captured by the secondary antibody (anti-goat IgG Ab_2) to produce a second dark-purple band (Figure 5.1C, right). In the absence of the target, only the band on the control zone was observed, and no band was observed in the test zone. In this case, the band in the control zone (control line) showed that the LFSB was working properly (Figure 5.1C, left). Quantitative analysis was achieved by reading the test-line intensities with a portable strip reader. The more analytes are present in the sample, the more conjugates would be captured on the test zone, leading to the increased signal.

To confirm the signal amplification of the GNP-SiNRs, the responses of the sample solutions at three concentration levels (0, 1.0, and 5.0 ng mL^{-1} IgG) on the GNP-SiNR-based LFSB were compared with the GNP-based LFSB. Figure 5.4 presents the photo images of the LFSBs after the assays were completed. When rabbit IgG was absent in the sample solutions, neither of the two LFSBs showed a response on the test zones (Figure 5.4A). No test line could be observed from the GNP-based LFSB in the presence of 1.0 ng mL^{-1} of rabbit IgG (Figure

5.4B, left) while there was a visible test line on the GNP-SiNR-based LFSB (Figure 5.4B, right). As shown in Figure 5.4C, the intensity of the test line on the GNP-SiNR-based LFSB in the presence of 5.0 ng mL^{-1} rabbit IgG was significantly higher than that of the GNP-based LFSB which exhibited a very weak response. Such dramatic signal enhancement on the GNP-SiNR-based LFSB is mostly due to the large surface area of the SiNRs where numerous GNPs were loaded. The number of the captured GNPs per antibody-antigen binding on the GNP-SiNR-based LFSB would be much higher than that of the GNP-based LFSB. In addition, the antibody density on the Ab_1-GNP-SiNR conjugates would be higher than that of the Ab_1-GNP conjugates. The immunoreaction efficiency on the GNP-SiNR-based LFSB was, thus, higher than that for the GNP-based LFSB with a short assay time.

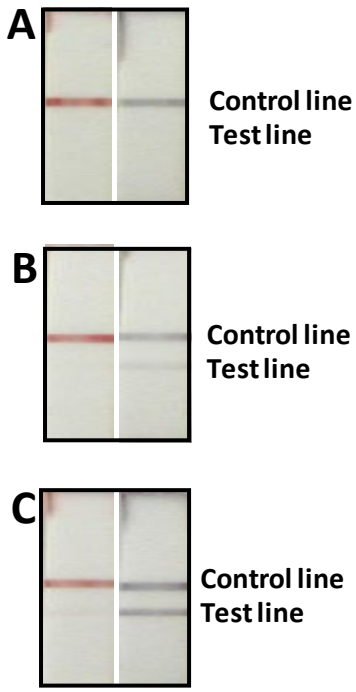

Figure 5.4. Photo images of the GNP-based LFSBs (left) and the GNP-SiNR-based LFSBs (right) in the presence of different concentrations of rabbit IgG. (A) 0 ng mL^{-1}, (B) 1.0 ng mL^{-1}, and (C) 5.0 ng mL^{-1}.

5.3.4. Optimization of experimental parameters

The amount of capture Ab_1 on the LFSB test zone affects the LFSB response. Figure 5.5A presents the effect for the capture Ab_1 amount on the signal-to-noise (S/N) ratio of the LFSB. The amount of Ab_1 on the test zone was determined by the dispensing cycles of the Ab_1. The S/N ratio was the highest for one dispensing cycle of 1.2 mg mL^{-1} (8×10^{-6} mol L^{-1}) Ab_1 on the test zone. The decreased S/N with more dispensing cycles resulted from the higher background signal. Therefore, one dispensing cycle (around 0.3 μL of solution) was used as the optimal condition in the following experiments.

The amount of Ab_1 on the GNP-SiNRs surface affects the LFSB's immunoreaction efficiency and sensitivity. We optimized the Ab_1 concentration in the conjugation solution. The LFSB's S/N ratio increased up to 10 μg mL^{-1} (~6.7×10^{-8} mol L^{-1}) Ab_1 in the conjugation solution; a further concentration increase caused a decreased S/N ratio (Figure 5.5B). The decrease of S/N ratio was due to the decreased immunoreaction efficiency when a higher amount of antibody was conjugated on the SiNRs. On the basis of the optimal concentration of Ab_1 antibodies for preparing the conjugate, there were approximately 11000 antibodies absorbed on a single silica nanorod. Concentrations exceeding the optimal condition may cause the steric hindrance of the antibodies absorbed on the surface and consequently result in the decreased antibody-antigen binding efficiency. Since the antibodies are polyclonal antibodies which could recognize multiple epitopes on one antigen, the molar ratio of antibody: antigen is at least 1:1. As a result, 10 μg mL^{-1} of Ab_1 antibodies were employed to prepare the Ab_1-GNP-SiNR conjugates in the following experiments.

The running buffer's composition is one of the main factors in developing a biosensor because it has a significant impact on the efficiency of antibody-antigen binding and the

elimination of nonspecific adsorption. Several buffers, including PBS (1% BSA), PBST (1% BSA), and Tris-HCl (1% BSA), were tested, and the results are shown in Figure 5.5C. The highest S/N ratio was obtained with the PBST (1% BSA) buffer. Therefore, a PBST (1% BSA) buffer was selected for the experiments.

The band intensities depended on the Ab_1-GNP-SiNR conjugates captured on the test and control zones which, in turn, corresponded to the amount of conjugates on the conjugate pad. To obtain a maximum response using a minimal amount of Ab_1-GNP-SiNR conjugates, the Ab_1-GNP-SiNRs on the conjugate pad were optimized by increasing the volume of the Ab_1-GNP-SiNR conjugates loaded on the conjugate pad. Figure 5.5D displays the histogram for the LFSB's S/N ratio with an increasing volume of conjugate solution (0.8 to 8 μL). It can be seen that the S/N ratio increased up to 4 μL; a further volume increase caused a decreased S/N ratio. The S/N ratio loss at a high volume may be attributed to the saturation of signal intensity and an increased nonspecific adsorption. Therefore, 4 μL of Ab_1-GNP-SiNR conjugate was employed as the optimal volume for the entire study.

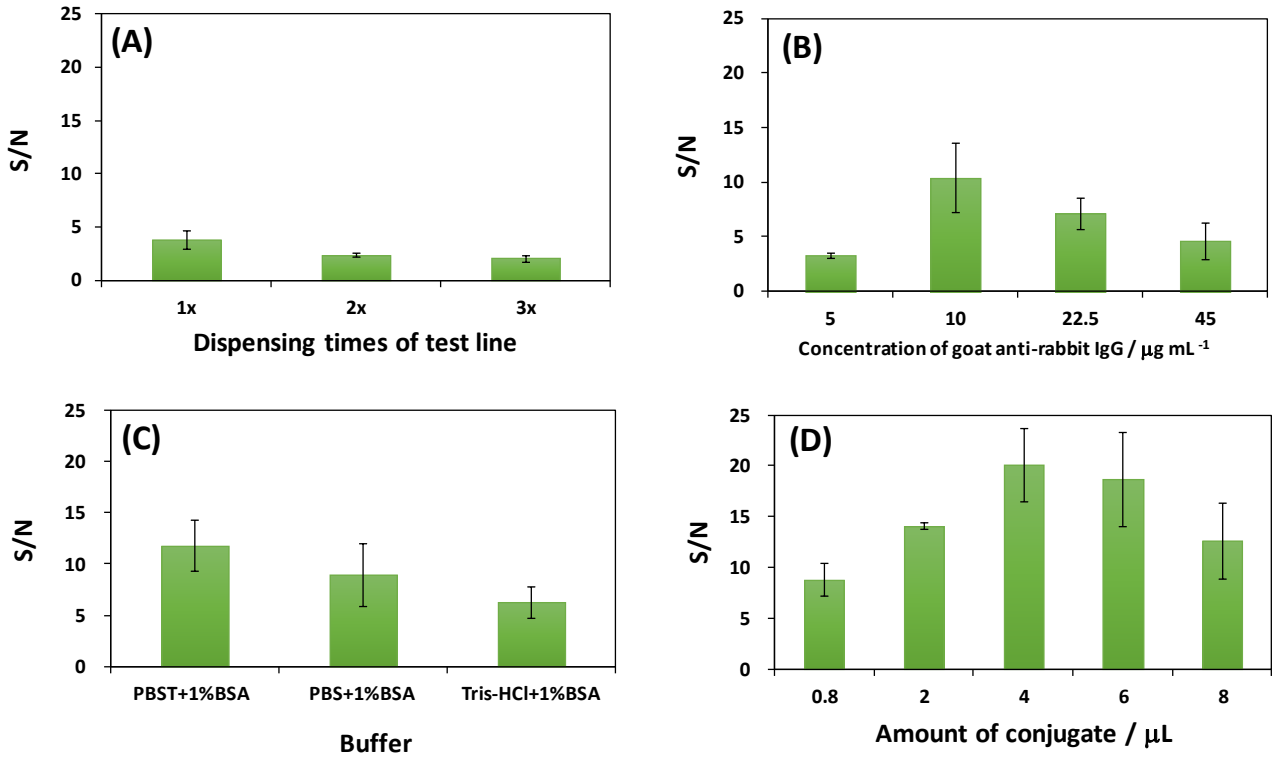

Figure 5.5. Optimization of experimental parameters. (A) Effect of dispensing cycles of Ab_1 on the LFSB's S/N ratio. Loading volume of Ab_1-GNP-SiNR conjugates: 2 µL, Ab_1 concentration in the conjugate: 5 µg mL^{-1}, running buffer: PBST (1% BSA). (B) Effect of Ab_1 concentration in the conjugate solution on the LFSB's S/N ratio. Dispensing cycle of Ab_1: 1 cycle, loading volume of Ab_1-GNP-SiNR conjugates: 2 µL, running buffer: PBST (1% BSA). (C) Effect of running buffer components on the LFSB's S/N ratio. Dispensing cycle of Ab_1: 1 cycle, loading volume of Ab_1-GNP-SiNR conjugates: 2 µL, Ab_1 concentration in the conjugate: 10 µg mL^{-1}. (D) Effect for the loading volume of Ab_1-GNP-SiNR conjugates on the LFSB's S/N ratio. Dispensing cycle of Ab_1: 1 cycle, Ab_1 concentration in the conjugate: 10 µg mL^{-1}, running buffer: PBST (1% BSA). Concentration of rabbit IgG: 1.0 ng mL^{-1}.

5.3.5. Analytical performance

Under optimal experimental conditions, we examined the performance of the GNP-SiNR-based LFSB with different concentrations of rabbit IgG. Figure 5.6 presents the typical photo images (right) and the corresponding optical response recorded with a portable strip reader in the presence of different concentrations of rabbit IgG (0 to 2.0 ng mL^{-1}). There was no test line observed on the LFSB test zone in the absence of rabbit IgG (control), indicating negligible

nonspecific adsorption under the optimized experimental condition. The test line was quite visible, even at 0.05 ng mL^{-1} rabbit IgG which can be used as the threshold for the visual determination (yes/no) of rabbit IgG without instrumentation.

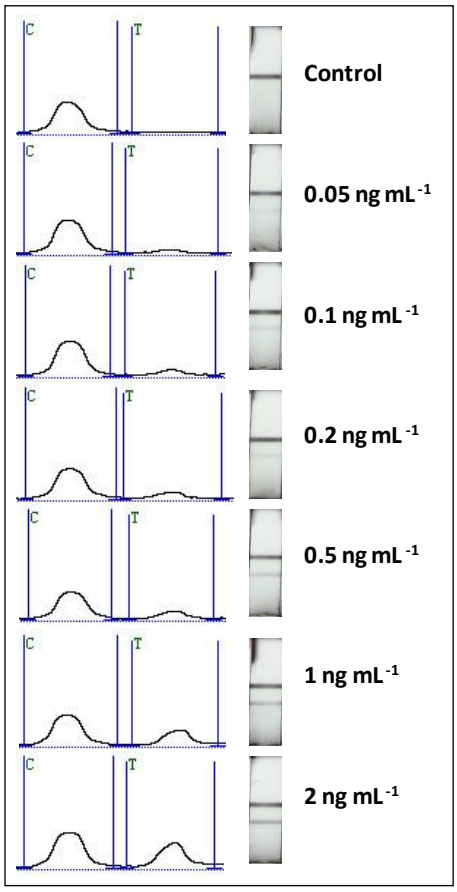

Figure 5.6. Typical response curves and photo images for the LFSB with an increasing rabbit IgG concentration (0.05 to 2.0 ng mL^{-1}).

In addition, quantitative detection was performed by recording the peak areas of the test bands with the aid of a portable strip reader (Figure 5.7). It was observed that the peak area increased with an increase in the rabbit IgG concentration until reaching a plateau at 100 ng mL^{-1}. The saturation of the calibration curve was caused by the physical size of the surface area of the test line limiting the number of GNP-SiNR that could bind. On the basis of response of 100 ng mL^{-1} (~6.7×10^{-10} mol L^{-1}) of rabbit IgG, the molar ratio of capture antibody (test line)/rabbit

IgG (target):/report antibody (GNP-SiNR-Ab) was estimated to be 10:1:4. The peak area had a linear correlation with the rabbit IgG concentration in the lower concentration range (0.05 – 2.0 ng mL^{-1}) as shown in the inset of Figure 5.7. The calibration equation was determined to be peak value A = 188.76 C + 61.908 with a correlation coefficient of 0.9941, where A and C represent the peak area and the concentration of rabbit IgG, respectively. The detection limit was estimated to be 0.01 ng mL^{-1} (~6.7×10^{-14} mol L^{-1}) from 3 times the standard deviation corresponding to the blank sample detection (S/N = 3). Compared to other labels for visual detection, the detection limit of GNP-SiNR-based LFSB is comparable with that of the fluorescent microspheres[27], almost 50-fold lower than GNP-based LFSB,[89] 1000-fold lower than the blue-colored latex particle-based LFSB,[175] and five orders of magnitude improved than a competitive liposome-based LFSB.[176]

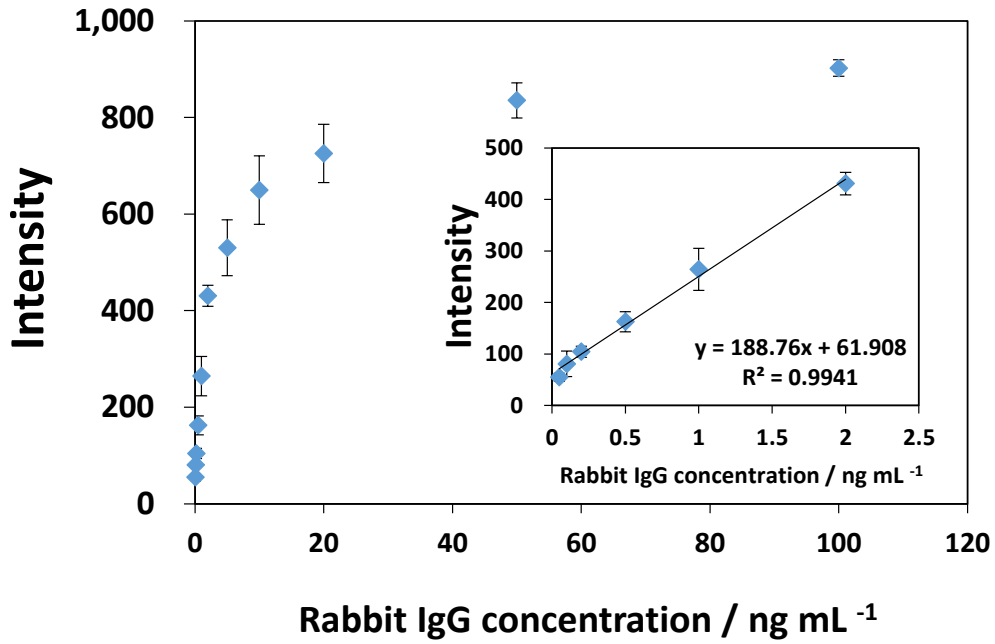

Figure 5.7. Calibration curve of the LFSB. (The inset shows the linear response for rabbit IgG. Each data point represents the average value obtained from three different measurements.)

5.3.6. Selectivity and reproducibility

Selectivity and reproducibility are two important parameters to evaluate a biosensor's performance. The selectivity of the GNP-SiNR-based LFSB was assessed by testing the responses of other proteins (thrombin, CEA, human IgG, and PDGF-BB) at 100 ng mL^{-1}, as well as the mixtures of rabbit IgG (1 ng mL^{-1}) and the nontarget protein (100 ng mL^{-1}). The histogram of the responses and the corresponding photo images are shown in Figure 5.8. Excellent selectivity for rabbit IgG, over other proteins, was achieved. The sensitive and specific response was coupled with high reproducibility.

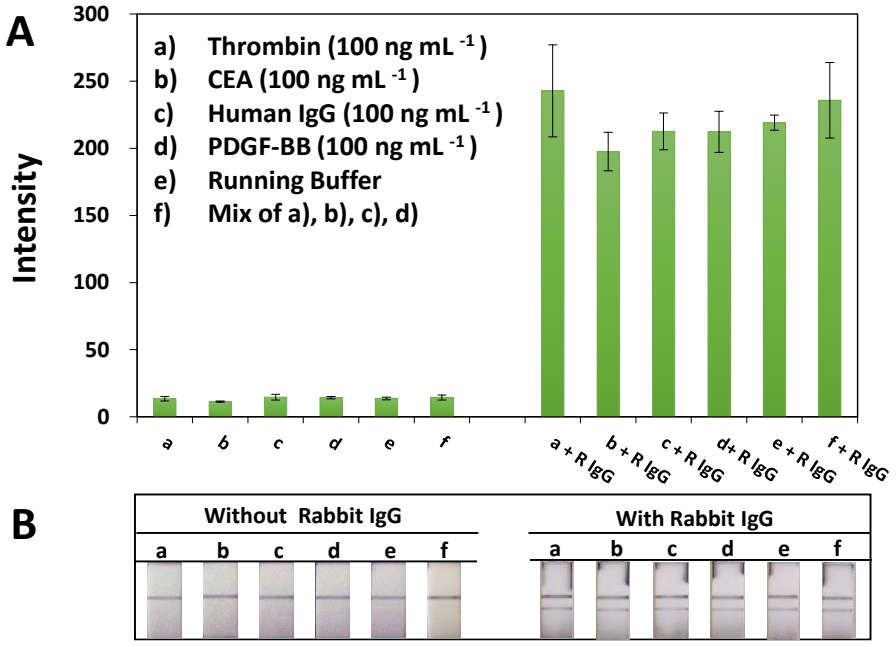

Figure 5.8. (A) Histogram of the LFSB responses and (B) the corresponding photo images. (Rabbit IgG concentration: 1 ng mL^{-1}.)

The reproducibility of the GNP-SiNR-based LFSB was studied by testing the sample solutions at different concentration levels (0, 0.5, 5, and 50 ng mL^{-1} of rabbit IgG). Samples from the same batch preparation and at the same concentration level were tested 6 times with 6 different LFSBs. Similar responses were obtained at the same concentration level (see the

histogram of the responses in Figure 5.9). The relative standard deviations for the signals were 1.80%, 6.63%, 3.93%, and 5.49% for 50, 5, 0.5, and 0 ng mL^{-1} of rabbit IgG, respectively, indicating an excellent reproducibility.

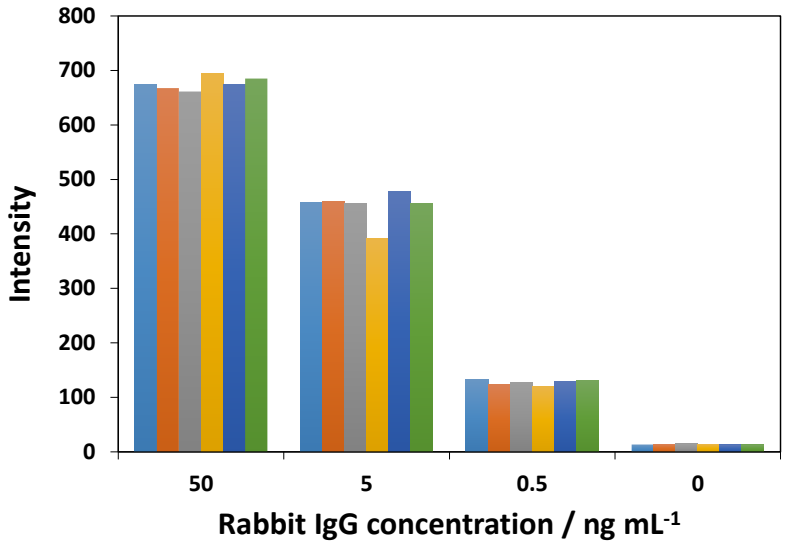

Figure 5.9. Reproducibility study in the presence of 50, 5, 0.5, and 0 ng mL^{-1} of rabbit IgG. (Tests were performed 6 times for each sample solution.)

5.4. Conclusion

We have developed a highly sensitive lateral-flow strip biosensor (LFSB) using GNP-SiNRs as labels. The LFSB detection limit was lowered 50 times compared to the traditional GNP-based lateral-flow assay. As demonstrated here, the significance of this work is to introduce a new type of nanolabel for signal enhancement on the lateral-flow immunoassay. In addition, the GNP-SiNRs can be used as nanolabels for nucleic acid and other biological molecular detection with high sensitivity. Future work will aim to detect cancer biomarkers (proteins and nucleic acids) in human blood or serum.

6. SUMMARY AND FUTURE PROSPECTS

The research work described in the dissertation demonstrated the improved sensitivity of LFSB based on using various labels and different measurement strategies. The amplified response signals were obtained from LFSB combing with novel nanomaterials, enzymes and advanced optical detection methods. Those ultrasensitive biosensors broadened the application field of LFSB for detection of proteins at trace level which could not be analyzed using conventional LFSB method. The improved LFSBs showed promising applications in early diagnosis of protein-related cancer, detection of infectious disease and maintaining cardiac health.

The signal amplifications were investigated by four strategies:

1. A dual-label based LFSB using both GNP and HRP was described for simple and low-cost protein assay. Rabbit IgG was used as a model system for the demonstration of the proof-of-concept. Combining the enzyme catalytic amplification of HRP and the unique optical property of GNP, the dual-label based biosensor could distinguish 0.02 ng mL^{-1} of rabbit IgG from the blank with the help of a portable strip reader. The detection limit was 25 times lower than that of the GNP-based LFSB.
2. An enzyme-based fluorescent LFSB has been developed for sensitive detection of protein. ALP was used as a label to conjugate with antibody. A sandwich immunoreaction was performed on a lateral flow strip resulting in the ALP accumulated at the test zone of the strip. The fluorescence signal was then obtained by adding the ALP substrate to generate fluorescent product located at the test zone. This enzyme-based fluorescent LFSB showed a good linear relationship over the range from 0.1 to 5 ng mL^{-1} of rabbit IgG with a detection limit of 0.1 ng mL^{-1} (S/N=3).

3. An improved chemiluminescent LFSB has been developed for sensitive analysis by taking advantages of ALP as a signal-trigger enzyme and GNP as enzymes' carrier. The detection signal was obtained by adding Lumigen APS-5 (ALP substrate) to generate sustained high-intensity chemiluminescence responses. The use of chemiluminescence detection allowed accurate and sensitive analyte detection. Under optimal conditions, a limit detection of 0.02 ng mL^{-1} for rabbit IgG was achieved, with an analytical working range of 0.05-2 ng mL^{-1}.
4. GNP-decorated silica nanorods (GNP-SiNRs) were synthesized and used as the labels for fabrication of LFSB. Owing to its biocompatibility and convenient surface modification, SiNRs were used as carriers to load numerous GNPs. Sandwich-type immunoreactions were performed on the lateral flow strips, and the accumulation of GNP-SiNRs on the test zone produced the characteristic colored bands, enabling visual detection of proteins without instrumentation. The quantitative detection of rabbit IgG was performed by reading the intensities of the colored bands with a portable strip reader. The response of the optimized device was highly linear for the range of 0.05-2 ng mL^{-1}, and the detection limit was estimated to be 0.01 ng mL^{-1}. The detection limit was lowered by 50 times compared to the traditional GNP-based lateral flow assay.

Even with highly enhanced sensitivity, the lateral flow strip biosensors are still faced with a number of challenges for point-of-care diagnosis or on-field application. The analytes tested with proposed biosensors are commercial products, without validation against real clinical samples. Successful and accurate detection of analytes in complex biological samples, such as human blood or saliva, is a greatly important future application. Moreover, to achieve an excellent specificity in validation of protein biomarkers for cancer development and progression,

accurate detection of multiple biomarkers is required due to the low specificity when using single tumor marker. Simultaneous analysis of multiplexed biomarkers with biosensor becomes particularly important in laboratory research and clinical diagnosis. Extensive experiments will be necessary to be carried out with analysis of patient samples for configuration of reliable detection platform; also more works will be focused on the multiplex detection on a single LFSB for diagnostics of the specific cancer-related disease.

7. REFERENCES

1. Winter, J. M.; Yeo, C. J.; Brody, J. R. Diagnostic, prognostic, and predictive biomarkers in pancreatic cancer. *J. Surg. Oncol.* **2013,** *107* (1), 15-22.
2. Rifai, N.; Gillette, M. A.; Carr, S. A. Protein biomarker discovery and validation: the long and uncertain path to clinical utility. *Nat. Biotechnol.* **2006,** *24* (8), 971-983.
3. American Cancer Society. *Cancer Facts & Figures* 2013. Atlanta: American Cancer Society; **2013**.
4. Zhang, Y.; Guo, Y.; Xianyu, Y.; Chen, W.; Zhao, Y.; Jiang, X. Nanomaterials for ultrasensitive protein detection. *Adv. Mater.* **2013,** *25* (28), 3802-3819.
5. Wu, S. L.; Amato, H.; Biringer, R.; Choudhary, G.; Shieh, P.; Hancock, W. S. Targeted proteomics of low-level proteins in human plasma by LC/MSn: using human growth hormone as a model system. *J. Proteome. Res.* **2002,** *1* (5), 459-465.
6. Barnidge, D. R.; Goodmanson, M. K.; Klee, G. G.; Muddiman, D. C. Absolute quantification of the model biomarker prostate-specific antigen in serum by LC-Ms/MS using protein cleavage and isotope dilution mass spectrometry. *J. Proteome. Res.* **2004,** *3* (3), 644-652.
7. Anderson, L.; Hunter, C. L. Quantitative mass spectrometric multiple reaction monitoring assays for major plasma proteins. *Mol. Cell. Proteomics* **2006,** *5* (4), 573-588.
8. Johnson, I. R.; Parkinson-Lawrence, E. J.; Butler, L. M.; Brooks, D. A. Prostate cell lines as models for biomarker discovery: performance of current markers and the search for new biomarkers. *Prostate* **2014,** *74* (5), 547-560.
9. Lichtenauer, A. M.; Herzog, R.; Tarantino, S.; Aufricht, C.; Kratochwill, K. Equalizer technology followed by DIGE-based proteomics for detection of cellular proteins in

artificial peritoneal dialysis effluents. *Electrophoresis* **2014,** *35* (10), 1387-1394.

10. Grandjean, M.; Dieu, M.; Raes, M.; Feron, O. A new method combining sequential immunoaffinity depletion and differential in gel electrophoresis to identify autoantibodies as cancer biomarkers. *J. Immunol. Methods* **2013,** *396* (1-2), 23-32.
11. Wayner, E. A.; Quek, S. I.; Ahmad, R.; Ho, M. E.; Loprieno, M. A.; Zhou, Y.; Ellis, W. J.; True, L. D.; Liu, A. Y. Development of an ELISA to detect the secreted prostate cancer biomarker AGR2 in voided urine. *Prostate* **2012,** *72* (9), 1023-1034.
12. Zong, C.; Wu, J.; Wang, C.; Ju, H.; Yan, F. Chemiluminescence imaging immunoassay of multiple tumor markers for cancer screening. *Anal. Chem.* **2012,** *84* (5), 2410-2415.
13. Wilson, M. S.; Nie, W. Multiplex measurement of seven tumor markers using an electrochemical protein chip. *Anal. Chem.* **2006,** *78* (18), 6476-6483.
14. Wu, M. S.; Shi, H. W.; He, L. J.; Xu, J. J.; Chen, H. Y. Microchip device with 64-site electrode array for multiplexed immunoassay of cell surface antigens based on electrochemiluminescence resonance energy transfer. *Anal. Chem.* **2012,** *84* (9), 4207-4213.
15. Lee, H.; Sun, E.; Ham, D.; Weissleder, R. Chip-NMR biosensor for detection and molecular analysis of cells. *Nat. Med.* **2008,** *14* (8), 869-874.
16. Shao, H.; Min, C.; Issadore, D.; Liong, M.; Yoon, T. J.; Weissleder, R.; Lee, H. Magnetic Nanoparticles and microNMR for Diagnostic Applications. *Theranostics* **2012,** *2* (1), 55-65.
17. Gubala, V.; Harris, L. F.; Ricco, A. J.; Tan, M. X.; Williams, D. E. Point of care diagnostics: status and future. *Anal. Chem.* **2012,** *84* (2), 487-515.
18. Farrell, B. O. Evolution in Lateral Flow–Based Immunoassay Systems. In *Lateral Flow*

Immunoassay; Wong, R. C., Tse, H. Y., Eds; Humana Press: New York, 2009; pp 1-4.

19. Posthuma-Trumpie, G. A.; Korf, J.; van Amerongen, A. Lateral flow (immuno)assay: its strengths, weaknesses, opportunities and threats. A literature survey. *Anal. Bioanal. Chem.* **2009,** *393* (2), 569-582.

20. Liu, J.; Mazumdar, D.; Lu, Y. A simple and sensitive "dipstick" test in serum based on lateral flow separation of aptamer-linked nanostructures. *Angew. Chem. Int. Ed. Engl.* **2006,** *45* (47), 7955-7959.

21. Xu, H.; Mao, X.; Zeng, Q.; Wang, S.; Kawde, A. N.; Liu, G. Aptamer-functionalized gold nanoparticles as probes in a dry-reagent strip biosensor for protein analysis. *Anal. Chem.* **2009,** *81* (2), 669-675.

22. Liu, G.; Mao, X.; Phillips, J. A.; Xu, H.; Tan, W.; Zeng, L. Aptamer-nanoparticle strip biosensor for sensitive detection of cancer cells. *Anal. Chem.* **2009,** *81* (24), 10013-10018.

23. Fernandez-Sanchez, C.; McNeil, C. J.; Rawson, K.; Nilsson, O.; Leung, H. Y.; Gnanapragasam, V. One-step immunostrip test for the simultaneous detection of free and total prostate specific antigen in serum. *J. Immunol. Methods* **2005,** *307* (1-2), 1-12.

24. Zeng, Q. M., X.; Xu, H.; Wang S.; Liu, G. Quantitative Immunochromatographic Strip Biosensor for the Detection of Carcinoembryonic Antigen Tumor Biomarker in Human Plasma. *Am. J. Biomed. Sci*. **2009,** *1* (1), 70-79.

25. Mikawa, A. Y.; Santos, S. A.; Kenfe, F. R.; da Silva, F. H.; da Costa, P. I. Development of a rapid one-step immunochromatographic assay for HCV core antigen detection. *J. Virol. Methods* **2009,** *158* (1-2), 160-164.

26. Zhu, J.; Zou, N.; Mao, H.; Wang, P.; Zhu, D.; Ji, H.; Cong, H.; Sun, C.; Wang, H.; Zhang,

F.; Qian, J.; Jin, Q.; Zhao, J. Evaluation of a modified lateral flow immunoassay for detection of high-sensitivity cardiac troponin I and myoglobin. *Biosens. Bioelectron.* **2013,** *42*, 522-525.

27. Worsley, G. J.; Attree, S. L.; Noble, J. E.; Horgan, A. M. Rapid duplex immunoassay for wound biomarkers at the point-of-care. *Biosens. Bioelectron.* **2012,** *34* (1), 215-220.

28. Pfender, N.; Lucassen, R.; Offermann, N.; Schulte-Pelkum, J.; Fooke, M.; Jakob, T. Evaluation of a Novel Rapid Test System for the Detection of Specific IgE to Hymenoptera Venoms. *J. Allergy (Cairo)* **2012,** *2012*, 862023.

29. Fang, Z.; Ge, C.; Zhang, W.; Lie, P.; Zeng, L. A lateral flow biosensor for rapid detection of DNA-binding protein c-jun. *Biosens. Bioelectron.* **2011,** *27* (1), 192-196.

30. Lie, P.; Liu, J.; Fang, Z.; Dun, B.; Zeng, L. A lateral flow biosensor for detection of nucleic acids with high sensitivity and selectivity. *Chem. Commun. (Camb)* **2012,** *48* (2), 236-238.

31. Glynou, K.; Ioannou, P. C.; Christopoulos, T. K.; Syriopoulou, V. Oligonucleotide-functionalized gold nanoparticles as probes in a dry-reagent strip biosensor for DNA analysis by hybridization. *Anal. Chem.* **2003,** *75* (16), 4155-4160.

32. Xiao, Z.; Lie, P.; Fang, Z.; Yu, L.; Chen, J.; Liu, J.; Ge, C.; Zhou, X.; Zeng, L. A lateral flow biosensor for detection of single nucleotide polymorphism by circular strand displacement reaction. *Chem. Commun. (Camb)* **2012,** *48* (68), 8547-8549.

33. Carter, D. J.; Cary, R. B. Lateral flow microarrays: a novel platform for rapid nucleic acid detection based on miniaturized lateral flow chromatography. *Nucleic Acids Res.* **2007,** *35* (10), e74.

34. Zuiderwijk, M.; Tanke, H. J.; Sam Niedbala, R.; Corstjens, P. L. An amplification-free

hybridization-based DNA assay to detect Streptococcus pneumoniae utilizing the up-converting phosphor technology. *Clin. Biochem.* **2003,** *36* (5), 401-403.

35. Gao, X.; Xu, H.; Baloda, M.; Gurung, A. S.; Xu, L. P.; Wang, T.; Zhang, X.; Liu, G. Visual detection of microRNA with lateral flow nucleic acid biosensor. *Biosens. Bioelectron.* **2014,** *54*, 578-584.

36. Delmulle, B. S.; De Saeger, S. M.; Sibanda, L.; Barna-Vetro, I.; Van Peteghem, C. H. Development of an immunoassay-based lateral flow dipstick for the rapid detection of aflatoxin B1 in pig feed. *J. Agric. Food Chem.* **2005,** *53* (9), 3364-3368.

37. Zhang, C.; Zhang, Y.; Wang, S. Development of multianalyte flow-through and lateral-flow assays using gold particles and horseradish peroxidase as tracers for the rapid determination of carbaryl and endosulfan in agricultural products. *J. Agric. Food Chem.* **2006,** *54* (7), 2502-2507.

38. Wang, S.; Quan, Y.; Lee, N.; Kennedy, I. R. Rapid determination of fumonisin B1 in food samples by enzyme-linked immunosorbent assay and colloidal gold immunoassay. *J. Agric. Food Chem.* **2006,** *54* (7), 2491-2495.

39. Verheijen, R. O., I. K.; Dietrich, R.; Haasnoot, W. Development of a One Step Strip Test for the Detection of (Dihydro)streptomycin Residues in Raw Milk. *Food Agric. Immunol.* **2000,** *12* (1), 31-40.

40. He, Y.; Zhang, X.; Zeng, K.; Zhang, S.; Baloda, M.; Gurung, A. S.; Liu, G. Visual detection of Hg^{2+} in aqueous solution using gold nanoparticles and thymine-rich hairpin DNA probes. *Biosens. Bioelectron.* **2011,** *26* (11), 4464-4470.

41. Liu, X.; Xiang, J. J.; Tang, Y.; Zhang, X. L.; Fu, Q. Q.; Zou, J. H.; Lin, Y. Colloidal gold nanoparticle probe-based immunochromatographic assay for the rapid detection of

chromium ions in water and serum samples. *Anal. Chim. Acta.* **2012,** *745*, 99-105.

42. Lopez Marzo, A. M.; Pons, J.; Blake, D. A.; Merkoci, A. All-integrated and highly sensitive paper based device with sample treatment platform for Cd^{2+} immunodetection in drinking/tap waters. *Anal. Chem.* **2013,** *85* (7), 3532-3538.

43. Mazumdar, D.; Liu, J.; Lu, G.; Zhou, J.; Lu, Y. Easy-to-use dipstick tests for detection of lead in paints using non-cross-linked gold nanoparticle-DNAzyme conjugates. *Chem. Commun. (Camb)* **2010,** *46* (9), 1416-1418.

44. Fang, Z.; Huang, J.; Lie, P.; Xiao, Z.; Ouyang, C.; Wu, Q.; Wu, Y.; Liu, G.; Zeng, L. Lateral flow nucleic acid biosensor for Cu^{2+} detection in aqueous solution with high sensitivity and selectivity. *Chem. Commun. (Camb)* **2010,** *46* (47), 9043-9045.

45. Hossain, S. M.; Ozimok, C.; Sicard, C.; Aguirre, S. D.; Ali, M. M.; Li, Y.; Brennan, J. D. Multiplexed paper test strip for quantitative bacterial detection. *Anal. Bioanal. Chem.* **2012,** *403* (6), 1567-1576.

46. Li, C. Z.; Vandenberg, K.; Prabhulkar, S.; Zhu, X.; Schneper, L.; Methee, K.; Rosser, C. J.; Almeide, E. Paper based point-of-care testing disc for multiplex whole cell bacteria analysis. *Biosens. Bioelectron.* **2011,** *26* (11), 4342-4348.

47. Salomone, A. M., M.; Roggero, P.; Boscia, D. Reliability of detection of citrus tristeza virus by an immunochromatographic lateral flow assay in comparison with ELISA. *J. Plant Pathol.* **2004,** *86* (1), 43-48.

48. Zhang, G. P.; Guo, J. Q.; Wang, X. N.; Yang, J. X.; Yang, Y. Y.; Li, Q. M.; Li, X. W.; Deng, R. G.; Xiao, Z. J.; Yang, J. F.; Xing, G. X.; Zhao, D. Development and evaluation of an immunochromatographic strip for trichinellosis detection. *Vet. Parasitol* **2006,** *137* (3-4), 286-293.

49. Leung, W.; Chan, C. P.; Leung, M.; Lehmann, K.; Renneberg, I.; Lehmann, M.; Hempel, A.; Glatz, J. F. C.; Renneberg, R. Novel "Digital-Style" Rapid Test Simultaneously Detecting Heart Attack and Predicting Cardiovascular Disease Risk. *Anal. Lett.* **2005,** *38* (3), 423-439.

50. Klewitz, T. G., F.; Beer, H.; Pflanz, K.; Scheper, T. Immunochromatographic assay for determination of botulinum neurotoxin type D. *Sens. Actuators, B* **2006,** *113* (2), 582-589.

51. He, J. Z. S.-P.; Liu, W.; Deng, A.-X.; Nan, T.-G.; Wang, B.-M.; Zhai, Z.-X.; Li, Z.-H., Development of a lateral flow dipstick immunoassay for the rapid detection of glycyrrhizic acid. *Food Agric. Immunol.* **2006,** *17* (3-4), 173-181.

52. Huo, T.; Peng, C.; Xu, C.; Liu, L. Development of colloidal gold-based immunochromatographic assay for the rapid detection of medroxyprogesterone acetate residues. *Food Agric. Immunol.* **2006,** *17* (3-4), 183-190.

53. Chou, S. F. Development of a manual self-assembled colloidal gold nanoparticle-immunochromatographic strip for rapid determination of human interferon-gamma. *Analyst* **2013,** *138* (9), 2620-2623.

54. Madersbacher, S.; Mian, C.; Maier, U.; Simak, R. Validation of a 10-minute dipstick test for serum prostate-specific antigen. *Eur. Urol.* **1996,** *30* (4), 446-450.

55. Lee, E. Y.; Kang, J. H.; Kim, K. A.; Chung, T. W.; Kim, H. J.; Yoon, D. Y.; Lee, H. G.; Kwon, D. H.; Kim, J. W.; Kim, C. H.; Song, E. Y. Development of a rapid, immunochromatographic strip test for serum asialo alpha1-acid glycoprotein in patients with hepatic disease. *J. Immunol. Methods* **2006,** *308* (1-2), 116-123.

56. Adams, J.; Carder, P. J.; Downey, S.; Forbes, M. A.; MacLennan, K.; Allgar, V.;

Kaufman, S.; Hallam, S.; Bicknell, R.; Walker, J. J.; Cairnduff, F.; Selby, P. J.; Perren, T. J.; Lansdown, M.; Banks, R. E. Vascular endothelial growth factor (VEGF) in breast cancer: comparison of plasma, serum, and tissue VEGF and microvessel density and effects of tamoxifen. *Cancer Res.* **2000,** *60* (11), 2898-2905.

57. Riedel, F.; Zaiss, I.; Herzog, D.; Gotte, K.; Naim, R.; Hormann, K. Serum levels of interleukin-6 in patients with primary head and neck squamous cell carcinoma. *Anticancer Res.* **2005,** *25* (4), 2761-2765.

58. Cho, I. H.; Seo, S. M.; Paek, E. H.; Paek, S. H. Immunogold-silver staining-on-a-chip biosensor based on cross-flow chromatography. *J. Chromatogr. B Analyt. Technol. Biomed. Life Sci.* **2010,** *878* (2), 271-277.

59. Rohrman, B. A.; Leautaud, V.; Molyneux, E.; Richards-Kortum, R. R. A lateral flow assay for quantitative detection of amplified HIV-1 RNA. *PLoS One* **2012,** *7* (9), e45611.

60. Choi, D. H.; Lee, S. K.; Oh, Y. K.; Bae, B. W.; Lee, S. D.; Kim, S.; Shin, Y. B.; Kim, M. G. A dual gold nanoparticle conjugate-based lateral flow assay (LFA) method for the analysis of troponin I. *Biosens. Bioelectron.* **2010,** *25* (8), 1999-2002.

61. Tang, D.; Sauceda, J. C.; Lin, Z.; Ott, S.; Basova, E.; Goryacheva, I.; Biselli, S.; Lin, J.; Niessner, R.; Knopp, D. Magnetic nanogold microspheres-based lateral-flow immunodipstick for rapid detection of aflatoxin B2 in food. *Biosens. Bioelectron.* **2009,** *25* (2), 514-518.

62. Nash, M. A.; Waitumbi, J. N.; Hoffman, A. S.; Yager, P.; Stayton, P. S. Multiplexed enrichment and detection of malarial biomarkers using a stimuli-responsive iron oxide and gold nanoparticle reagent system. *ACS Nano* **2012,** *6* (8), 6776-6785.

63. Qin, Z.; Chan, W. C. W.; Boulware, D. R.; Akkin, T.; Butler, E. K.; Bischof, J. C.

Significantly Improved Analytical Sensitivity of Lateral Flow Immunoassays by Using Thermal Contrast. *Angew. Chem., Int. Ed.* **2012,** *51* (18), 4358-4361.

64. Cho, J. H.; Paek, E. H.; Cho, I. H.; Paek, S. H. An enzyme immunoanalytical system based on sequential cross-flow chromatography. *Anal. Chem.* **2005,** *77* (13), 4091-4097.

65. He, Y.; Zhang, S.; Zhang, X.; Baloda, M.; Gurung, A. S.; Xu, H.; Liu, G. Ultrasensitive nucleic acid biosensor based on enzyme-gold nanoparticle dual label and lateral flow strip biosensor. *Biosens. Bioelectron.* **2011,** *26* (5), 2018-2024.

66. Mirasoli, M.; Buragina, A.; Dolci, L. S.; Simoni, P.; Anfossi, L.; Giraudi, G.; Roda, A. Chemiluminescence-based biosensor for fumonisins quantitative detection in maize samples. *Biosens. Bioelectron.* **2012,** *32* (1), 283-287.

67. Mirasoli, M.; Buragina, A.; Dolci, L. S.; Guardigli, M.; Simoni, P.; Montoya, A.; Maiolini, E.; Girotti, S.; Roda, A. Development of a chemiluminescence-based quantitative lateral flow immunoassay for on-field detection of 2,4,6-trinitrotoluene. *Anal. Chim. Acta* **2012,** *721*, 167-172.

68. Li, Z.; Wang, Y.; Wang, J.; Tang, Z.; Pounds, J. G.; Lin, Y. Rapid and sensitive detection of protein biomarker using a portable fluorescence biosensor based on quantum dots and a lateral flow test strip. *Anal. Chem.* **2010,** *82* (16), 7008-7014.

69. Bai, Y.; Tian, C.; Wei, X.; Wang, Y.; Wang, D.; Shi, X. A sensitive lateral flow test strip based on silica nanoparticle/CdTe quantum dot composite reporter probes. *RSC Advances* **2012,** *2* (5), 1778-1781.

70. Xia, X.; Xu, Y.; Zhao, X.; Li, Q. Lateral flow immunoassay using europium chelate-loaded silica nanoparticles as labels. *Clin. Chem.* **2009,** *55* (1), 179-182.

71. Suarez-Pantaleon, C.; Wichers, J.; Abad-Somovilla, A.; van Amerongen, A.; Abad-

Fuentes, A. Development of an immunochromatographic assay based on carbon nanoparticles for the determination of the phytoregulator forchlorfenuron. *Biosens. Bioelectron.* **2013,** *42*, 170-176.

72. Kalogianni, D. P.; Boutsika, L. M.; Kouremenou, P. G.; Christopoulos, T. K.; Ioannou, P. C. Carbon nano-strings as reporters in lateral flow devices for DNA sensing by hybridization. *Anal. Bioanal. Chem.* **2011,** *400* (4), 1145-1152.

73. Abera, A.; Choi, J.-W. Quantitative lateral flow immunosensor using carbon nanotubes as label. *Anal. Methods* **2010,** *2* (11), 1819-1822.

74. Ouellette, A. L.; Li, J. J.; Cooper, D. E.; Ricco, A. J.; Kovacs, G. T. Evolving point-of-care diagnostics using up-converting phosphor bioanalytical systems. *Anal. Chem.* **2009,** *81* (9), 3216-3221.

75. Shuman, M. A.; Majerus, P. W. The measurement of thrombin in clotting blood by radioimmunoassay. *J. Clin. Invest.* **1976,** *58* (5), 1249-1258.

76. Bichler, J.; Siebeck, M.; Maschler, R.; Pelzer, H.; Fritz, H. Determination of thrombin-hirudin complex in plasma with an enzyme-linked immunosorbent assay. *Blood Coagul. Fibrinolysis* **1991,** *2* (1), 129-133.

77. Reboli, A. C. Diagnosis of invasive candidiasis by a dot immunobinding assay for Candida antigen detection. *J. Clin. Microbiol.* **1993,** *31* (3), 518-523.

78. Kandan, A.; Ramanathan, A.; Raguchander, T.; Balasubramanian, P.; Samiyappan, R. Development and evaluation of an enzyme-linked immunosorbent assay (ELISA) and dot immunobinding assay (DIBA) for the detection of Ganoderma infecting palms. *rch. Phytopathol. Plant Prot.* **2010,** *43* (15), 1473-1484.

79. Liao, W.; Guo, S.; Zhao, X. S. Novel probes for protein chip applications. *Front. Biosci.*

2006, *11*, 186-197.

80. Hu, M.; He, Y.; Song, S.; Yan, J.; Lu, H. T.; Weng, L. X.; Wang, L. H.; Fan, C. DNA-bridged bioconjugation of fluorescent quantum dots for highly sensitive microfluidic protein chips. *Chem. Commun. (Camb)* **2010,** *46* (33), 6126-6128.

81. Poltronieri, P.; Cimaglia, F.; Santino, A.; De Blasi, M. D.; Krizkova-Kudlikova, I.; Liu, S.; Wang, Y.; Wang, Y. Protein chips for detection of mite allergens using Kunitz-type protease inhibitors. *Biotechnol. J.* **2010,** *5* (6), 582-587.

82. Zhang, X.; Jiang, L.; Zhang, C.; Li, D.; Wang, C.; Gao, F.; Cui, D. A silicon dioxide modified magnetic nanoparticles-labeled lateral flow strips for HBs antigen. *J. Biomed. Nanotechnol.* **2011,** *7* (6), 776-781.

83. Lawn, S. D.; Dheda, K.; Kerkhoff, A. D.; Peter, J. G.; Dorman, S.; Boehme, C. C.; Nicol, M. P. Determine TB-LAM lateral flow urine antigen assay for HIV-associated tuberculosis: recommendations on the design and reporting of clinical studies. *BMC Infect. Dis.* **2013,** *13*, 407.

84. Zheng, M. Z.; Richard, J. L.; Binder, J. A review of rapid methods for the analysis of mycotoxins. *Mycopathologia* **2006,** *161* (5), 261-273.

85. Leuvering, J. H.; Thal, P. J.; van der Waart, M.; Schuurs, A. H. Sol particle immunoassay (SPIA). *J. Immunoassay* **1980,** *1* (1), 77-91.

86. Klewitz, T.; Gessler, F.; Beer, H.; Pflanz, K.; Scheper, T. Immunochromatographic assay for determination of botulinum neurotoxin type D. *Sens. Actuators, B* **2006,** *113* (2), 582-589.

87. Aveyard, J.; Mehrabi, M.; Cossins, A.; Braven, H.; Wilson, R. One step visual detection of PCR products with gold nanoparticles and a nucleic acid lateral flow (NALF) device.

Chem. Commun. (Camb) **2007,** (41), 4251-4253.

88. Nielsen, K.; Yu, W. L.; Kelly, L.; Bermudez, R.; Renteria, T.; Dajer, A.; Gutierrez, E.; Williams, J.; Algire, J.; de Eschaide, S. T., Development of a lateral flow assay for rapid detection of bovine antibody to Anaplasma marginale. *J. Immunoassay Immunochem.* **2008,** *29* (1), 10-18.

89. Kawde, A. N.; Mao, X.; Xu, H.; Zeng, Q.; He, Y.; Liu, G. Moving Enzyme-Linked ImmunoSorbent Assay to the Point-of-Care Dry-Reagent Strip Biosensors. *Am. J. Biomed. Sci.* **2010,** *2* (1), 23-32.

90. Cho, J. H.; Han, S. M.; Paek, E. H.; Cho, I. H.; Paek, S. H. Plastic ELISA-on-a-chip based on sequential cross-flow chromatography. *Anal. Chem.* **2006,** *78* (3), 793-800.

91. Pal, A.; Dhar, T. K. An analytical device for on-site immunoassay. Demonstration of its applicability in semiquantitative detection of aflatoxin B1 in a batch of samples with ultrahigh sensitivity. *Anal. Chem.* **2004,** *76* (1), 98-104.

92. Ahn, J. S.; Choi, S.; Jang, S. H.; Chang, H. J.; Kim, J. H.; Nahm, K. B.; Oh, S. W.; Choi, E. Y. Development of a point-of-care assay system for high-sensitivity C-reactive protein in whole blood. *Clin. Chim. Acta* **2003,** *332* (1-2), 51-59.

93. Khreich, N.; Lamourette, P.; Boutal, H.; Devilliers, K.; Creminon, C.; Volland, H. Detection of Staphylococcus enterotoxin B using fluorescent immunoliposomes as label for immunochromatographic testing. *Anal. Biochem.* **2008,** *377* (2), 182-188.

94. Dequaire, M.; Degrand, C.; Limoges, B. An electrochemical metalloimmunoassay based on a colloidal gold label. *Anal. Chem.* **2000,** *72* (22), 5521-5528.

95. Wang, J.; Liu, G.; Jan, M. R. Ultrasensitive electrical biosensing of proteins and DNA: carbon-nanotube derived amplification of the recognition and transduction events. *J. Am.*

Chem. Soc. **2004,** *126* (10), 3010-3011.

96. Zheng, G.; Patolsky, F.; Cui, Y.; Wang, W. U.; Lieber, C. M. Multiplexed electrical detection of cancer markers with nanowire sensor arrays. *Nat. Biotechnol.* **2005,** *23* (10), 1294-1301.

97. Wu, Y.; Chen, C.; Liu, S. Enzyme-functionalized silica nanoparticles as sensitive labels in biosensing. *Anal. Chem.* **2009,** *81* (4), 1600-1607.

98. An, Y.; Jiang, X.; Bi, W.; Chen, H.; Jin, L.; Zhang, S.; Wang, C.; Zhang, W. Sensitive electrochemical immunosensor for alpha-synuclein based on dual signal amplification using PAMAM dendrimer-encapsulated Au and enhanced gold nanoparticle labels. *Biosens. Bioelectron.* **2012,** *32* (1), 224-230.

99. Schramm, W.; Angulo, G. B.; Torres, P. C.; Burgess-Cassler, A. A simple saliva-based test for detecting antibodies to human immunodeficiency virus. *Clin. Diagn. Lab. Immunol.* **1999,** *6* (4), 577-580.

100. Fernandez-Sanchez, C.; McNeil, C. J.; Rawson, K.; Nilsson, O. Disposable noncompetitive immunosensor for free and total prostate-specific antigen based on capacitance measurement. *Anal. Chem.* **2004,** *76* (19), 5649-5656.

101. Vaughn, D. W.; Nisalak, A.; Kalayanarooj, S.; Solomon, T.; Dung, N. M.; Cuzzubbo, A.; Devine, P. L. Evaluation of a rapid immunochromatographic test for diagnosis of dengue virus infection. *J. Clin. Microbiol.* **1998,** *36* (1), 234-238.

102. Zhu, J.; Chen, W.; Lu, Y.; Cheng, G. Development of an immunochromatographic assay for the rapid detection of bromoxynil in water. *Environ. Pollut.* **2008,** *156* (1), 136-142.

103. Zhou, P.; Lu, Y.; Zhu, J.; Hong, J.; Li, B.; Zhou, J.; Gong, D.; Montoya, A. Nanocolloidal Gold-Based Immunoassay for the Detection of the N-Methylcarbamate Pesticide

Carbofuran. *J. Agric. Food Chem.* **2004,** *52* (14), 4355-4359.

104. Delmulle, B. S.; De Saeger, S. M. D. G.; Sibanda, L.; Barna-Vetro, I.; Van Peteghem, C. H. Development of an Immunoassay-Based Lateral Flow Dipstick for the Rapid Detection of Aflatoxin B1 in Pig Feed. *J. Agric. Food Chem.* **2005,** *53* (9), 3364-3368.

105. Molinelli, A.; Grossalber, K.; Führer, M.; Baumgartner, S.; Sulyok, M.; Krska, R. Development of Qualitative and Semiquantitative Immunoassay-Based Rapid Strip Tests for the Detection of T-2 Toxin in Wheat and Oat. *J. Agric. Food Chem.* **2008,** *56* (8), 2589-2594.

106. Blazkova, M.; Mickova-Holubova, B.; Rauch, P.; Fukal, L. Immunochromatographic colloidal carbon-based assay for detection of methiocarb in surface water. *Biosens. Bioelectron.* **2009,** *25* (4), 753-758.

107. Song, C.; Zhi, A.; Liu, Q.; Yang, J.; Jia, G.; Shervin, J.; Tang, L.; Hu, X.; Deng, R.; Xu, C.; Zhang, G. Rapid and sensitive detection of beta-agonists using a portable fluorescence biosensor based on fluorescent nanosilica and a lateral flow test strip. *Biosens. Bioelectron.* **2013,** *50*, 62-65.

108. Paragas, V. B.; Kramer, J. A.; Fox, C.; Haugland, R. P.; Singer, V. L. The ELF -97 phosphatase substrate provides a sensitive, photostable method for labelling cytological targets. *J. Microsc.* **2002,** *206* (Pt 2), 106-119.

109. Cox, W. G.; Singer, V. L. A high-resolution, fluorescence-based method for localization of endogenous alkaline phosphatase activity. *J. Histochem. Cytochem.* **1999,** *47* (11), 1443-1456.

110. Reiter, E.; Zentek, J.; Razzazi, E. Review on sample preparation strategies and methods used for the analysis of aflatoxins in food and feed. *Mol. Nutr. Food Res.* **2009,** *53* (4),

508-524.

111. Fung, K. K.; Chan, C. P.; Renneberg, R. Development of enzyme-based bar code-style lateral-flow assay for hydrogen peroxide determination. *Anal. Chim. Acta* **2009,** *634* (1), 89-95.

112. Lin, Y. Y.; Wang, J.; Liu, G.; Wu, H.; Wai, C. M.; Lin, Y. A nanoparticle label/immunochromatographic electrochemical biosensor for rapid and sensitive detection of prostate-specific antigen. *Biosens. Bioelectron.* **2008,** *23* (11), 1659-1665.

113. Liu, G.; Lin, Y. Y.; Wang, J.; Wu, H.; Wai, C. M.; Lin, Y. Disposable electrochemical immunosensor diagnosis device based on nanoparticle probe and immunochromatographic strip. *Anal. Chem.* **2007,** *79* (20), 7644-7653.

114. Mao, X.; Baloda, M.; Gurung, A. S.; Lin, Y.; Liu, G. Multiplex electrochemical immunoassay using gold nanoparticle probes and immunochromatographic strips. *Electrochem. Commun.* **2008,** *10* (10), 1636-1640.

115. Roda, A.; Guardigli, M. Analytical chemiluminescence and bioluminescence: latest achievements and new horizons. *Anal. Bioanal. Chem.* **2012,** *402* (1), 69-76.

116. Roda, A.; Mirasoli, M.; Dolci, L. S.; Buragina, A.; Bonvicini, F.; Simoni, P.; Guardigli, M. Portable device based on chemiluminescence lensless imaging for personalized diagnostics through multiplex bioanalysis. *Anal. Chem.* **2011,** *83* (8), 3178-3185.

117. Kim, H.-S.; Ko, H.; Kang, M.-J.; Pyun, J.-C. Highly sensitive rapid test with chemiluminescent signal bands. *BioChip J.* **2010,** *4* (2), 155-160.

118. Grabar, K. C.; Freeman, R. G.; Hommer, M. B.; Natan, M. J. Preparation and Characterization of Au Colloid Monolayers. *Anal. Chem.* **1995,** *67* (4), 735-743.

119. Frens, G. Controlled Nucleation for the Regulation of the Particle Size in Monodisperse

Gold Suspensions. *Nature* **1973,** *241*, 20-22.

120. Torres-Chavolla, E.; Alocilja, E. C. Aptasensors for detection of microbial and viral pathogens. *Biosens. Bioelectron.* **2009,** *24* (11), 3175-3182.

121. Nam, J.-M.; Thaxton, C. S.; Mirkin, C. A. Nanoparticle-Based Bio-Bar Codes for the Ultrasensitive Detection of Proteins. *Science* **2003,** *301* (5641), 1884-1886.

122. Wang, J.; Cao, Y.; Xu, Y.; Li, G. Colorimetric multiplexed immunoassay for sequential detection of tumor markers. *Biosens. Bioelectron.* **2009,** *25* (2), 532-536.

123. Zhou, W.-H.; Zhu, C.-L.; Lu, C.-H.; Guo, X.; Chen, F.; Yang, H.-H.; Wang, X. Amplified detection of protein cancer biomarkers using DNAzyme functionalized nanoprobes. *Chem. Commun.* **2009,** *0* (44), 6845-6847.

124. Wang, H.; Wu, Z.; Tang, L.; Yu, R.; Jiang, J. Fluorescence Protection Assay: A Novel Homogeneous Assay Platform toward Development of Aptamer Sensors for Protein Detection. *Nucleic Acids Res.* **2011,** *39*, e122.

125. Akter, R.; Kyun Rhee, C.; Aminur Rahman, M. Sensitivity enhancement of an electrochemical immunosensor through the electrocatalysis of magnetic bead-supported non-enzymatic labels. *Biosens. Bioelectron.* **2014,** *54* (0), 351-357.

126. Du, S.; Guo, Z.; Chen, B.; Sha, Y.; Jiang, X.; Li, X.; Gan, N.; Wang, S. Electrochemiluminescence immunosensor for tumor markers based on biological barcode mode with conductive nanospheres. *Biosens. Bioelectron.* **2014,** *53* (0), 135-141.

127. Yu, Q.; Zhan, X.; Liu, K.; Lv, H.; Duan, Y. Plasma-Enhanced Antibody Immobilization for the Development of a Capillary-Based Carcinoembryonic Antigen Immunosensor Using Laser-Induced Fluorescence Spectroscopy. *Anal. Chem.* **2013,** *85* (9), 4578-4585.

128. Xia, H.; Mathew, B.; John, T.; Hegab, H.; Feng, J. Microfluidic based immunosensor for

detection and purification of carbonylated proteins. *Biomed. Microdevices* **2013,** *15* (3), 519-530.

129. Armani, A. M.; Kulkarni, R. P.; Fraser, S. E.; Flagan, R. C.; Vahala, K. J. Label-free single-molecule detection with optical microcavities. *Science* **2007,** *317*, 783-787.

130. Nie, S.; Emory, S. R. Probing Single Molecules and Single Nanoparticles by Surface-Enhanced Raman Scattering. *Science* **1997,** *275* (5303), 1102-1106.

131. Pang, Y.; Gordon, R. Optical Trapping of a Single Protein. *Nano Lett.* **2011,** *12* (1), 402-406.

132. Sorgenfrei, S.; Chiu, C.-y.; Gonzalez, R. L.; Yu, Y.-J.; Kim, P.; Nuckolls, C.; Shepard, K. L. Label-free single-molecule detection of DNA-hybridization kinetics with a carbon nanotube field-effect transistor. *Nature Nanotechnol.* **2011,** *6* (2), 126-132.

133. Srinivas, R. L.; Chapin, S. C.; Doyle, P. S. Aptamer-Functionalized Microgel Particles for Protein Detection. *Anal. Chem.* **2011,** *83* (23), 9138-9145.

134. Akter, R.; Rahman, M. A.; Rhee, C. K. Amplified Electrochemical Detection of a Cancer Biomarker by Enhanced Precipitation Using Horseradish Peroxidase Attached on Carbon Nanotubes. *Anal. Chem.* **2012,** *84* (15), 6407-6415.

135. Lin, D.; Wu, J.; Ju, H.; Yan, F. Signal amplification for electrochemical immunosensing by in situ assembly of host–guest linked gold nanorod superstructure on immunocomplex. *Biosens. Bioelectron.* **2013,** *45* (0), 195-200.

136. Shiddiky, M. J. A.; Kithva, P. H.; Rauf, S.; Trau, M. Femtomolar detection of a cancer biomarker protein in serum with ultralow background current by anodic stripping voltammetry. *Chem. Commun.* **2012,** *48* (51), 6411-6413.

137. Wang, J.; Han, H.; Jiang, X.; Huang, L.; Chen, L.; Li, N. Quantum Dot-Based Near-

Infrared Electrochemiluminescent Immunosensor with Gold Nanoparticle-Graphene Nanosheet Hybrids and Silica Nanospheres Double-Assisted Signal Amplification. *Anal. Chem.* **2012,** *84* (11), 4893-4899.

138. Zhang, J.; Yuan, Z.-F.; Wang, Y.; Chen, W.-H.; Luo, G.-F.; Cheng, S.-X.; Zhuo, R.-X.; Zhang, X.-Z. Multifunctional Envelope-Type Mesoporous Silica Nanoparticles for Tumor-Triggered Targeting Drug Delivery. *J. Am. Chem. Soc.* **2013,** *135* (13), 5068-5073.

139. Qiu, L.-P.; Wu, Z.-S.; Shen, G.-L.; Yu, R.-Q. Highly Sensitive and Selective Bifunctional Oligonucleotide Probe for Homogeneous Parallel Fluorescence Detection of Protein and Nucleotide Sequence. *Anal. Chem.* **2011,** *83* (8), 3050-3057.

140. Lu, L.; Liu, B.; Zhao, Z.; Ma, C.; Luo, P.; Liu, C.; Xie, G. Ultrasensitive electrochemical immunosensor for HE4 based on rolling circle amplification. *Biosens. Bioelectron.* **2012,** *33* (1), 216-221.

141. Zhang, Z.-z.; Zhang, C.-y. Highly Sensitive Detection of Protein with Aptamer-Based Target-Triggering Two-Stage Amplification. *Anal. Chem.* **2012,** *84* (3), 1623-1629.

142. Posthuma-Trumpie, G.; Korf, J.; Amerongen, A. Lateral flow (immuno)assay: its strengths, weaknesses, opportunities and threats. A literature survey. *Anal. Bioanal. Chem.* **2009,** *393* (2), 569-582.

143. Wang, Y.-K.; Yan, Y.-X.; Ji, W.-H.; Wang, H.-a.; Li, S.-Q.; Zou, Q.; Sun, J.-H. Rapid Simultaneous Quantification of Zearalenone and Fumonisin B1 in Corn and Wheat by Lateral Flow Dual Immunoassay. *J. Agric. Food Chem.* **2013,** *61* (21), 5031-5036.

144. Parolo, C.; Medina-Sanchez, M.; de la Escosura-Muniz, A.; Merkoci, A. Simple paper architecture modifications lead to enhanced sensitivity in nanoparticle based lateral flow immunoassays. *Lab Chip* **2013,** *13* (3), 386-390.

145. Hou, S.-Y.; Hsiao, Y.-L.; Lin, M.-S.; Yen, C.-C.; Chang, C.-S. MicroRNA detection using lateral flow nucleic acid strips with gold nanoparticles. *Talanta* **2012,** *99* (0), 375-379.

146. Mao, X.; Ma, Y.; Zhang, A.; Zhang, L.; Zeng, L.; Liu, G. Disposable Nucleic Acid Biosensors Based on Gold Nanoparticle Probes and Lateral Flow Strip. *Anal. Chem.* **2009,** *81* (4), 1660-1668.

147. Shyu, R.-H.; Shyu, H.-F.; Liu, H.-W.; Tang, S.-S. Colloidal gold-based immunochromatographic assay for detection of ricin. *Toxicon* **2002,** *40* (3), 255-258.

148. López_Marzo, A. M.; Pons, J.; Blake, D. A.; Merkoçi, A. High sensitive gold-nanoparticle based lateral flow Immunodevice for Cd^{2+} detection in drinking waters. *Biosens. Bioelectron.* **2013,** *47* (0), 190-198.

149. Suárez-Pantaleón, C.; Wichers, J.; Abad-Somovilla, A.; van Amerongen, A.; Abad-Fuentes, A. Development of an immunochromatographic assay based on carbon nanoparticles for the determination of the phytoregulator forchlorfenuron. *Biosens. Bioelectron.* **2013,** *42* (0), 170-176.

150. Ye, L.; Haider, H.; Esa, W. B.; Su, L.; Law, P. K.; Zhang, W.; Lim, Y.; Poh, K. K.; Sim, E. K. Liposome-based vascular endothelial growth factor-165 transfection with skeletal myoblast for treatment of ischaemic limb disease. *J. Cell. Mol. Med.* **2010,** *14* (1-2), 323-336.

151. Zou, Z.; Du, D.; Wang, J.; Smith, J. N.; Timchalk, C.; Li, Y.; Lin, Y. Quantum Dot-Based Immunochromatographic Fluorescent Biosensor for Biomonitoring Trichloropyridinol, a Biomarker of Exposure to Chlorpyrifos. *Anal. Chem.* **2010,** *82* (12), 5125-5133.

152. Li, X.; Lu, D.; Sheng, Z.; Chen, K.; Guo, X.; Jin, M.; Han, H. A fast and sensitive immunoassay of avian influenza virus based on label-free quantum dot probe and lateral

flow test strip. *Talanta* **2012,** *100* (0), 1-6.

153. Liu, C.; Jia, Q.; Yang, C.; Qiao, R.; Jing, L.; Wang, L.; Xu, C.; Gao, M. Lateral Flow Immunochromatographic Assay for Sensitive Pesticide Detection by Using Fe_3O_4 Nanoparticle Aggregates as Color Reagents. *Anal. Chem.* **2011,** *83* (17), 6778-6784.

154. Fang, Z.; Ge, C.; Zhang, W.; Lie, P.; Zeng, L. A lateral flow biosensor for rapid detection of DNA-binding protein c-jun. *Biosens. Bioelectron.* **2011,** *27* (1), 192-196.

155. Chao, C.-H.; Wu, C.-S.; Huang, C.-C.; Liang, J.-C.; Wang, H.-T.; Tang, P.-T.; Lin, L.-Y.; Ko, F.-H. A rapid and portable sensor based on protein-modified gold nanoparticle probes and lateral flow assay for naked eye detection of mercury ion. *Microelectron. Eng.* **2012,** *97* (0), 294-296.

156. Anfossi, L.; Baggiani, C.; Giovannoli, C.; D'Arco, G.; Giraudi, G. Lateral-flow immunoassays for mycotoxins and phycotoxins: a review. *Anal. Bioanal. Chem.* **2013,** *405* (2-3), 467-480.

157. Kapaki, E. K., K.; Paraskevas, G. P.; Michalopoulou, M.; Patsouris, E. Highly increased CSF tau protein and decreased β-amyloid (1–42) in sporadic CJD: a discrimination from Alzheimer's disease? *J. Neurol. Neurosurg. Psychiatry* **2001,** *71* (3), 401-403.

158. Choi, D. H.; Lee, S. K.; Oh, Y. K.; Bae, B. W.; Lee, S. D.; Kim, S.; Shin, Y.-B.; Kim, M.-G. A dual gold nanoparticle conjugate-based lateral flow assay (LFA) method for the analysis of troponin I. *Biosens. Bioelectron.* **2010,** *25* (8), 1999-2002.

159. Mei, Z.; Qu, W.; Deng, Y.; Chu, H.; Cao, J.; Xue, F.; Zheng, L.; El-Nezamic, H. S.; Wu, Y.; Chen, W. One-step signal amplified lateral flow strip biosensor for ultrasensitive and on-site detection of bisphenol A (BPA) in aqueous samples. *Biosens. Bioelectron.* **2013,** *49* (0), 457-461.

160. He, Y.; Zhang, S.; Zhang, X.; Baloda, M.; Gurung, A. S.; Xu, H.; Zhang, X.; Liu, G. Ultrasensitive nucleic acid biosensor based on enzyme–gold nanoparticle dual label and lateral flow strip biosensor. *Biosens. Bioelectron.* **2011,** *26* (5), 2018-2024.

161. Tang, D.; Sauceda, J. C.; Lin, Z.; Ott, S.; Basova, E.; Goryacheva, I.; Biselli, S.; Lin, J.; Niessner, R.; Knopp, D. Magnetic nanogold microspheres-based lateral-flow immunodipstick for rapid detection of aflatoxin B2 in food. *Biosens. Bioelectron.* **2009,** *25* (2), 514-518.

162. Tanaka, H.; Mitsuishi, M.; Miyashita, T. Tailored-Control of Gold Nanoparticle Adsorption onto Polymer Nanosheets. *Langmuir* **2003,** *19* (8), 3103-3105.

163. Tseng, R. J.; Huang, J.; Ouyang, J.; Kaner, R. B.; Yang, Y. Polyaniline nanofiber/gold nanoparticle nonvolatile memory. *Nano Lett.* **2005,** *5* (6), 1077-1080.

164. Chu, H.; Wang, J.; Ding, L.; Yuan, D.; Zhang, Y.; Liu, J.; Li, Y. Decoration of gold nanoparticles on surface-grown single-walled carbon nanotubes for detection of every nanotube by surface-enhanced Raman spectroscopy. *J. Am. Chem. Soc.* **2009,** *131* (40), 14310-14316.

165. Minati, L.; Antonini, V.; Dalla Serra, M.; Speranza, G. Multifunctional branched gold-carbon nanotube hybrid for cell imaging and drug delivery. *Langmuir* **2012,** *28* (45), 15900-15906.

166. Vallet-Regi, M.; Balas, F.; Arcos, D. Mesoporous Materials for Drug Delivery. *Angew. Chem. Int. Ed.* **2007,** *46*, 7548-7558.

167. Bae, S. W.; Tan, W.; Hong, J.-I. Fluorescent dye-doped silica nanoparticles: new tools for bioapplications. *Chem. Commun.* **2012,** *48* (17), 2270-2282.

168. Fan, H.; Jiao, F.; Chen, H.; Zhang, F.; Wang, Q.; He, P.; Fang, Y. Qualitative and

quantitative detection of DNA amplified with HRP-modified SiO_2 nanoparticles using scanning electrochemical microscopy. *Biosens. Bioelectron.* **2013,** *47* (0), 373-378.

169. Qi, W.; Wu, D.; Zhao, J.; Liu, Z.; Zhang, W.; Zhang, L.; Xu, G. Electrochemiluminescence Resonance Energy Transfer Based on $Ru(phen)_3^{2+}$-Doped Silica Nanoparticles and Its Application in "Turn-on" Detection of Ozone. *Anal. Chem.* **2013,** *85* (6), 3207-3212.

170. Zhang, Y.; Yuan, Q.; Chen, T.; Zhang, X.; Chen, Y.; Tan, W. DNA-Capped Mesoporous Silica Nanoparticles as an Ion-Responsive Release System to Determine the Presence of Mercury in Aqueous Solutions. *Anal. Chem.* **2012,** *84* (4), 1956-1962.

171. Xu, S.; Hartvickson, S.; Zhao, J. X. Engineering of SiO_2−Au−SiO_2 Sandwich Nanoaggregates Using a Building Block: Single, Double, and Triple Cores for Enhancement of Near Infrared Fluorescence. *Langmuir* **2008,** *24* (14), 7492-7499.

172. Xu, H.; Mao, X.; Zeng, Q.; Wang, S.; Kawde, A.-N.; Liu, G. Aptamer-Functionalized Gold Nanoparticles as Probes in a Dry-Reagent Strip Biosensor for Protein Analysis. *Anal. Chem.* **2008,** *81* (2), 669-675.

173. Lin, W.; Huang, Y.-w.; Zhou, X.-D.; Ma, Y. In vitro toxicity of silica nanoparticles in human lung cancer cells. *Toxicol. Appl. Pharmacol.* **2006,** *217* (3), 252-259.

174. Jin, Y.; Kannan, S.; Wu, M.; Zhao, J. X. Toxicity of Luminescent Silica Nanoparticles to Living Cells. *Chem. Res. Toxicol.* **2007,** *20* (8), 1126-1133.

175. Birnbaum, S.; Uden, C.; Magnusson, C. G.; Nilsson, S. Latex-based thin-layer immunoaffinity chromatography for quantitation of protein analytes. *Anal. Biochem.* **1992,** *206* (1), 168-171.

176. Wen, H. W.; Borejsza-Wysocki, W.; DeCory, T. R.; Durst, R. A. Development of a

competitive liposome-based lateral flow assay for the rapid detection of the allergenic peanut protein Ara h1. *Anal. Bioanal. Chem.* **2005,** *382* (5), 1217-1226.